Seabed mapping in the shallow waters of the Gulf of Bothnia - A joint Finnish - Swedish initiative for the management of shallow habitats

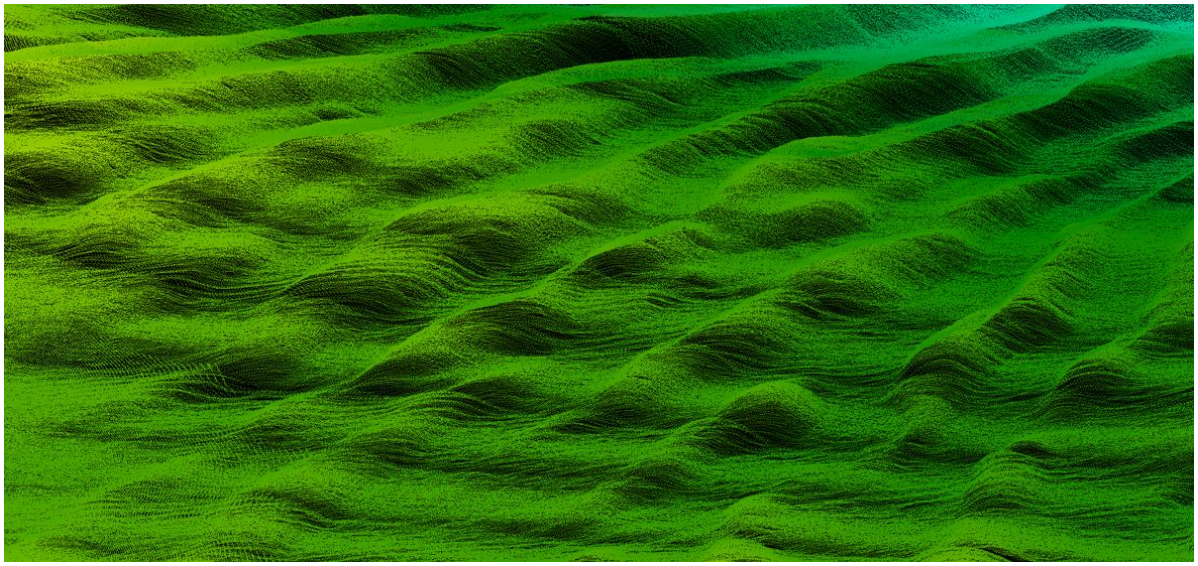

Interreg
Aurora

Co-funded by
the European Union

SeaMoreEco

Interreg Aurora
Co-funded by the European Union
SeaMoreEco
County Administrative Board of Norrbotten
Länsstyrelsen Västerbotten
County administrative board of Västerbotten
Centre for Economic Development, Transport and the Environment
GTK
Swedish Agency for Marine and Water Management
REGIONAL COUNCIL OF LAPLAND
SGU Geological Survey of Sweden

Title:	Seabed mapping in the shallow waters of the Gulf of Bothnia - A joint Finnish - Swedish initiative for the management of shallow habitats
Authors:	Francis Freire[1], Tarikul Islam[1], Aarno Kotilainen[2], Elina Lindsberg[2], Meri Sahiluoto[2], Olli Sallasmaa[2], Peter Slagbrand[1], Riku-Olli Valta[2], Anton Wagner[1] & Pichaya Zerne[1] [1] The Geological Survey of Sweden [2] The Geological Survey of Finland
Publication year:	2025
How to refer to this report	Freire et al., 2025, *Seabed mapping in the shallow waters of the Gulf of Bothnia - A joint Finnish - Swedish initiative for the management of shallow habitats*, SeaMoreEco Technical Report WP 2: Collecting marine data from the coastal waters, p.106, Doria

Preface

The shallow coastal areas of the northern Gulf of Bothnia represent ecologically vital zones within the broader marine environment, distinguished by their rich biodiversity and unique habitats. However, these areas are increasingly vulnerable to the pressures of human activity and the accelerating impacts of climate change. A challenge for management today is the lack of knowledge of occurring species and habitats and practical solutions on how to improve their environmental status.

SeaMoreEco is a Finnish-Swedish initiative that during the years of 2023 – 2025 brought together expertise in marine biology and geology to map coastal habitats as well as develop, test, and demonstrate methods for monitoring, conservation, and restoration in shallow marine environments in the northern Gulf of Bothnia.

This report is published as one output of the project, with the aim to share the results of the marine geological seabed mapping. Through these efforts, the project aims to strengthen the knowledge of marine habitat and their management and foster long-term resilience in the northern Gulf of Bothnia's shallow ecosystems.

The project was financed by Interreg Aurora and co-financed by Regional Council of Lapland and Swedish Agency for Marine and Water Management.

Participating organisations:

County Administrative Board of Norrbotten
County Administrative Board of Västerbotten
Geological Survey of Finland
Geological Survey of Sweden
Centre for Economic development, Transport and Environment Northern Ostrobothnia
Centre for Economic development, Transport and Environment Southern Ostrobothnia

Uppsala December 2025

Contents

ABBREVIATIONS & ACRONYMS

EMODnet – European Marine Observation and Data Network system

Ga – Billions of years

GTK – Geological Survey of Finland

HAV - Swedish Agency for Marine and Water Management

HELCOM – Helsinki Convention

HELCOM HUB – HELCOM Underwater Biotope and Habitat Classification

LOI – Loss on Ignition

Ma – Millions of years ago

MBES – Multibeam echosounder

MDPS - Meridata data processing and interpretation software

PSA – Particle Size Analysis

RTK – Real Time Kinematic positioning system

R/V – Research Vessel

SAV – Submerged aquatic vegetation

SBP – Sub-bottom profiler

SGU – Geological Survey of Sweden

SLU - Environment at the Swedish University of Agricultural Sciences

S/V – Sailing vessel

SVP – Sound velocity profiler

Abstract

The Gulf of Bothnia contains ecologically important marine environments that are undergoing rapid environmental changes driven by climate change, tectonic uplift processes and increasing human pressure. Detailed baseline information is needed to carry out effective marine spatial planning and habitat conservation. This document details the results of an Interreg Aurora funded, joint Finnish - Swedish seabed mapping project across the shallow water areas in the Gulf of Bothnia for the purpose of producing high resolution geological and habitat maps needed for environmental management. The project conducted intensive seabed mapping surveys that utilized acoustic instruments, i.e., multibeam echosounders, sub-bottom profiling and reflection seismic sounding, together with underwater video observations and sediment sampling to characterize both surface and subsurface seabed conditions. In addition, satellite and airborne drone imagery was also utilized to determine seabed conditions in shallow water areas. The survey results were used as inputs to the predictive modeling process that used advanced AI and machine learning techniques to create sediment and habitat distribution maps. Together, these approaches provided a robust foundation for understanding spatial patterns in sediment composition and benthic habitats, while also offering a reproducible workflow that can be applied in future marine mapping initiatives. These map product outputs were standardized with the requirements of HELCOM and EMODnet, to allow for its submission to these broader, European and regional mapping initiatives. Finally, this project highlights the benefits of cross-border cooperation, such as sharing of methodologies, datasets and modelling approaches that foster harmonization of mapping standards and conservation strategies across the Gulf of Bothnia.

1. Introduction

The shallow coastal areas of the northern Gulf of Bothnia, the Baltic Sea, are undergoing rapid environmental change driven by climate change, post-glacial land uplift, shifting sediment dynamics, and increasing human use. Despite their ecological and societal importance, these coastal zones in Finland and in Västerbotten and Norrbotten in Sweden remain poorly mapped, especially with respect to seabed substrate types, seabed morphology, and benthic habitats. This lack of detailed information limits Finland's and Sweden's ability to carry out effective marine spatial planning, evaluate environmental status, and meet national and EU requirements for coastal monitoring and habitat protection.

To address these gaps, the Geological Survey of Finland (GTK) and the Geological Survey of Sweden (SGU) conducted targeted seabed mapping mission in 2023–2025 across representative shallow-water areas, six in Finland and three in Sweden. The purpose of this work is to:

1. **Produce high-resolution geological and habitat maps** for previously unmapped or sparsely surveyed near-shore areas,
2. **Support environmental management**, including identification of sensitive substrates, vulnerable habitats, and areas at risk from coastal development, and
3. **Develop and test a consistent mapping workflow** that integrates hydroacoustic data, ground-truth sampling, and machine-learning modelling.

The surveys combined multibeam bathymetry, backscatter, sub-bottom profiling and reflection seismic sounding with underwater video observations and sediment sampling to characterize both surface and subsurface seabed conditions. In addition, satellite and airborne drone imagery was also utilized to determine seabed conditions in shallow water areas. These datasets were then processed and used as inputs to a modelling framework designed to generate spatially explicit predictions of substrate and habitat types. In addition, satellite and airborne drone derived data were used in the analysis.

This report presents the field methods, data processing procedures, interpretation and modelling workflow used to produce these maps, providing a transparent and reproducible basis for future SGU and GTK coastal mapping efforts.

1.1. Geological background

The Gulf of Bothnia, a shallow brackish-water basin, represents the northernmost part of the Baltic Sea. Its geological history is closely linked to

that of Finland and Sweden, reflecting their shared proximity and extensive coastlines along the Baltic Sea.

The Gulf of Bothnia occupies a depression within the Fennoscandian Shield. Bedrock along the Swedish and Finnish coasts is largely similar, consisting predominantly of Precambrian crystalline rocks that form the ancient basement of both countries. In the Swedish coast gneiss dominates terrestrial areas near the project sites along the Swedish coastline (Ahlberg, 1986; Berggrund 1:50 000–250 000, 2025). In the Finnish coast Granite and granodiorite are the primary rock types (Koistinen et al., 2001).

In the central parts of the Bothnian Sea and Bothnian Bay, crystalline bedrock is overlain by younger sedimentary rocks—such as limestone and sandstone—that tend to smooth seabed topography. These sedimentary units include deposits from the Proterozoic Ectasian period (ca. 1.4–1.2 Ga), such as the Muhos Formation near Oulu and the Satakunta region, occasionally covered by younger Ediacaran strata (ca. 635 Ma).

The basin's morphology reflects repeated glacial advances and subsequent deglaciation during the Pleistocene and Holocene. The retreat of the Fennoscandian Ice Sheet exposed the Gulf of Bothnia last within the Baltic Sea basin, leaving extensive glacial deposits and triggering rapid isostatic rebound—a process that continues today. And at the same time making it one of the youngest marine regions on Earth.

The Swedish coastline exhibits diverse coastal types, ranging from mainland shores in southern Sweden to fjord and archipelago coasts extending through the Baltic Proper into the Gulf of Bothnia (Schiewer, 2008). In the Swedish coast the seabed slopes steeply and is more fragmented. In the Finnish side the coast is gentler, with a flat and gradually deepening profile.

Overall, the Gulf of Bothnia is characterized by a gently sloping eastern side and a sharply deepening western side.

In the Bothnian Bay, land uplift reaches up to 10 mm yr^{-1} (Ekman, 1996; Kakkuri, 2012). Accounting for global sea-level rise, the effective relative uplift rate is approximately 7–9 mm yr^{-1} (Poutanen & Steffen, 2014). Under mid-range climate scenarios, this differential suggests a projected relative sea-level decline of about 0.35 m during the 21st century (Grinsted, 2015).

Postglacial development involved alternating freshwater and brackish phases, driven by fluctuations in water level, salinity, and land uplift. These changes influenced sedimentation patterns, ranging from varved clays to organic-rich muds. Today, the Gulf of Bothnia is marked by low salinity, substantial river input, and ongoing land uplift—creating a dynamic environment where geological processes remain active.

Seafloor conditions vary significantly across the basin. Exposed bottoms composed of coarse material are more affected by wave energy and bottom currents than areas with finer substrates (Hjulström, 1935). Sheltered zones accumulate fine sediments, whereas exposed areas experience erosion and transport of finer material.

2. Methods

2.1. Field surveys

The geological surveys at the study areas were executed in the summers of 2023, 2024 and 2025 (GTK and SGU). The aim was to provide full-coverage bathymetry and seabed substrate data from the study/pilot areas, as well as seabed sediment samples and underwater images of the seafloor.

Seafloor geological information was obtained using various acoustic-seismic investigations, underwater video recording, and seabed sediment sampling methods. Acoustic-seismic data and sediment cores were collected onboard the Finnish research vessel R/V Geomari, the survey boat Gridi, and SGU's small research vessel S/V Ugglan. The vessels and their survey systems were continuously positioned using GPS. GTK and SGU used mainly similar but slightly different survey systems as described below. In this project, a total of nine areas were surveyed comprising six along the Finnish coast and three along the Swedish coast (Fig. 1).

Figure 1. *The SeaMoreEco project area in the Gulf of Bothnia, the northern Baltic Sea, with geological survey areas in Finland and in Sweden.*

2.1.1. Acoustic seismic surveys

GTK

GTK's data on seafloor characteristics and bathymetry was gathered employing acoustic-seismic derived shipborne methods, including sediment echo sounding, side-scan sonar, reflection seismic sounding and multibeam echo sonar (MBES) or phase differencing bathymetric sonar (PDBS).

MBES determines depth mainly by measuring the travel time of sound at known beam angles. Each transmit pulse produces several narrow beams across track, and each beam typically yields one depth point. The measured values are corrected using motion data and sound-speed profiles to produce accurate depth results. PDBS (also known as interferometric sonar) determines depth by combining travel time with arrival angles derived from phase differences between multiple receivers. This method produces many depth points across a very wide swath, but uncertainty increases directly under the vessel, and the results are more sensitive to phase errors, calibration, and sound-speed variability (Zhao et al., 2020). In practice, PDBS provides wider coverage in shallow water but generally lower depth accuracy and resolution than MBES, especially at the lower frequencies commonly used in interferometric systems.

The bathymetry data on R/V Geomari was collected with PDBS in 2023 and 2024. In 2025 MBES was installed, and it replaced the bathymetric sounding system. On R/V Gridi there was no bathymetric sonar in 2023. The MBES was installed in 2024.

The acoustic instruments were operated simultaneously to ensure comparability and temporal alignment of the datasets. The survey speed was 2-3 knots on R/V Gridi and approximately 5 knots with R/V Geomari. Sound velocity profiles (SVP) were measured during the survey to correct the sound velocity variations in the water column. On R/V Geomari the SVPs were measured with Teledyne Oceanscience RapidCast system and on R/V Gridi with Reson SVP 15T sound velocity probe. The used acoustic seismic devices are listed in Table 1 and Table 2.

Table 1. *Survey equipment used on R/V Geomari.*

Survey instrument	Model	Frequency [kHz]
PDBS	GeoSwath 4	125
MBES	R2Sonic 2022	170–450 / 700
Side-scan sonar	EdgeTech 4205	230/540/800
Sub bottom profiler	MD HF-Chirp	20-36
Sub bottom profiler	Massa TR-61-A LF-Chirp	3-12
Reflection seismic system	SIG Pulse S1	0.2-14

Table 2. *Survey equipment used on R/V Gridi.*

Survey instrument	Model	Frequency [kHz]
MBES	R2Sonic 2020	200–450
Side-scan sonar	Sonarbeam S150Ai	400/900
Sub bottom profiler	MD HF-Chirp	20-36
Sub bottom profiler	MASSA TR-1075D LF-Chirp	2,5-10
Reflection seismic system	C-Boom (ELMA in 2023)	0.2-1

SGU

SGU's smaller survey vessel S/V Ugglan is equipped with state-of-the-art hydroacoustic instruments which were utilized during the survey, namely, a Kongsberg EM2040C multibeam echosounder system (MBES), a Kongsberg Topas 120 sub-bottom profiler (SBP) system, and the Valeport SWiFT SVP sound velocity profiler (SVP), to measure the change in the water column sound speed and address refraction issues in the MBES. The hydroacoustic survey was undertaken at the start of the sampling period and was run following a dynamic line planning approach, where the first line of the survey started from the shallow towards the deeper portion of the survey area. This was done to account for unexpected shallow areas in the survey area. MBES and SBP were run simultaneously with a 100% overlap between the survey lines and a survey speed ranging from 3 to 4 knots to ensure a full-area coverage mapping and collecting high acoustic density data. The used acoustic seismic devices are listed in Table 3.

Table 3. *Survey equipment used on S/V Ugglan.*

Survey instrument	Model	Frequency [kHz]
MBES	Kongsberg EM2040C	300
Sub bottom profiler	Kongsberg Topas 120	Primary: 70-100 Parametric: 2-30
Sound velocity profiler	Valeport SWiFT SVP	

2.1.2. Seabed sampling

GTK

All the sampling locations on R/V Geomari were first filmed with a drop camera. The sediment sampler was chosen based on the seabed substrate seen in the video. If the seabed substrate seemed too hard or rocky for sampling, only a video was taken.

The sediment samples were collected after the acoustic seismic surveys based on the profiles. The main purpose of the sampling was to support the geological interpretation. From areas with soft recent mud, longer samples were collected to date the sediment layers and to determine the sedimentation rate.

In 2025 in Lapuanjoki area the sampling sites were determined by using The Sampling Toolbox developed by SGU.

On R/V Geomari, a Gemax sampler was used to collect sediment cores up to 70 cm in length. Surface sediment samples, with a maximum depth of 20 cm, were collected using an Ekman box corer and a Van Veen grab. On Gridi, a Kajak sampler was used to obtain cores up to 50 cm long, while a Ponar grab sampler was employed for samples up to 10 cm deep. The longer cores

collected with the Gemax and Kajak samplers were sectioned into 1 cm sub-samples.

SGU

Seabed sampling was executed following the hydroacoustic survey to collect sediment samples and to ground-truth (verify by physical samples and observations) the geophysical data. The results from sampling were not only used to verify but also to modify the interpretation of hydroacoustic and modelled data. These samples were the only verification of the sediment condition in the seabed, and thus, interpretation of the hydroacoustic data should conform with the results from the seabed sampling.

The sampling site locations for the ground truthing were identified using the SGU developed ArcGIS (v. 3.1) sampling toolbox, which utilized the interpreted hydroacoustic data to generate sampling locations across the three study areas. The Sampling Toolbox consisted of two main components. The first component involved preprocessing the source data. In this component, input raster datasets such as bathymetry and backscatter were processed to produce a combined, classified raster layer through a series of statistical and geospatial operations. The workflow generated grids of Bathymetric Position Index (BPI), standardized BPIs, slope, and terrain ruggedness, which collectively describe seafloor morphology and variability. Additionally, the toolbox included two terrain classification tools that produced zone and structure classifications, allowing users to define and analyze spatial relationships between geomorphological features. The second component, the final sampling modeling, was where the classified raster outputs generated during the first component were used to create sampling points and corresponding sampling area polygons. The model applied probabilistic sampling methods, including random and stratified random sampling, to ensure statistically representative coverage of the study area based on the spatial distribution of depth and backscatter characteristics.

The tool also allows users to define key parameters during the process, such as the number or percentage of samples, minimum distance between sampling points, and distance from area boundaries. The tool then automatically generates the sampling points within the specified extent and produces corresponding shapefiles for both points and sampling polygons. This second component ensures that the sampling design is spatially balanced and reproducible, providing a statistically sound basis for ground-truthing and subsequent field validation.

Sediment samples were collected with a Van Veen grab sampler (Fig. 2B), while underwater video surveys were carried out to record benthic habitats and biological features at identified sampling locations. At each identified sampling site, the seafloor was filmed in transects using either SubC Imaging Rayfin Mk2 Coastal (Fig. 2A), GoPro Hero 12 Black (Fig. 2C) or a Chasing M2 ROV as drop-cameras (Fig. 2D). Evaluating the bottom type from the video

was essential in order to avoid damaging the substrate sampler. The specific sampler used in this project is suitable for fine sediments such as mud or loose silt, and sand in some cases. If the bottom type was identified as gravel or coarser, the sampler risked being damaged and no samples were taken in such substrates.

During the fieldwork in 2023 and 2024, positions of underwater video and substrate samples were logged using Ugglan's RTK (Real Time Kinematic) positioning system which has centimeter-level accuracy. Ugglan was not available for the 2025 field season and led to the use of a handheld Bad Elf GPS connected to an iPad mini gen 5, which has a meter-level accuracy.

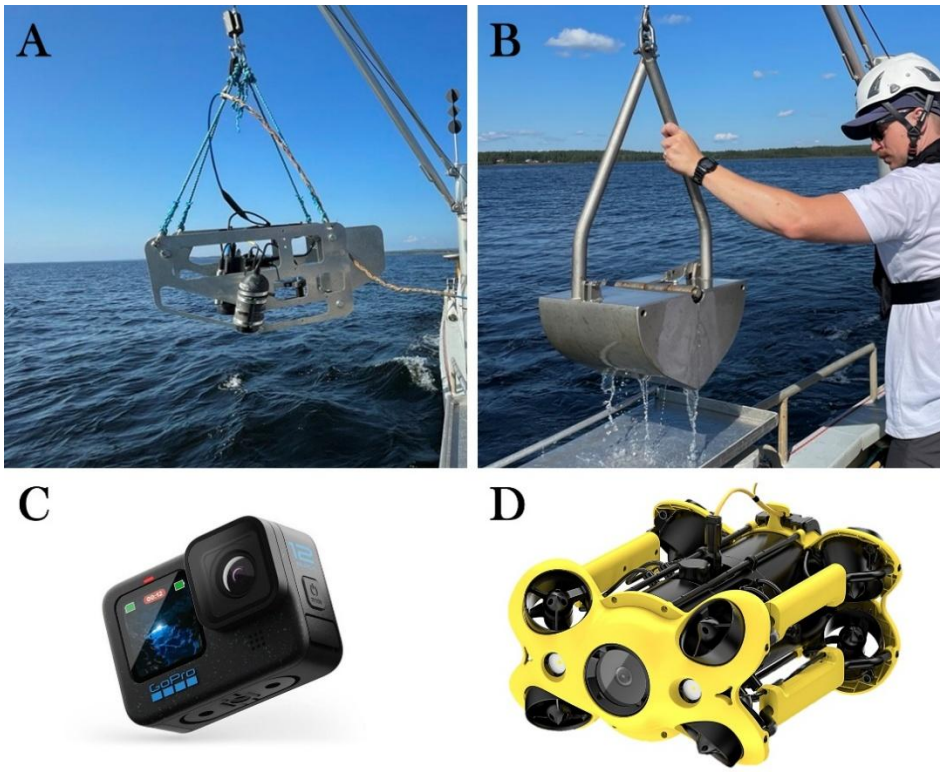

Figure 1. *Collage of the sampling equipment used by SGU: A) SubC Imaging Rayfin Mk2 Coastal with a custom camera sled designed by SGU, B) Van Veen grab sampler, C) GoPro Hero 12 Black (image curtesy: GoPro), D) Chasing M2 ROV (image curtesy: Chasing).*

2.1.3. Airborne drone imaging

GTK's UAV imaging data was collected with DJI Mavic 3 Multispectral drone in 2024. Flights were performed at altitude of 120 m, speed of 10 m/s and with 75 % vertical and horizontal overlap. Camera gimbal angle was modified 10-15 degrees from orthogonal to reduce sun reflectance from the water surface in the images. Flight direction was fixed to a set angle so that the drone was always facing away from the sun.

2.2. Data processing

2.2.1. Shipborne acoustic-seismic data

GTK

The Finnish bathymetry data collected with PDBS was collected and processed with Hypack, while the MBES data was collected and processed with Meridata data processing and interpretation software (MDPS). Bathymetry models were interpolated from the point cloud data. Final depth data will be provided as a 25 m resolution raster.

The bathymetry models of the shallowest areas surveyed by Gridi in 2023 were interpolated from the HF-Chirp profiles that include point-based depth information of the seabed surface. The point distance is 5 meters. This depth model does not allow for very detailed features to be distinguished, but it provides a general overview of the seabed contours. In 2024 there were also some issues with the PDBS system, thus the bathymetry model from Kalajoki collected with R/V Geomari is also produced using only the HF-Chirp profiles.

SGU

MBES data files (i.e., *.all files) were processed using software from QPS (www.qps.nl). The files were imported into both Qimera, to extract bathymetry, and FMGT software to extract the backscatter. In both datasets, data processing involved extensive data cleaning using different processing techniques to remove artifacts and produce the final data products. These are then exported to a generic raster format where it was used to extract secondary derivatives for the modelling (Fig. 3).

Bathymetry and backscatter were the primary products derived from MBES. Bathymetry records the changes in depth over the study area by measuring the travel time of acoustic signal, while backscatter records the strength of the acoustic signal returning from the surface of the seabed to the receiver mounted on the vessel. Backscatter can indicate the “hardness” or “softness” of the sediment being ensonified. Additional “secondary” derivatives are then extracted from these two datasets using additional software namely, ArcGIS, ENVI and R. These additional secondary datasets serve as predictor variables for use in the modelling process and are described in detail in Table 4.

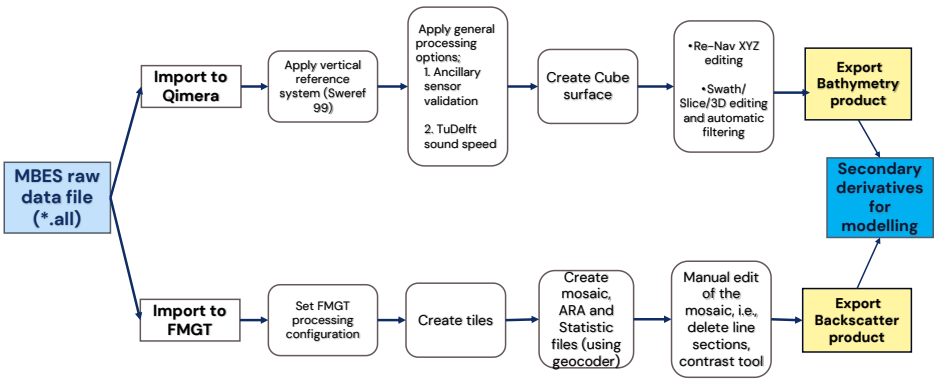

Figure 2. *Geophysical data processing workflow.*

The sub-bottom profile data was processed using MDPS software. The features used for interpreting the characteristics and defining the boundaries between different sedimentary units are reflectors, which are interpreted lines lying parallel to the seafloor. The sub-bottom-profiles are displayed in grayscale colours with dark grey to black colours implying a strong signal and a hard sediment, while a weak signal is lighter grey to almost white indicating a soft sediment. The top-most reflector, usually the strongest, represents the seafloor. The characteristic of this reflector gives an indication of the type of sediment found in the seabed surface, with "rugged" reflector indicating an uneven seabed surface that could be scattered with stones or boulders. The matrix of a reflector unit with internal reflectors, point reflectors, hyperbola etc. indicates the geological composition of the unit. Hyperbola for instance indicates possible stones in a matrix of softer sediments, such as clay or silt. An internal reflector which meets an overlaying reflector at an angle indicates an erosive phase in the sedimentary sequence. The maps produced based on the sub-bottom interpretations also take into account the substrate samples, bathymetry and backscatter in order to validate the interpreted seafloor type from the SBP.

2.2.2. Sediment analysis

GTK

Dating of surface sediment cores and estimation of recent sedimentation rates were based on radionuclide 137Cs, which serves as a time marker in the sediment column (e.g., Kankaanpää et al. 1997; Meili et al. 1998; Mattila et al. 2006; Ilus 2007; Zaborska et al. 2014; Moros et al. 2017; Kotilainen et al. 2021). In undisturbed, non-bioturbated Baltic Sea sediments, the sharp increase in 137Cs activity corresponds to fallout from the Chernobyl nuclear power plant accident in April 1986. Measurements of 137Cs activity in fresh subsamples were conducted at the Geological Survey of Finland using an EG&G Ortec ACE™-2K gamma spectrometer equipped with a four-inch NaI(Tl) detector, with a counting time of 60 minutes.

Grain size distribution of the sediments was determined using sieving and Sedigraph analysis. For the chemical analysis of environmentally harmful

substances (e.g., heavy metals), several analytical techniques were applied, including ICP-MS, ICP-OES, and Leco (C, N, S). In the laboratory, samples were first weighed for wet weight, freeze-dried, and re-weighed for dry weight. All samples were sieved to <2 mm to remove coarse material such as plant and animal remains and Fe–Mn concretions. Subsamples from different depths of all cores were analysed for carbon and nitrogen using a Leco CHN-600 instrument. For elemental analysis, the samples were treated with a hydrofluoric acid–perchloric acid leach, and element concentrations were determined using either inductively coupled plasma mass spectrometry (ICP-MS) or inductively coupled plasma optical emission spectroscopy (ICP-OES), depending on the target element. Mercury concentrations were measured using an Hg-analyser with pyrolytic extraction (US EPA Method 7473). All laboratory analyses were carried out at Eurofins Environment Testing Finland Oy, Jyväskylä, Finland.

SGU

A total of 316 sampling site locations from the three different study areas were investigated using underwater videos. Results as seen from underwater videos determine the sediment conditions of the seabed. In locations with soft sediments, sediment samples were collected using Van veen grab samplers. Sediment samples were collected from a total of 170 sites, of which 37 of these were retrained and delivered for loss on ignition (LOI) analysis and particle size analysis (PSA), using the PARIO analysis method, to the Department of Soil and Environment at the Swedish University of Agricultural Sciences (SLU). PARIO-analysis is a method based on the sedimentation of dispersed particles in suspension. The result of this method is categorized according to the German classification system KA 5 (Boden, 2005). Samples that were not sent in for analysis were interpreted by experienced geologists in the field. This was done by physical examination the sediment and estimating the approximate grainsize, consistency, sorting, color, redox-state, texture, genesis and age. The grainsize classification that SGU uses adhere to the Swedish Geotechnical Society classification of soils and sediment (SGF, 2016).

2.2.3. Video analysis (SGU)

Analysis of videos were done after the field sampling to estimate the percentage cover of both sediment and biological classes in the seabed. The length of the videos at each site ranged from approximately 1 - 2 minutes, representing a transect that is estimated to cover 5 m^2 of seafloor. For each video, the percentage cover (%) of different sediment types and biological species observed, were estimated. This protocol followed the recommendation stated in the visual observation's guideline manual developed by HAV (HAV, 2017).

2.2.4. Drone images (GTK)

The collected RGB images were processed into orthomosaics with Agisoft metashape software following Over et al. (2021). Orthomosaics were further processed with ArcGIS Pro segmentation tool using ground truth data and classified into areas depending on vegetation coverage. As a result, a map was created with classified areas containing vegetation and without vegetation (i.e. bare sea floor) and rocks.

2.2.5. Satellite data (GTK)

Sentinel-2 satellite data was used for shallow shore bathymetry estimation and substrate mapping. Satellite images were obtained from "Copernicus browser" -service provided by European Space Agency (ESA).

Satellite bathymetry estimation –method (Kulha et al. 2024) compares multi-temporal derivatives of images with in-situ measurements of water depth. Visible light channels red, green, blue and coastal aerosol from Sentinel-2 images were used in varying combinations to reach optimal results in each of the six study sites.

Substrate mapping

Substrate mapping was done following partly the methodological framework established by Huber et al. (2022). Substrate mapping was done only for Kalajoki area as it was the only site for which background data (both, drone surveys and ground truth data) was available. A map was created with three classes: 1) areas containing vegetation and 2) without vegetation and 3) optically deep areas. The data was processed with SNAP - ESA Sentinel Application Platform v 11.0.0, http://step.esa.int and Sen2Coral Toolbox v 2.0.0 http://step.esa.in. S2 Level 2A data was used. All bands were resampled to spatial resolution of 10 m × 10 m. Water areas were masked using the scene classification algorithm run by ESA. Sun glint correction was tested using the Sen2Coral Deglint processor; however, this did not yield any notable improvement in the quality of the results. Spatial datasets were processed, and substrate maps were generated using ArcGIS Desktop version 10.8.2.

Drone surveys were done in early July 2024, covering both the harbour and wetland areas in Kalajoki. A substrate classification was done for the wetland site. In addition, ground truth data sampling was carried out in 2023 and 2024 by Centre for Economic development, Transport and Environment Northern Ostrobothnia.

Cloud-free Sentinel-2 L2A True color images from Kalajoki 05 - 09/2024 are in the Figure 4. Influence of river Kalajoki in the eastern part can be seen in all images. Satellite imagery was sorted to achieve the best possible temporal correspondence with the drone surveys and ground truth collecting dates and good quality. Image selected for further processing was 2024-08-17.

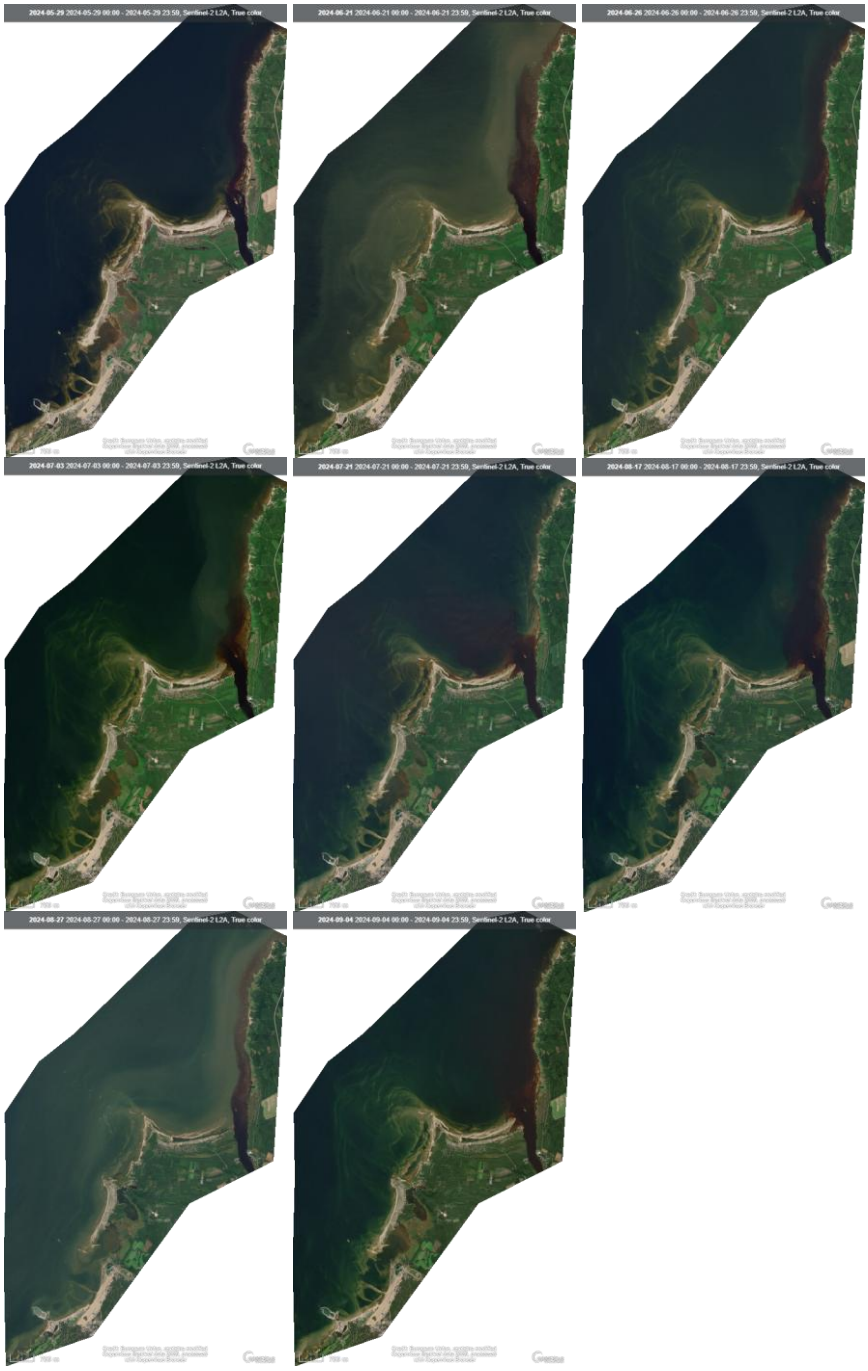

Figure 4. *Sentinel-2 L2A True color images from Kalajoki 05 - 09/2024. Contains modified Copernicus Sentinel Data 2025, processed with Copernicus Browser.*

Satellite-derived bathymetry was used to mask shallow coast (<6 m depth). Sen2coral Depth Invariant Indices processor (water column correction) was used to produce depth invariant bands from pairs of image bands.

Substrate mapping was done using a supervised classification approach, employing the maximum likelihood algorithm to delineate classes. Ground truth data along with Kalajoki harbor drone survey imagery, were used to

generate training vectors representing vegetated and unvegetated bottom and optically deep-water areas.

2.3. Geological interpretations

GTK's geological maps were generated based on sediment core analysis, manual interpretation of the acoustic-seismic profiles and the acoustic properties of the seabed substrates. The theoretical vertical resolution of the HF- and LF-Chirp sub-bottom profilers is 20–30 cm, so surface sediment units thinner than 30 cm were excluded from interpretation.

Nine different geological units were interpreted: bedrock, till, mixed glacial outwash, glaciofluvial sand/gravel, glacial clay, post-glacial clay, brackish-water mud, recent mud, and erosional secondary sand. These defined units are modified from Virtasalo et al. (2014) classification. Additionally, dredged material was distinguished as its own separate class. Meridata MDPS software was used to digitize boundaries between different geological units in the profiles. The gaps between the profiles were interpreted and interpolated using orthomosaics, bathymetric data, and side-scan images, which provided broader coverage along the survey line.

2.4. Modeling process (SGU)

This section describes the modeling process, where each step undertaken in the substrate and habitat modeling workflow is defined. The modelling approach used in this project was structured to ensure flexibility and consistency across different classification schemes with a goal to generate spatially explicit predictions of substrate composition and habitat types by integrating observed biological and sediment data with a suite of environmental predictors. The modeling process used eXtream Gradient Boosting (XGBoost) algorithm (Chen & Guestrin, 2016) in the Caret package (Kuhn, 2008) as deployed in an R programming environment (R Core Team, 2024). The process involved the following general steps; data preparation, model training and testing and selecting relevant predictor variables, the production of final classified and continuous maps, and finally accuracy assessment (Fig. 5).

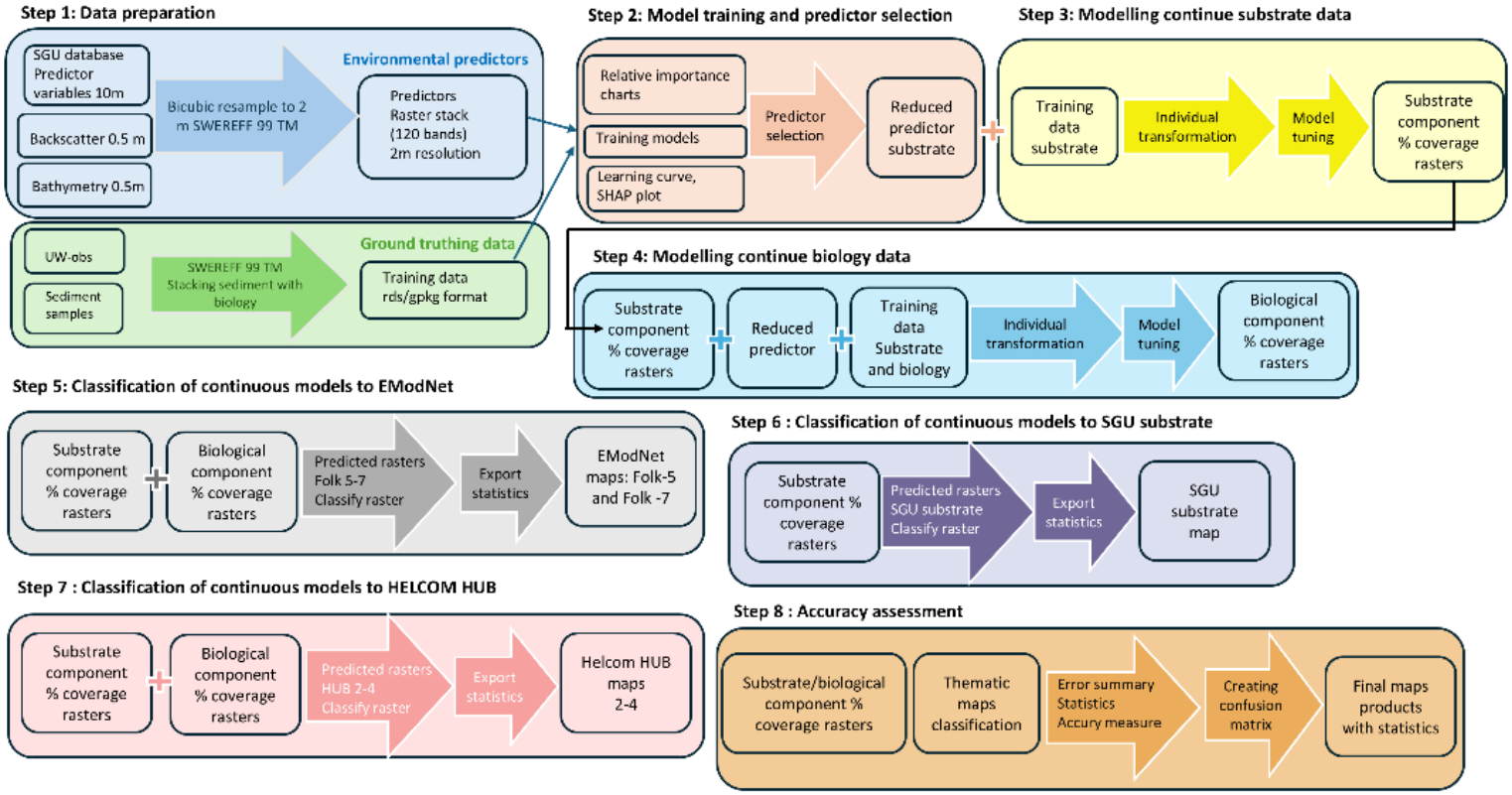

Figure 5. *Workflow flowchart that highlights the steps taken throughout the modeling process.*

2.4.1. Data preparation

Data preparation involves selecting spatial predictor variables that could affect or help predict the spatial distribution of the modeled parameter, i.e., the seafloor substrate and biological distribution. In this study, the predictor variables came from a variety of sources that included outputs from field studies, secondary (derived) variables, and spatial variables incorporated from SGU's machine learning database. A list of these spatial variables and their description is shown in Table 4.

Bathymetry and Backscatter outputs from geophysical surveys were used as primary predictor variables to further generate other statistical and geometrical predictors of the seafloor. This was done by analyzing them using Object-Based Image Analysis (OBIA) segmentation and edge detection algorithms using eCognition in ENVI software. The same method has been successfully applied in several marine habitat mapping studies in Baltic Sea (Kågesten et al., 2020; Janowski, et al., 2021). Outputs from this analysis were then spatially reduced using Principal Component Analysis (PCA) to capture only significant variances in the data. Additionally, another secondary derivative, Bathymetric Position Index (BPI), was computed using the Benthic Terrain Modeler (Walbridge et al. 2018). BPI belongs to a suite of morphometrics that are used to describe seafloor morphological characteristics.

Some predictor variables were sourced from the national-scale environmental dataset collated by SGU. These predictors, originally at a 10-meter resolution, were resampled to 2x2 meters to align with high-resolution input data. The predictor groups that were taken from the national data cube include morphology, photosynthesis, physical chemistry, wave action, geographic position (latitude and longitude), anthropogenic disturbance, RGB satellite mosaics, sedimentation rate, and substrate-related variables, which are described in Table 4.

Finally, all variables were standardized by ensuring that all their spatial parameters were consistent. This was done by cropping all variables to a raster mask, setting a uniform 2x2 meter grid, projecting to SWEREF99 TM, and finally, exporting the raster in Geotiff format. The raster files were then stacked into a single multi-band raster to verify their spatial uniformity in both extent and resolution. Ground validation points from interpreted field data were superimposed on the raster stack to extract values for each variable at each validation point. This procedure established a direct linkage between observed substrate characteristics and underlying environmental gradients, resulting in an integrated dataset suitable for model training and validation.

Table 4. *Predictor variables used for substrate and habitat distribution modeling. Predictor groups, individual variables, and their descriptions are listed.*

Predictor Group	Morphology	Photosynthesis	Physical Chemistry	Wave Action	Geographic Position	Anthropogenic Disturbance	RGB Satellite Mosaics
Variables	1. BPI (5 m) 2. BPI (20 m) 3. BPI (100 m) 4. Composite BPI 5. Negative openness 6. Positive openness	1. Chlorophyll concentration (warm temperature) 2. Light at seabed 3. Secchi depth gradient 4. Secchi depth mean	1. Bottom salinity (cold) 2. Bottom salinity (warm) 3. Surface salinity 4. Dissolved oxygen at seabed 5. Ice cover 6. Phosphate concentration (warm)	1. Surface water movement 2. Water movement	1. Latitude 2. Longitude	1. Total disturbance 2. Average disturbance (150 m radius) 3. Sum of disturbances (150 m radius) 4. Dredging 5. Trawling	1. Band 2 (Sentinel-2) 2. Band 3 (Sentinel-2) 3. Band 4 (Sentinel-2)
Description / Notes	Seafloor shape, terrain enclosure, and exposure; captures fine- and broad-scale morphological features	Light availability and photosynthetic activity; Secchi depth measures water transparency	Chemical environment of water column affecting benthic habitats	Hydrodynamic forces shaping seabed and influencing habitat distribution	Spatial context for integrating environmental variables	Captures human impacts on seabed habitats	High-resolution visual information of seabed surface

Table 4. *Continuation.*

Predictor Group	Sedimentation Rate	Substrate-related Variables	Observation Data	OBIA Derived	Backscatter Derived	Depth Derived
Variables	1. Sediment accumulation over time	1. Hardness 2. Total soft-bottom coverage 3. Organic mud 4. Benthic predator layers	1. Bathymetry 2. Backscatter 3. Track line uncertainty	1. PCA-Backscatter 1 2. PCA-Backscatter 2 3. PCA-Backscatter 3 4. PCA-Backscatter 4 5. PCA-depth 1 6. PCA-depth 2 7. PCA-depth 3 8. PCA-depth 4	1. Characterization 2. Distance 3. Gradient 4. Grazing angle 5. Impedance 6. Intercept 7. Kurtosis 8. M3 9. M4 10. Max 11. Mean 12. Minimum 13. Mode 14. Phi 15. Quartile range 16. Roughness 17. Standard deviation 18. Skewness	1. Aspect 2. Roughness 3. Rugosity 4. Segment 5. Slope 6. TRI (Terrain Ruggedness Index)
Description / Notes	Influences benthic habitat structure and dynamics	Composition, texture, and distribution of seafloor materials	Provides additional seafloor characteristics and data reliability	OBIA-based principal components derived from high-resolution hydroacoustic data	Statistical and geometric descriptors derived from backscatter data	Depth-derived terrain features capturing seabed complexity

2.4.2. Model training and testing and selecting relevant predictor variables

Model training and testing were done using the CARET package in R. The comprehensive set of predictor variables were fed into the model using an iterative selection procedure to identify the most influential variables. Predictor importance was evaluated using Gain, Cover and Frequency system. Initially all predictors were fed in the training process to identify the relative importance matrix. Using this initial pool of predictors, any predictors that were neither physically nor biologically relevant to a targeted response variable was removed from the predictor set. Only the top-ranked predictors, i.e., the predictor variables that contribute most to the model, were retained for final model training run while the other predictors were disregarded. Results of the analysis are shown in (Fig. 6).

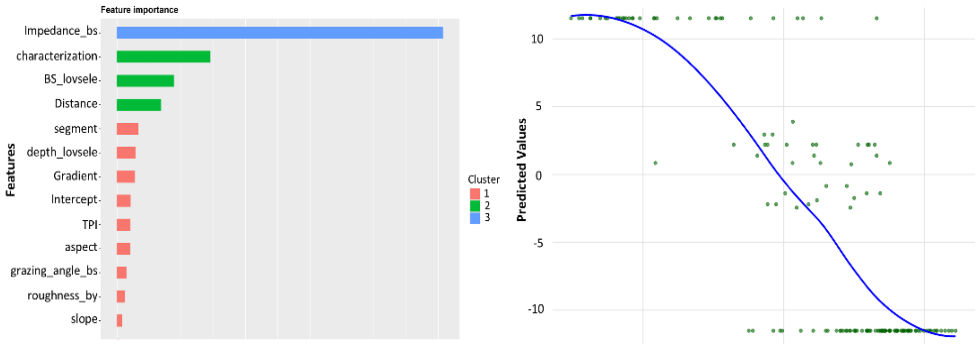

Figure 6. *The result of training process to determine the relative importance of predictor variables as an example. The left panel shows the top best predictors that have a relationship with returning clay sediments in Lövsele area. The right-hand panel shows the relationship between clay in the x-axis and impedance value extracted from the backscatter in the y-axis.*

Continuous substrate and biological maps of percentage coverage were then produced for each area using XGBoost algorithm via the CARET package in R. Further refinement of the algorithm function setting was done to optimize model performance by hyper-tunning the parameters and then re-running the algorithm. The hyper tunning parameters and a sample algorithm loop are provided in APPENDIX 1.

The sediment maps produced in the sediment modelling were then used as "input" predictor variables to create the biological distribution maps to account for species-substrate associations. For each of the continuous biological and sediment distribution maps that was produced, associated uncertainty layers and statistical tables were also created to show the modelling accuracy (APPENDIX 2).

2.4.3. Production of continuous and thematic maps

The continuous sediment and biological map outputs were then translated into thematic habitat maps in accordance with HELCOM HUB (Avellan, et al.,

2013) and the European Marine Observation and Data Network classification framework (Kaskela et al., 2019). The methodology employed to produce the maps ensured that the resulting maps were compatible with the established and standardized classification systems, while still providing flexibility to examine individual components in finer-scale details when required. The spatial modeling workflow used in this process generated both EMODnet Folk sediment classification maps, and the HELCOM HUB (Avellan, et al., 2013) maps based on environmental predictor data and ground-truth sediment samples.

Environmental predictor layers representing key sediment components—such as boulders, sand, clay, gravel, and pebbles—were compiled and combined into derived variables describing dominant substrate characteristics, including "rock and boulders" and "coarse substrate." The classification was performed at multiple spatial resolutions to capture sediment variation across different spatial scales. Using established threshold criteria from the EMODnet Folk system, each raster cell was assigned to a sediment class according to the relative proportions of coarse, sandy, and fine material.

EMODnet Sediment Classification implemented the Folk5 classification system wherein the sediments were categorized into five principal classes (rock, coarse, mixed, muddy, and sandy sediment classes. Calculations of the area cover (in km^2) and percentage cover of each sediment class in relation to the total mapped area were undertaken to provide a quantitative measure of class dominance and spatial distribution. Classification rules were implemented using logical thresholds for sediment proportions—for instance, pixels dominated by rock and boulders were classified as "Rock and Boulders," those with ≥80% coarse fraction or ≥90% sand and ≥5% coarse fraction as "Coarse Sediment," and remaining classes according to clay, sand, and coarse substrate proportions.

HELCOM HUB maps up to level 5 classification were produced in the study using the continuous map outputs from both sediment and biological modelling as ground truth validation and predictors in the modeling process. In the HUB Level 2 (photic vs. aphotic) classification, pixels shallower than –15 m were classified as photic, while deeper as aphotic.

For HUB Level 3 (substrate classification), continuous sediment cover models were combined and reclassified into discrete thematic maps corresponding to HELCOM HUB Level 3 substrate classes. The workflow included grouping, normalization, and rule-based classification of modelled sediment layers. The maximum sediment coverage value for each pixel was first extracted to identify the dominant substrate type. Sediment components were then grouped into two main categories: Hard substrates – bedrock, boulders, and large stones and soft sediments – clay, sand, gravel, pebbles, and stones. This classification distinguished hard-bottom from soft-bottom environments, which represent major ecological divisions in benthic habitats. Within the soft sediment group, subcategories were defined as muddy, coarse, or sandy

based on the dominant fine fraction. Each pixel was then classified according to the dominant component using a hierarchical rule set: pixels with ≥90% coverage by a single substrate were assigned to that dominant class, while more heterogeneous pixels were classified as mixed sediments. The resulting raster map provided a spatially explicit classification of seabed substrate following the HELCOM HUB (2013) framework. Class statistics, including area (km^2) and percentage coverage, were calculated to quantify the extent of each substrate type.

The HUB Level 4 classification (macrofauna and macrophyte influence) refined the Level 3 substrate map by incorporating biological information on macrophyte and macrofauna cover derived from predictive models. These biological layers represented ecologically important indicators, for example: the presence and abundance of *Cladophora spp*. and *Potamogeton perfoliatus*, which were used to distinguish between vegetated and unvegetated seabed areas. The maximum predicted macrophyte coverage was calculated to identify areas with substantial vegetation. Pixels with ≥10% cover were classified as vegetated, while those with lower or no cover were assigned as sparsely vegetated or unvegetated, depending on threshold values. The classification function then combined the substrate type (HUB Level 3) with biological cover (macrophytes and sessile or infaunal fauna) to assign each pixel to a HELCOM HUB Level 4 habitat class. After classification, summary statistics were calculated for each Level 4 class, including total area (km^2) and proportional coverage (%). These were linked to an external reference table containing official HELCOM Level 4 codes and names to ensure consistent and standardized class attribution and classified further down to level 5.

2.4.4. Accuracy Assessment

Accuracy assessment workflow was developed to compile and summarize the performance metrics of previously trained models used for substrate and habitat classification. The process does not perform model training; instead, it imports the saved model objects and extracts their evaluation statistics, including confusion matrices, producer and user accuracy (PA and UA), overall accuracy (OA), kappa coefficient, and F1-score. These metrics are retrieved for each model through an automated loop based on predefined class categories, ensuring consistent handling across all model outputs. The extracted values are then merged into a unified results table, where variable names are cleaned and standardized to align with reporting conventions, and the final dataset is exported to an Excel file to facilitate further analysis, comparison across models, and inclusion in scientific reporting. After this data preparation, the actual accuracy assessment workflow for habitat mapping is implemented to calculate confusion matrices, user's and producer's accuracy, overall accuracy, Tau statistics, and export the results in multiple formats for different thematic classification systems, including HELCOM HUB Levels 2–5 and EMODNet Folk 5.

The workflow was structured to process multiple spatial resolutions, enabling evaluation of model performance at different scales, which is critical for capturing habitat heterogeneity. For each classification system and raster resolution, the workflow imports the observed vs. predicted class tables generated in earlier steps, identifies all unique classes present in the dataset, constructs confusion matrices including all possible classes, extracts diagonal elements to calculate user's and producers' accuracy, and computes overall accuracy, Tau, variance of Tau, and 95% confidence limits for Tau. Numeric class codes are replaced with descriptive names using lookup tables from external Excel files, producing labelled outputs suitable for publication-ready reporting. Results are saved in multiple formats, including Excel tables, PNG images of tables, and interactive HTML reports for each classification system and resolution, while individual outputs are compiled into organized lists for systematic storage and easy retrieval. This automated structure ensures consistent evaluation across multiple models, resolutions, and thematic classification levels, producing reproducible and transparent outputs. By integrating confusion matrix calculations, accuracy metrics, Tau statistics, labelling, and formatted exports, this workflow provides a complete, publication-ready suite of results for reporting applications.

3. Results

3.1. Surveys

GTK

Approximately 1090 km of acoustic-seismic profiles were collected across six study sites in Finland: Lapväärtti, Lohtaja, Kalajoki, Lapuanjoki, Kiiminkijoki and Iijoki, covering 76,4 km² (Fig. 7). Distance between survey lines varies from 40 to 150 meters depending on the water depth in the area. The total length of the survey lines, area coverage and depths in each study area is presented in Table 5. In addition, 84 surface sediment cores (41 box cores, 15 Gemax cores, 15 Kayak cores, and 13 van Veen grab samples) and 8 beach samples were recovered from the seafloor. Underwater videos were collected from 70 sites The surface sediment cores were used to provide information on the seabed surface substrates, sedimentation rates and distribution of harmful substances in the sediments.

Table 5. *GTK Fieldwork statistics.*

Study area	Area (km²)	Depth (m)	Survey lines (km)	Number of seabed samples
Iijoki	4,9	1,3 – 19	77	8
Kiiminkijoki	21,2	1 – 41,4	164	7
Kalajoki	13,9	1,1 – 25	216	12
Lohtajanjoki	19,8	0,7 – 15,4	277	20
Lapuanjoki	10,2	0,5 – 21,7	205	42
Lapväärtinjoki	6,4	1,6 - 13,6	81	6
Total	76,4	0,5 - 41,4	1020	95

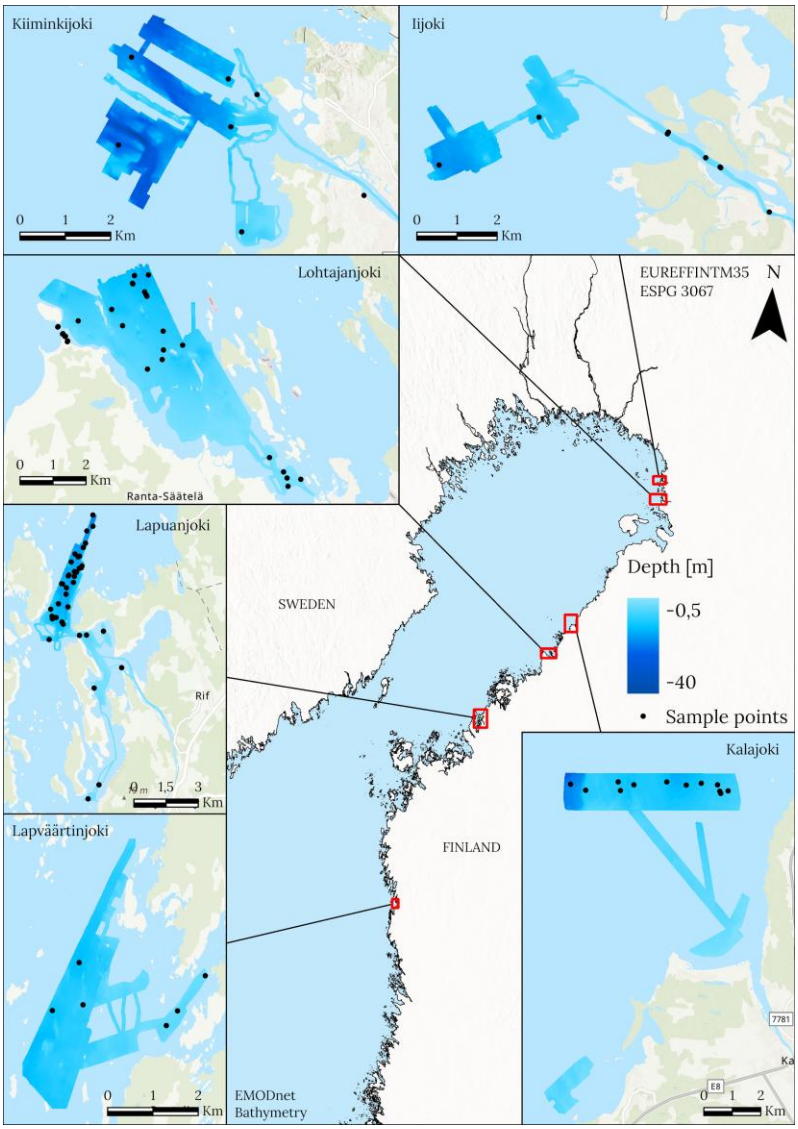

Figure 7. *Map of GTK's survey areas and sampling sites on the coast of Finland.*

SGU

The results of the field surveys are summarized in Table 6. Field survey days totalled more than four weeks that resulted in a combined survey line length of 487,2 km and produced a total surveyed area of 11.5 km^2 for the three different locations (Fig. 8). The depth measured during the survey ranged from ~1 to 14 m.

Table 6. *SGU fieldwork statistics.*

Area Working Name	Study area	Area km^2	Depth (m)	Survey lines (km)	Number of seabed samples
A	Västerbotten, Tavasten	2,5	1 – 13,7	101	50

B & D	Norrbotten, Piteå	6,9	0.7 – 11,2	288	117
C	Västerbotten, Lövsele	2,1	1,4 – 13,9	98	149
Total		11,5	0,7 – 13,9	487	316

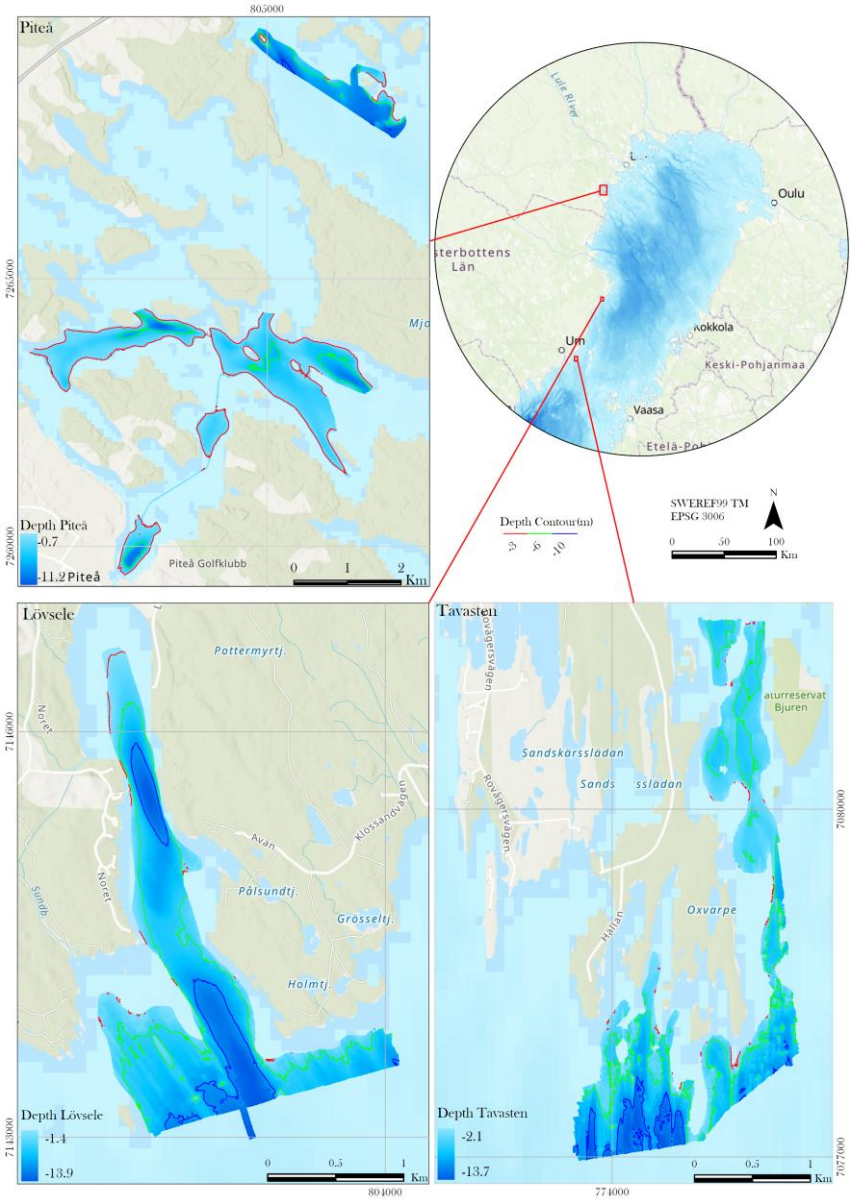

Figure 8. *Map highlighting SGU's three different survey areas. The coloured contour lines show the -3-, -6- and -10-meter depth levels.*

3.2. Geological interpretations (SGU)

The two counties' areas differ from each other, where the survey areas in Norrbotten were more sheltered from the open sea while the two areas in Västerbotten were more exposed, resulting in differences in seafloor compositions. These were particularly prevalent in southern parts of the Västerbotten survey areas, where ground validation samples revealed a coarser fraction ranging mostly from sandy-gravel to boulders distribution (Fig. 9 - Fig. 11).

APPENDIX 3 contains field data documents, extracted from SGU's sample database, of the 316 sites that were filmed and sampled where possible. On some selected sample sites, grain size analysis was conducted on sediment with low mud (gyttja) content, as indicated by the low LOI. The grain size results varied between the areas depending on the depositional environment, where Tavasten and Lövsele was dominated by sand and LOI <2% compared Piteå, with higher silt content as well as LOI up to 5.6% as can be seen in Figure 9 - Figure 11. Results from the graphs only provide grainsized classifications of the samples that were sent in for analysis. Most sites visited were not sent in for analysis such as sites having a high amount of clayey gyttja, which would show an overrepresentation of organic matter, or sites consisting mostly of rocky bottoms that were not suitable for sediment sampling.

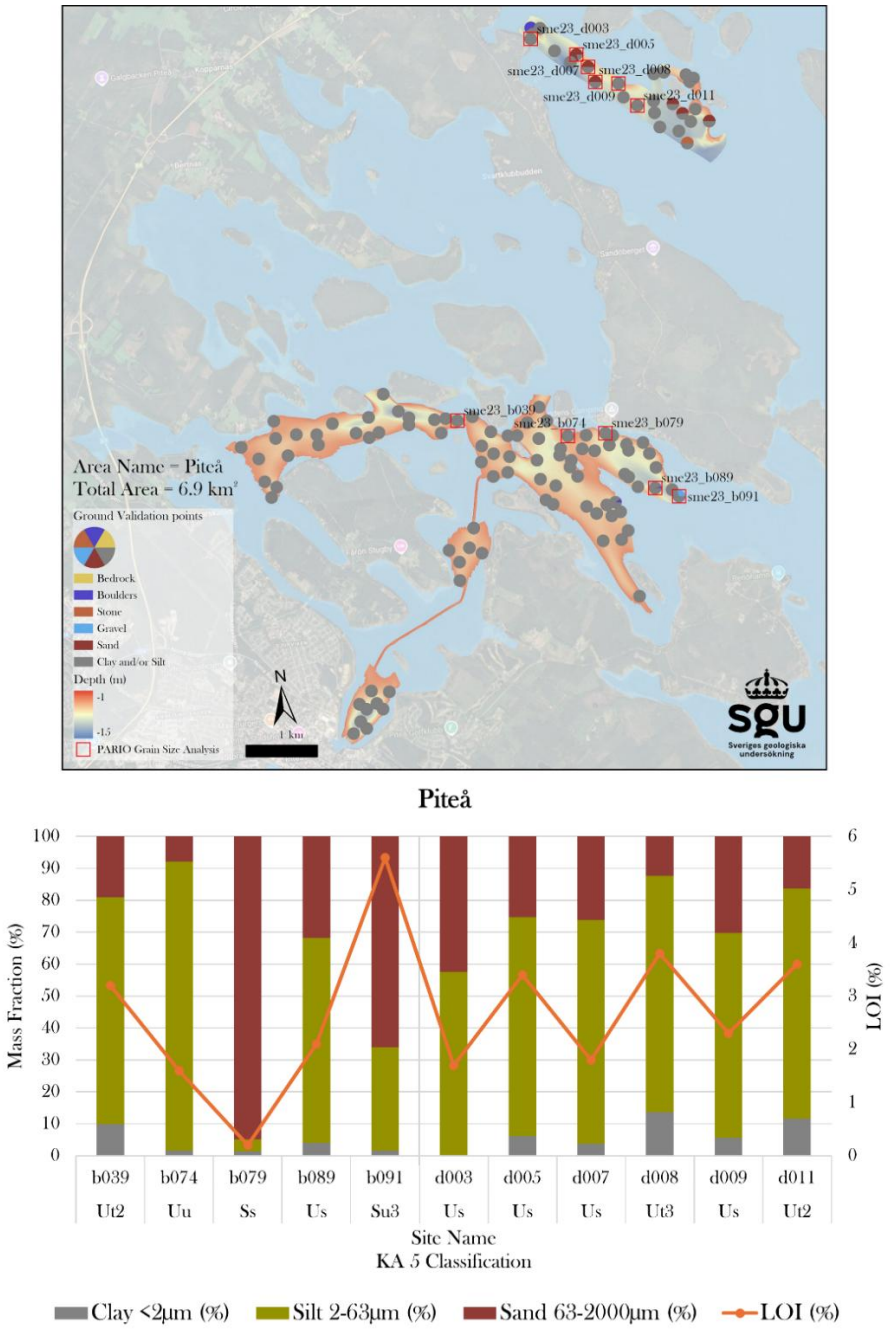

Figure 9. *Map showing the sample locations from Piteå along with a pie-chart of the interpreted substrate coverage for each site. The bar graph below shows the PARIO grainsize, along with the sample name and soil classification (Ut2 = slightly clayey silt, Uu = pure silt, Ss = pure sand, Us = sandy silt, Su3 = medium silty sand, Ut3 = medium clayey silt) according to the German classification KA 5 (Boden, 2005), as provided by SLU and LOI results from Piteå in Norrbotten. Sample sites selected for grain size analysis are marked as squares and labelled in the map.*

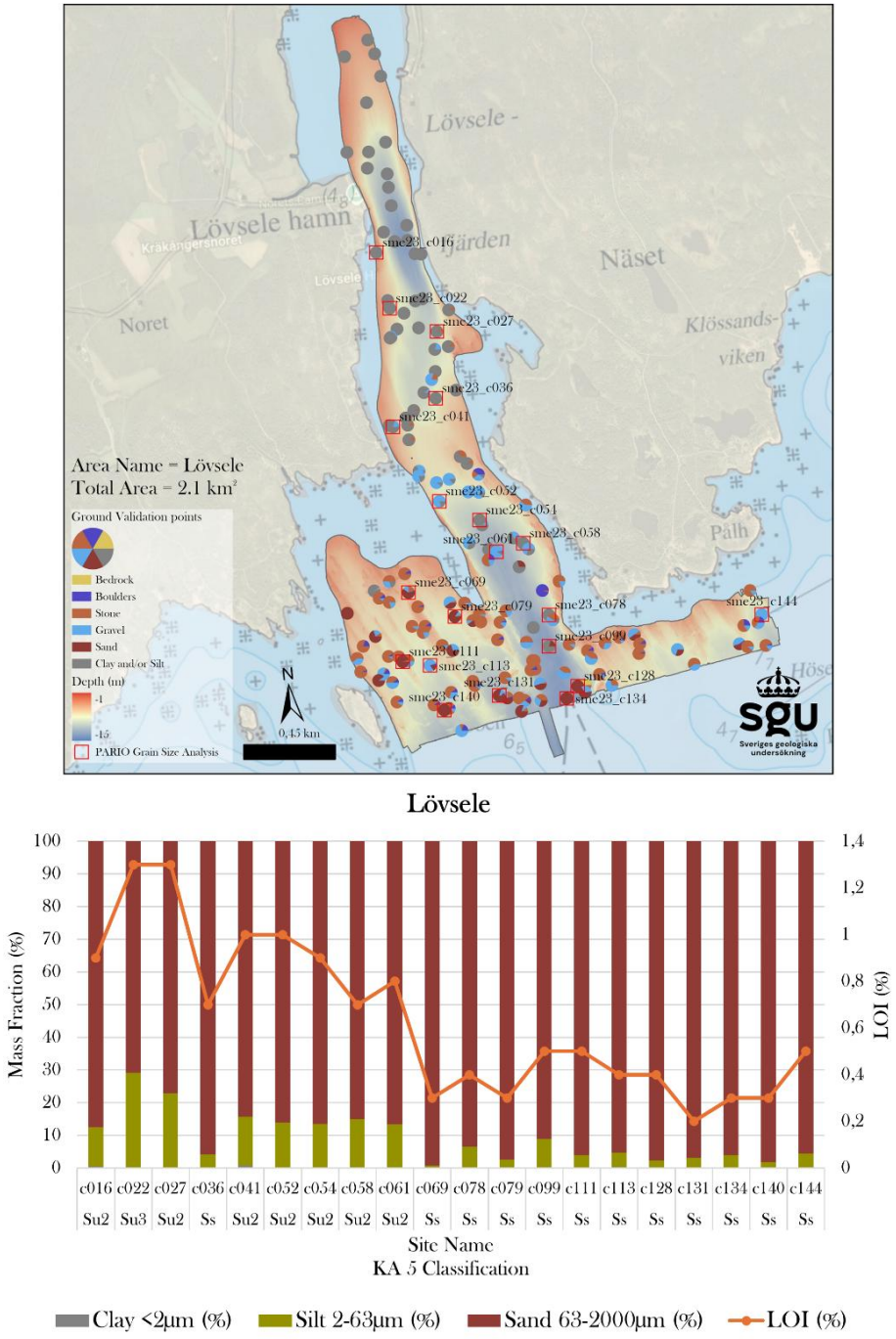

Figure 10. *Map showing the sample locations from Lövsele along with a pie-chart of the interpreted substrate coverage for each site. The bar graph below shows the PARIO grainsize, along with the sample name and soil classification (Su2 = slightly silty sand, Su3 = medium silty sand, Ss = pure sand) according to the German classification KA 5 (Boden, 2005), as provided by SLU and LOI results from Lövsele in Västerbotten. Sample sites selected for grain size analysis are marked as squares and labelled on the map.*

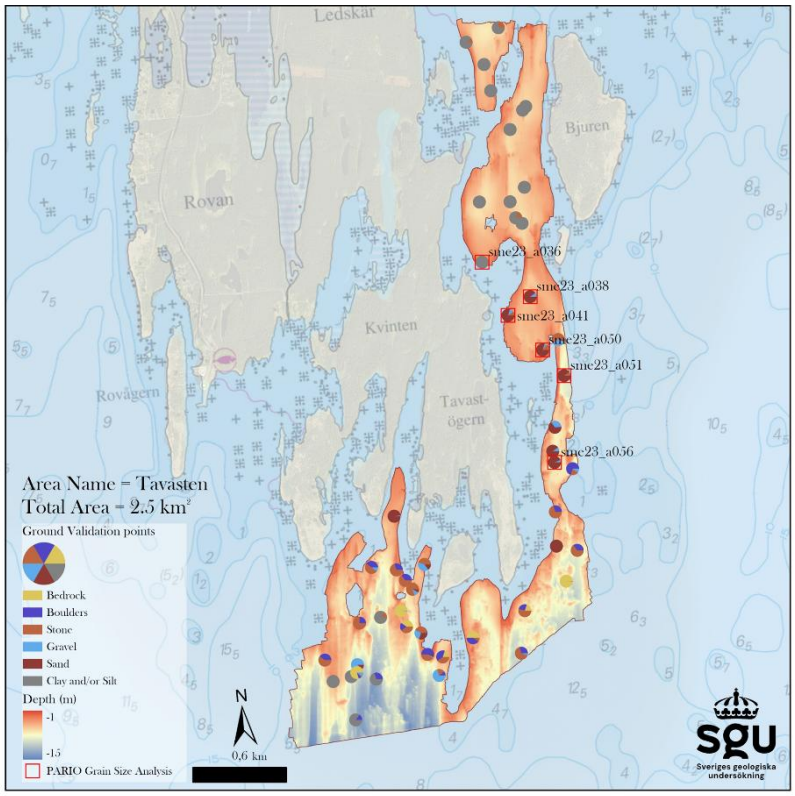

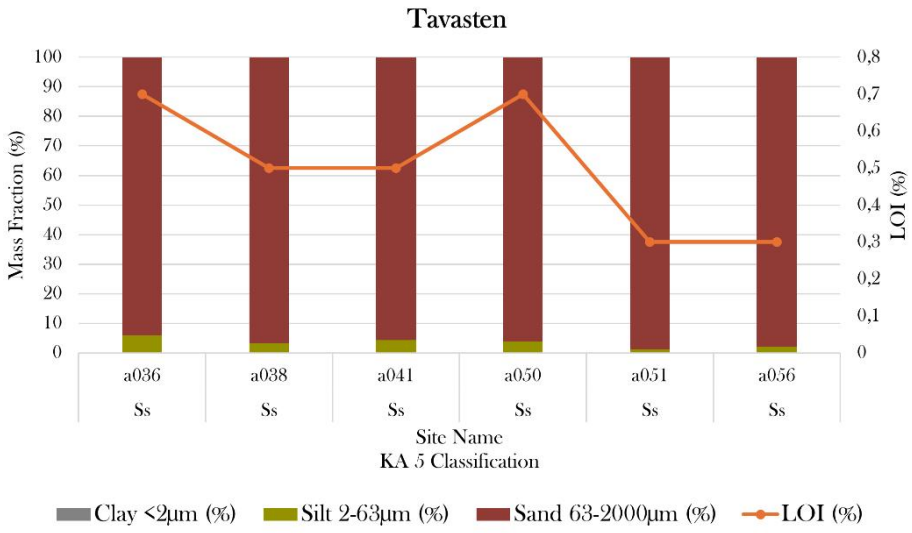

Figure 11. *Map showing the sample locations from Tavasten along with a pie-chart of the interpreted substrate coverage for each site. The bar graph below shows the PARIO grainsize, along with the sample name and soil classification (Ss = pure sand) according to the German classification KA 5 (Boden, 2005), as provided by SLU, and LOI results from Tavasten in Västerbotten. Sample sites selected for grain size analysis are marked as squares and labelled in the map.*

3.2.1. Sub bottom Interpretations (SGU)

The sediment type distribution based on the sub bottom profile interpretations show a diverse seafloor both in Lövsele and Tavasten (Fig. 12). Fine sediments such as *clay* or *mud* were predominantly found in the sheltered bays in the northern parts of both areas and cover approximately 48% and 25% of the area (Table 7). *Till* consists of unsorted, often coarser material and cover a significant part of Lövsele and Tavasten, 41% and 47% respectively, and is found in the southern exposed parts of the areas. *Sand* is found intermittently mostly in the more exposed parts of both areas. SBP-data from Piteå was unfortunately compromised during data-backup which is why no interpretation from this area is included in this section.

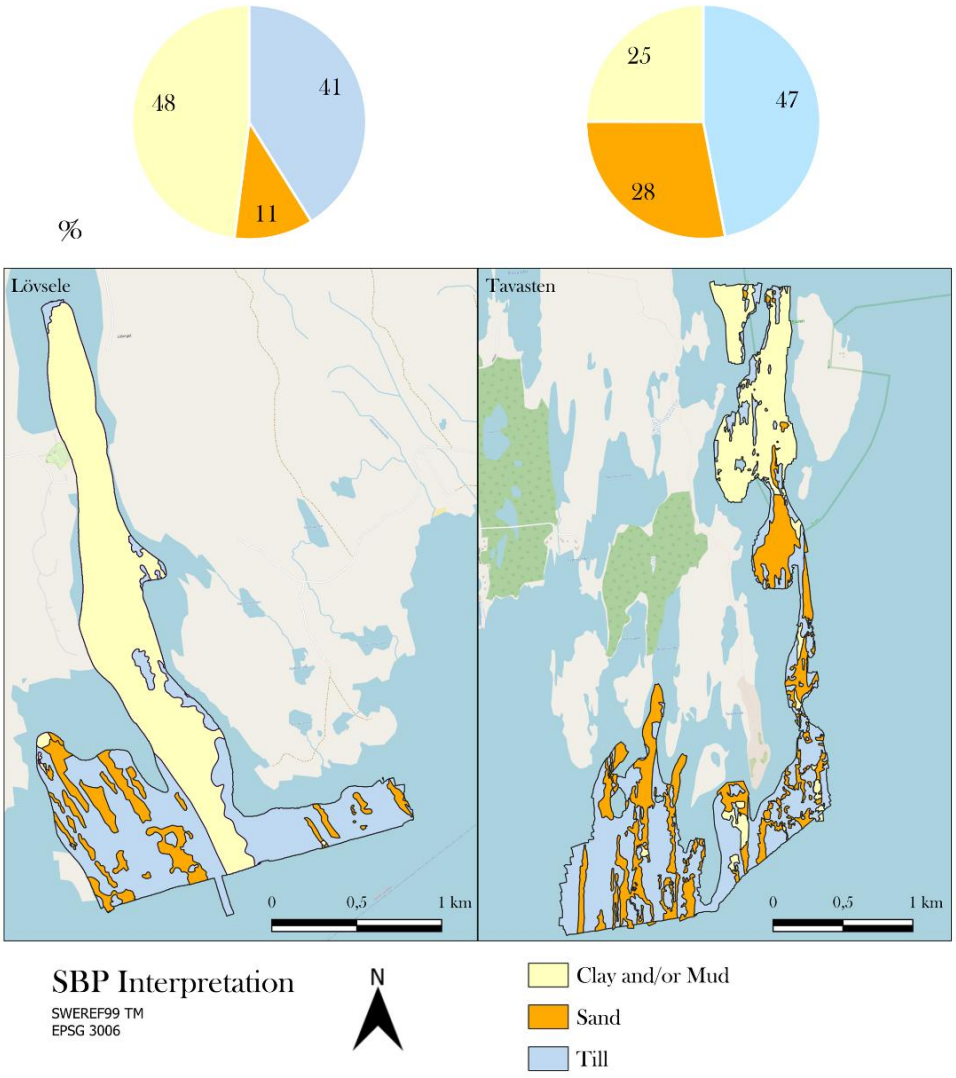

Figure 12. *Pie-charts with accompanying maps for each area that describe the coverage of sediment type according to the interpreted SBP-data.*

Table 7. *Table showing the coverage in km2 and percentage for each substrate type according to the interpreted SBP-data.*

	Lövsele	Lövsele	Tavasten	Tavasten
Substrate Type	**Coverage (km^2)**	**Coverage (%)**	**Coverage (km^2)**	**Coverage (%)**
Clay	1,01	48,0	0,62	25,0
Sand	0,23	10,9	0,70	28,0
Till	0,86	41,1	1,18	47,0

3.3. Biological distribution summary

Results from the analysis of underwater videos show that there were several species that were found in all three project areas (Fig. 13). In Piteå the total number of observation locations was 117, followed by 149 in Lövsele and 50 in Tavasten. The common species found in all three locations included *Myriophyllum spp*; *Potamogeton spp*; and *Chara spp*., while there were also some species were found in one location but not in other, e.g., *Elodea sp*, *Ceratophyllum*, and others, were only found in Piteå but not in other sites.

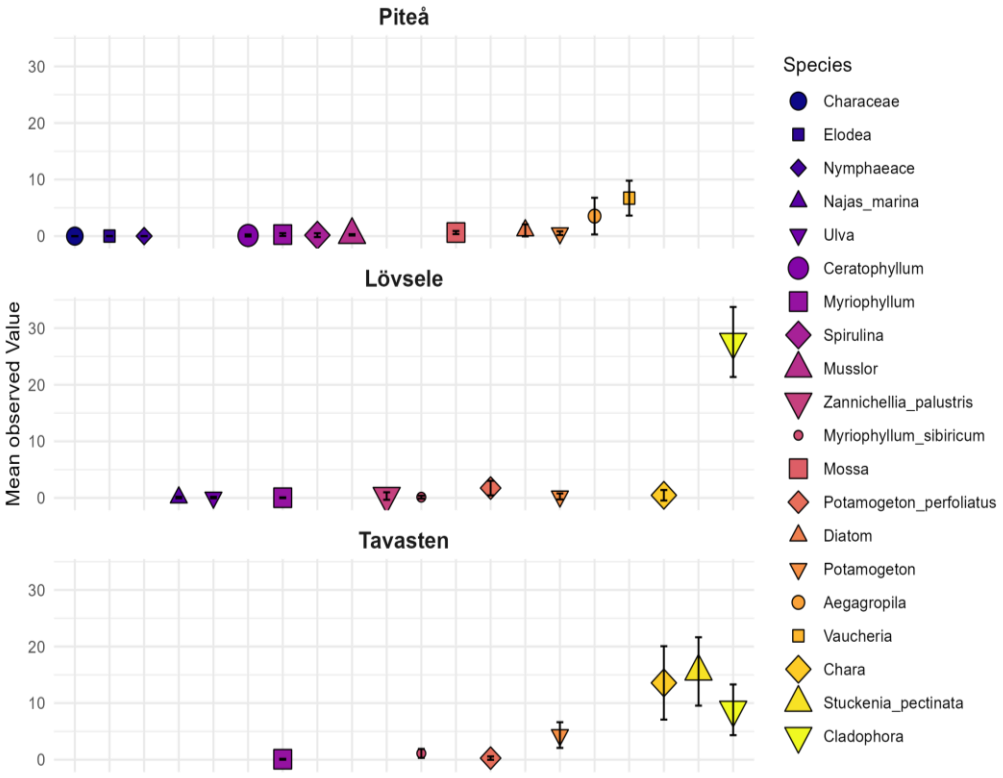

Figure 13. *Mean observed percentage values (%) with confidence interval of present species per observation location in the study area.*

3.4. Seabed substrate and habitat maps

This section presents GTK's interpreted seabed substrate maps, and SGU's continuous and thematic maps generated from spatial modeling. Further details on SGU's map accuracy, including statistical description can be found in APPENDIX 2.

3.4.1. Seabed substrate maps – Finland (GTK)

3.4.1.1. GTK Classification – seabed substrates distribution Finland

According to GTK classification scheme, nine different substrate classes were found in the study areas. The seabed substrate maps with GTK classification can be seen in Figures 14 and 15. Recent brackish water mud and brackish water mud were the dominant substrate types across most areas. The coverage areas and percentage for each class are presented in Tables 8 and 9.

In Iijoki, recent brackish water mud covered 44.8 % of the seabed, while in Kiiminkijoki, brackish water mud accounted for 34 % and recent brackish water mud 25.3 %. In Lohtajanjoki, brackish water mud made up 56,3 % of the seabed, with secondary sand comprising 18.6 %. Thin sand layers were also present over a larger area in Lohtaja, but because the substrate interpretation is based on sub-bottom profiles, layers thinner than 30 cm were not included.

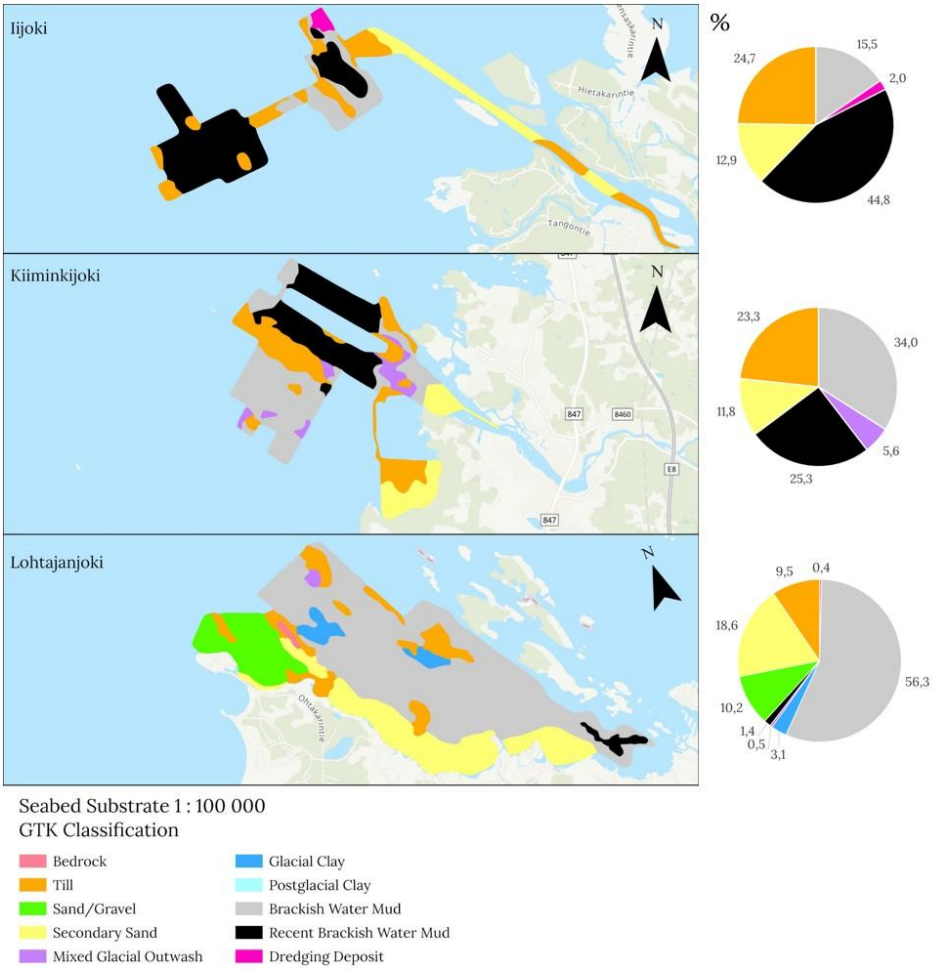

Figure 14. *Seabed substrate maps of the Iijoki, Kiiminkijoki and Lohtajanjoki areas. The seabed substrate classification is based on GTK's classification scheme.*

Table 8. *Table showing the coverage in km2 and percentage for each class in GTK's substrate classes in Iijoki, Kiiminkijoki and Lohtajanjoki.*

Class name	Iijoki		Kiiminkijoki		Lohtajanjoki	
	Coverage (km^2)	Coverage (%)	Coverage (km^2)	Coverage (%)	Coverage (km^2)	Coverage (%)
Recent mud	2,2	44,8	5,4	25,3	0,3	1,4
Brackish water mud	0,8	15,5	7,2	34	11,2	56,3
Glacial Clay	N/A	N/A	N/A	N/A	0,6	3,1
Mixed Glacial Outwash	N/A	N/A	1,2	5,6	0,1	0,5
Secondary Sand	0,6	12,9	2,5	11,8	3,7	18,6
Sand/Gravel	N/A	N/A	N/A	N/A	2,0	10,2
Till	1,2	24,7	4,9	23,3	1,9	9,5
Bedrock	N/A	N/A	N/A	N/A	0,1	0,4
Dredging deposit	0,1	2,0	N/A	N/A	N/A	N/A

In Läpväärtinjoki, recent brackish water mud dominates with 56 %, followed by 36.5 % till. In Lapuanjoki, brackish water mud covers 47.4 %, and recent brackish water mud 43 %. In contrast, Kalajoki area is mostly sandy, with 37.1 % secondary sand and 30.6 % sand/gravel. The Kalajoki and Lohtajanjoki study areas are located near prominent northwest–southeast-oriented esker formations that extend onto the seafloor, which explains the expected presence of sandy deposits in these areas.

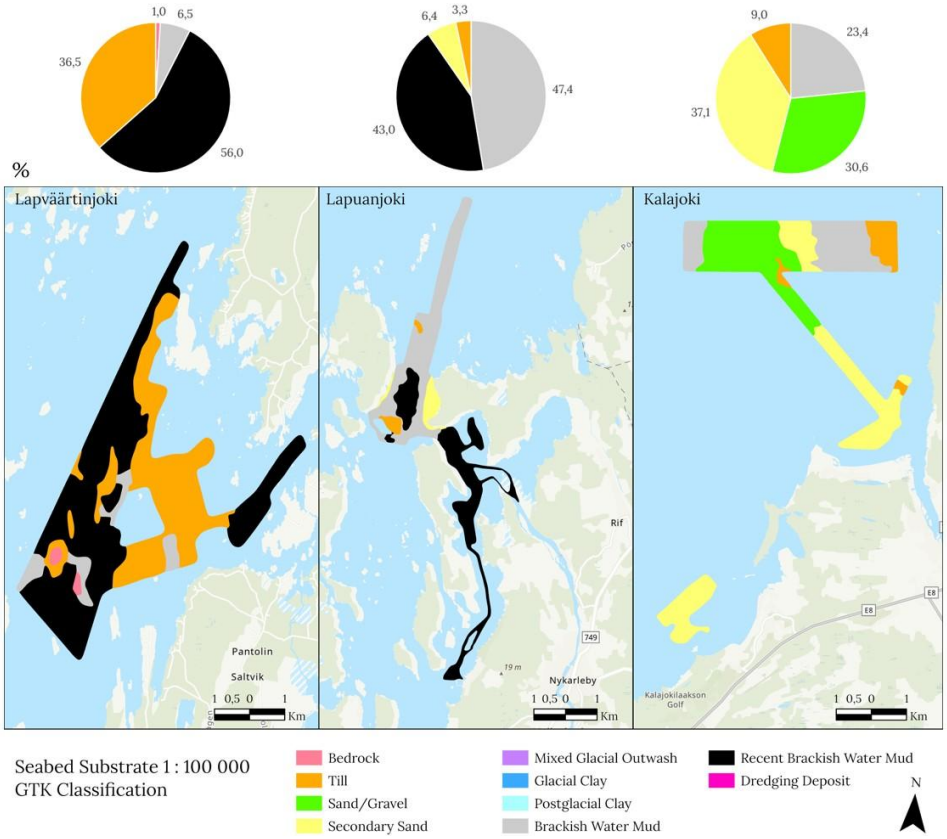

Figure 15. *Seabed substrate maps of the Lapväärtinjoki, Lapuanjoki and Kalajoki areas. The classification is based on GTK's classification scheme.*

Table 9. *Table showing the coverage in km2 and percentage for each class in GTK's substrate classes in Lapväärtinjoki, Lapuanjoki and Kalajoki.*

Class name	Lapväärtinjoki		Lapuanjoki		Kalajoki	
	Coverage (km^2)	Coverage (%)	Coverage (km^2)	Coverage (%)	Coverage (km^2)	Coverage (%)
Recent mud	3,6	56,0	4,4	43,0	N/A	N/A
Brackish water mud	0,4	6,5	4,8	47,4	3,3	23,4
Glacial Clay	N/A	N/A	N/A	N/A	N/A	N/A
Mixed Glacial Outwash	N/A	N/A	N/A	N/A	N/A	N/A
Secondary Sand	N/A	N/A	0,7	6,4	5,2	37,1
Sand/Gravel	N/A	N/A	N/A	N/A	4,3	30,6
Till	2,3	36,5	0,3	3,3	1,2	9,0
Bedrock	0,1	1,0	N/A	N/A	N/A	N/A

3.4.1.2. EMODnet Classification – seabed substrates in Finland

Seabed substrate maps were also produced using the EMODnet Folk-5 classification scheme. The maps were first produced with GTK's classification system and then converted to EMODnet classification system (Figures 16 and 17). In five of the six study areas, the seabed is dominated by mud to muddy sand. The Kalajoki area is the exception, primarily covered by sand or coarser substrates. In Iijoki there was 60,3 % coverage of mud to muddy sand followed with 24,7 % coverage of mixed sediments. In Kiiminkijoki survey area, which is located quite close to the Iijoki area, the trend was very similar with 59,3 % of mud to muddy sand and 28,9 % of mixed sediment. In Lohtajanjoki the coverage of mud to muddy sand was 57,7 % followed by 18,6 % of sand. The coverage areas and percentage for each class are presented in Tables 10 and 11.

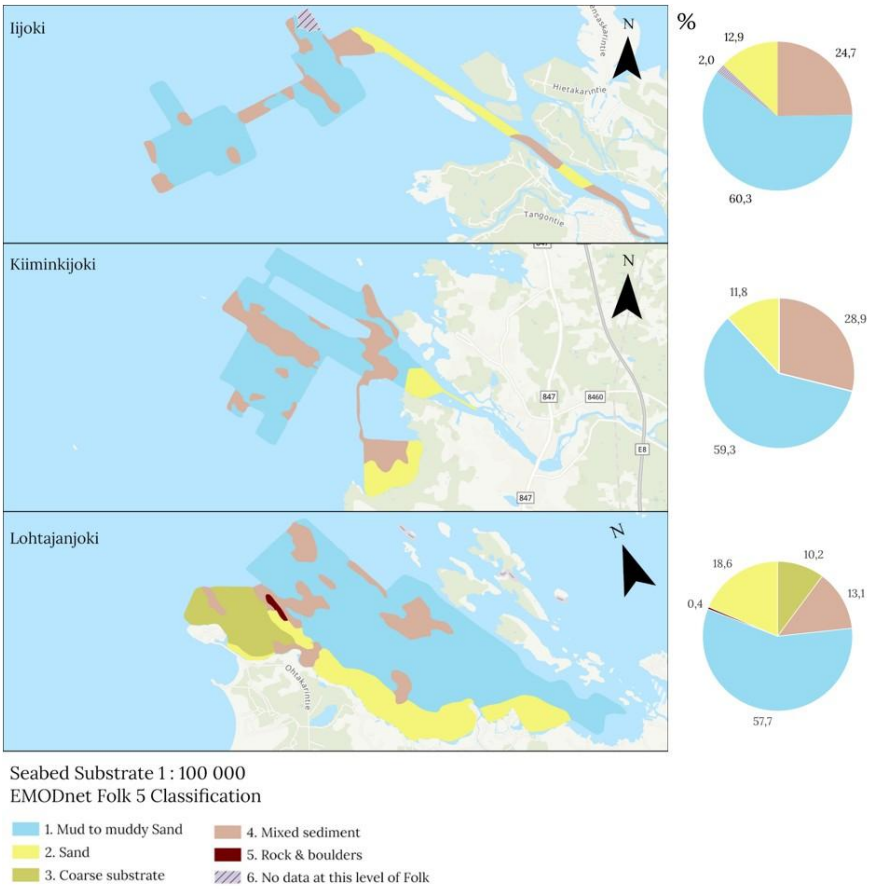

Figure 16. *Seabed substrate maps of the Iijoki, Kiiminkijoki and Lohtajanjoki areas with EMODnet Folk 5 classification scheme.*

Table 10. *Table showing the coverage in km2 and percentage for each class in EMODnet Folk 5 in Iijoki, Kiiminkijoki and Lohtajanjoki.*

Class name	Iijoki		Kiiminkijoki		Lohtajanjoki	
	Coverage (km^2)	Coverage (%)	Coverage (km^2)	Coverage (%)	Coverage (km^2)	Coverage (%)
Mud to muddy sand	3,0	60,3	12,6	59,3	11,4	57,7
Sand	0,6	12,9	2,5	11,8	3,7	18,6
Coarse sediment	N/A	N/A	N/A	N/A	2,0	10,2
Mixed sediment	1,2	24,7	6,1	28,9	2,6	13,1
Rock & Boulders	N/A	N/A	N/A	N/A	0,1	0,4
No data at this level	0,1	2,0	N/A	N/A	N/A	N/A

In Lapväärtinjoki, there was no sand at all according to EMODnet Folk 5 classification; instead, the area consisted mainly of mud to muddy sand (62,5 %) and mixed sediment (36,5 %). Lapuanjoki contains the most amount of mud to muddy sand with 90,3 %. In Kalajoki there is 37,1 & of sand and 30,6 % of coarse substrate.

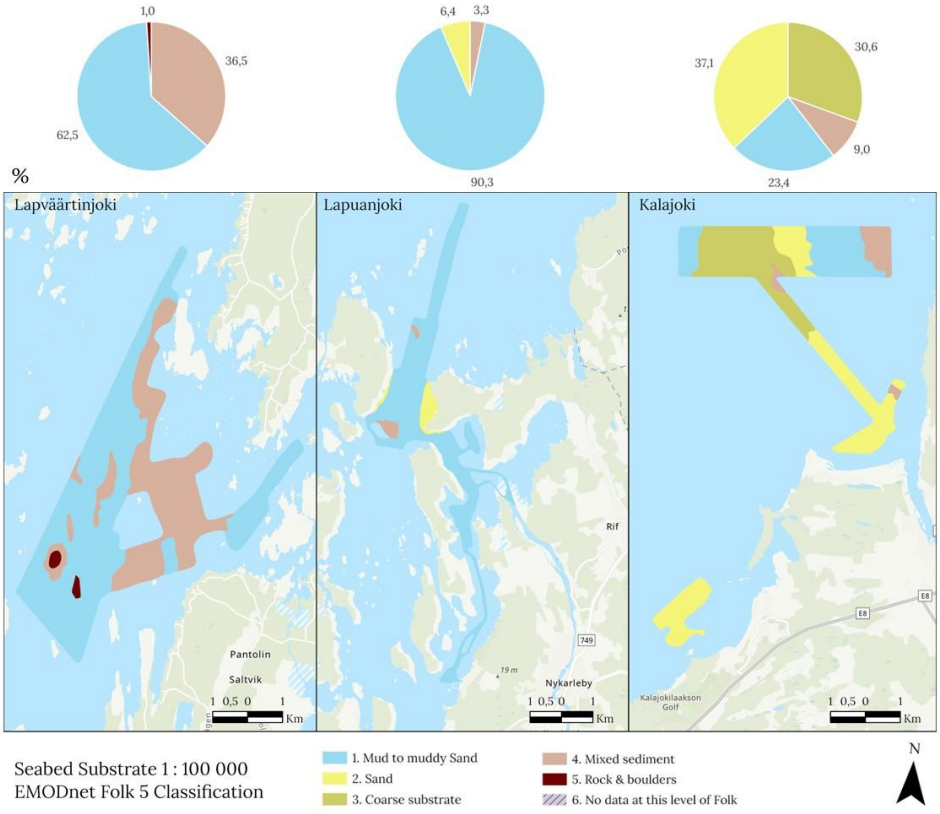

Figure 17. *Seabed substrate maps of the Lapväärtinjoki, Lapuanjoki and Kalajoki areas with EMODnet Folk 5 classification scheme.*

Table 11. *Table showing the coverage in km2 and percentage for each class in EMODnet Folk 5 in Lapväärtinjoki, Lapuanjoki and Kalajoki.*

Class name	Lapväärtinjoki		Lapuanjoki		Kalajoki	
	Coverage (km^2)	Coverage (%)	Coverage (km^2)	Coverage (%)	Coverage (km^2)	Coverage (%)
Mud to muddy sand	4,0	62,5	9,2	90,3	3,3	23,4
Sand	N/A	N/A	0,7	6,4	5,2	37,1
Coarse sediment	N/A	N/A	N/A	N/A	4,3	30,6
Mixed sediment	2,3	36,5	0,3	3,3	1,2	9,0
Rock & Boulders	0,1	1,0	N/A	N/A	N/A	N/A

3.4.2 Seabed substrate and habitat maps – Sweden (SGU)

The mapped areas in Piteå, Lövsele and Tavasten ranged in depth from approximately 1 to 14 m, well within the photic zone. In the Piteå area, mud to muddy sand were the dominant substrate types, covering roughly 98% of the seabed, with a grain size ≤0.002mm. with the remaining 2.2 % consisting of Mixed sediment. For Helcom HUB, the current study included level 2 to level 5 where several habitats were identified. Corresponding to EMODNet folk level 5, all classes was found in two of the three study areas (Lövsele and Tavasten) whereas three classes was found in the remaining area (Piteå).

This project, as shown in the following paragraphs, has produced the first comprehensive, high-resolution benthic habitat maps for the shallow regions of Piteå in Norrbotten, Lövsele, and Tavasten in Västerbotten. The total seabed area covered by the maps from the different areas approximated to 11,5 km^2. The maps feature spatial resolutions ranging from 2 m to higher up and include thematic information on geomorphology, substrate, and biological components.

3.4.2.1. Dominant sediment types

3.4.2.1.1. Clay sediment

The clay type sediment was the most predominant sediment in all three study areas from both video observation and modelled data. Piteå had the largest percent coverage of clay having 98% of clay coverage. In the case of Lövsele, the dominant coverage range for each pixel in the model were 0-20% of clay coverage which was followed by the 80-100% coverage range as presented in the table below. 0-20% of clay coverage was the dominant pixel class and followed by the 80-100% coverage group (Table 12). Clay was distributed

throughout the area in Piteå but more confined to the northern tip in Lövsele and Tavasten (Fig. 18). The accuracy of the modelled data at the ground-truthing location was 100%, 94% and 96% in Piteå, Lövsele and Tavasten respectively. This means that the modeled data for clay, in Piteå for example, 100% correspond to the interpreted coverage of clay from the samples at the sampling location.

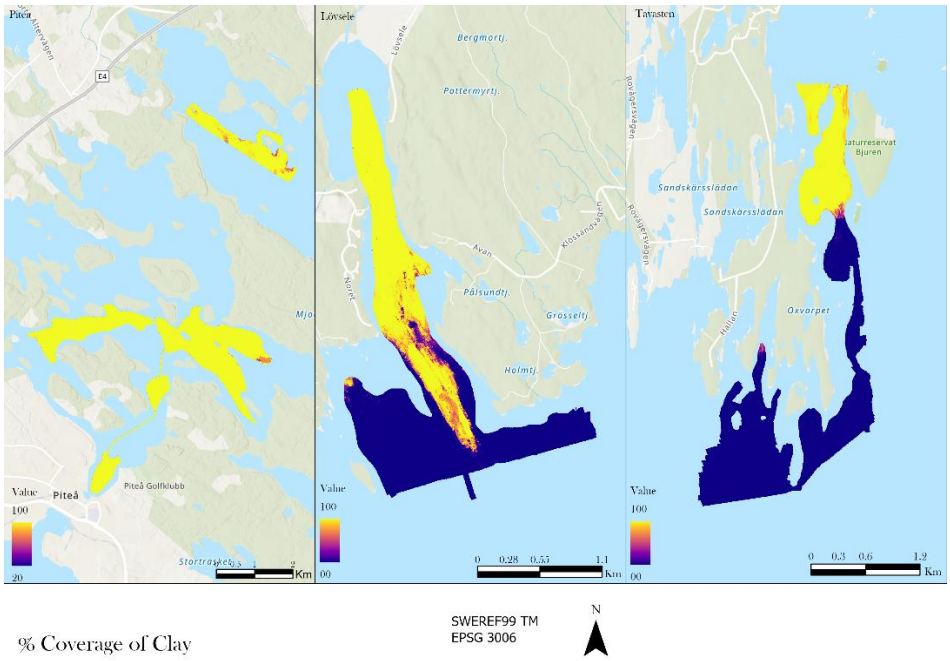

Figure 18. *Continuous coverage map showing the coverage of clay in % as indicated by the color-bar for each area.*

Table 12. *Table showing the classification percentage, coverage in km², coverage in percentage for each class and accuracy percentage of modelled clay.*

Classes	Piteå		Lövsele		Tavasten	
	Coverage (km²)	Coverage (%)	Coverage (km²)	Coverage (%)	Coverage (km²)	Coverage (%)
0–20%	0	0	1,11	54,9	1,74	73,5
20–40%	0	0	0,03	1,2	0,01	0,3
40–60%	0,01	0,2	0,03	1,5	0,01	0,3
60–80%	0,12	1,7	0,05	2,6	0,01	0,3
80-100%	6,82	98,1	0,81	39,8	0,61	25,6
Accuracy of model compared to sample (%)	100		94		96	

3.4.2.1.2. Stones & Pebbles

The stone pebbles type sediment was the second most dominant sediment in all three study areas from both video observation and modelled data.

Modelling stones pebbles at Piteå, most of the pixels (2x2m) in the modelled data was in 80-20% coverage group which had 99% of sediment coverage. In the case of Lövsele, pixels that had 0-20% of stones and pebbles coverage was the most dominant group (64%) followed by 80-100% group (18%) as presented in the table below. In the case of Tavasten again 0-20% group (51%) topped for stones pebbles followed by 80-100% group (16%) (Table 13). The stone pebbles sediment percentage group (0-20% group) within each pixel was distributed overall area in Piteå but in the southern tip of Lövsele and Tavasten (Fig. 19). The accuracy of the modelled data at the ground- truthing location was 100%, 85%, and 84% respectively in Piteå, Lövsele and Tavasten. This means that the modelled data for stones and pebbles, in Lövsele for example, 85% correspond to the interpreted coverage of clay from the samples at the sampling location.

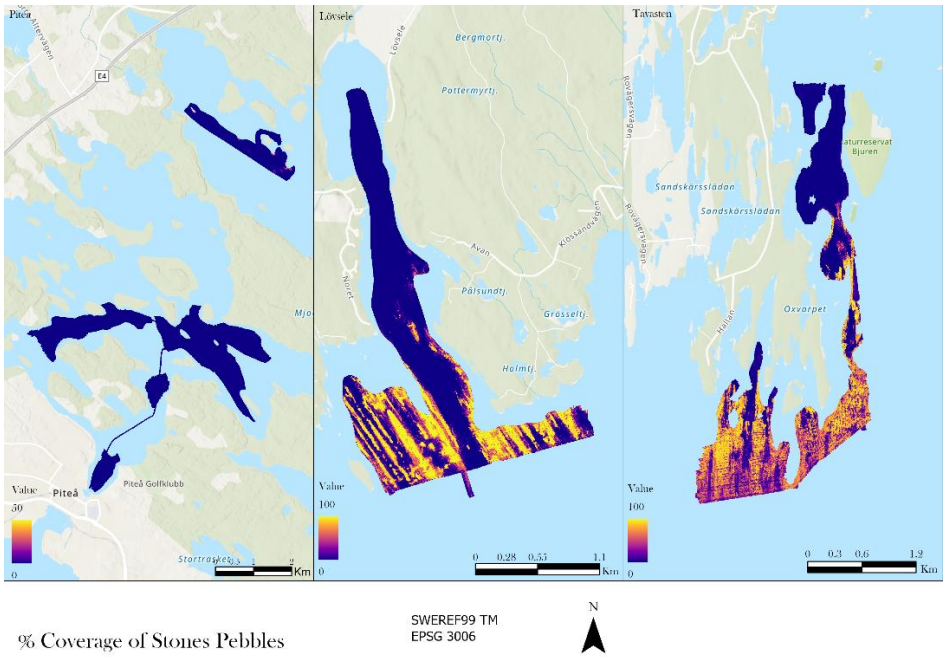

Figure 19. *Continuous coverage map showing the coverage of stones and pebbles in % as indicated by the colour-bar for each area.*

Table 13. *Table showing the classification percentage, coverage in km², coverage in percentage for each class and accuracy percentage of modelled stones and pebbles.*

Classes	Piteå		Lövsele		Tavasten	
	Coverage (km²)	Coverage (%)	Coverage (km²)	Coverage (%)	Coverage (km²)	Coverage (%)
0–20%	6,93	99,8	1,31	64,8	1,23	51,9
20–40%	0,01	0,2	0,10	5,1	0,21	8,8
40–60%	0	0	0,12	5,8	0,22	9,3
60–80%	0	0	0,12	6,0	0,33	13,9
80-100%	0	0	0,37	18,5	0,39	16,3
Accuracy of model compared to sample (%)	100		85		84	

3.4.2.2. SGU Classification - seabed substrate distribution Sweden

Five different substrate classes (according to the SGU classification scheme) were found in two of the three investigated areas. Three classes were found in Piteå were *clay/silt* dominated with 100% coverage (Fig. 20). *Sand* and *gravel* only showed up in a few pixels and were thus too few to register as any meaningful coverage. *Clay/silt* was also the dominant class in Lövsele with 46% coverage, followed by *pebbles, cobbles and boulders* at 34%. Unlike Lövsele, sand cover the largest area in Tavasten with 37% were clay/silt cover 30%. See Table 14 for the remaining classes for each area along with the coverage in km².

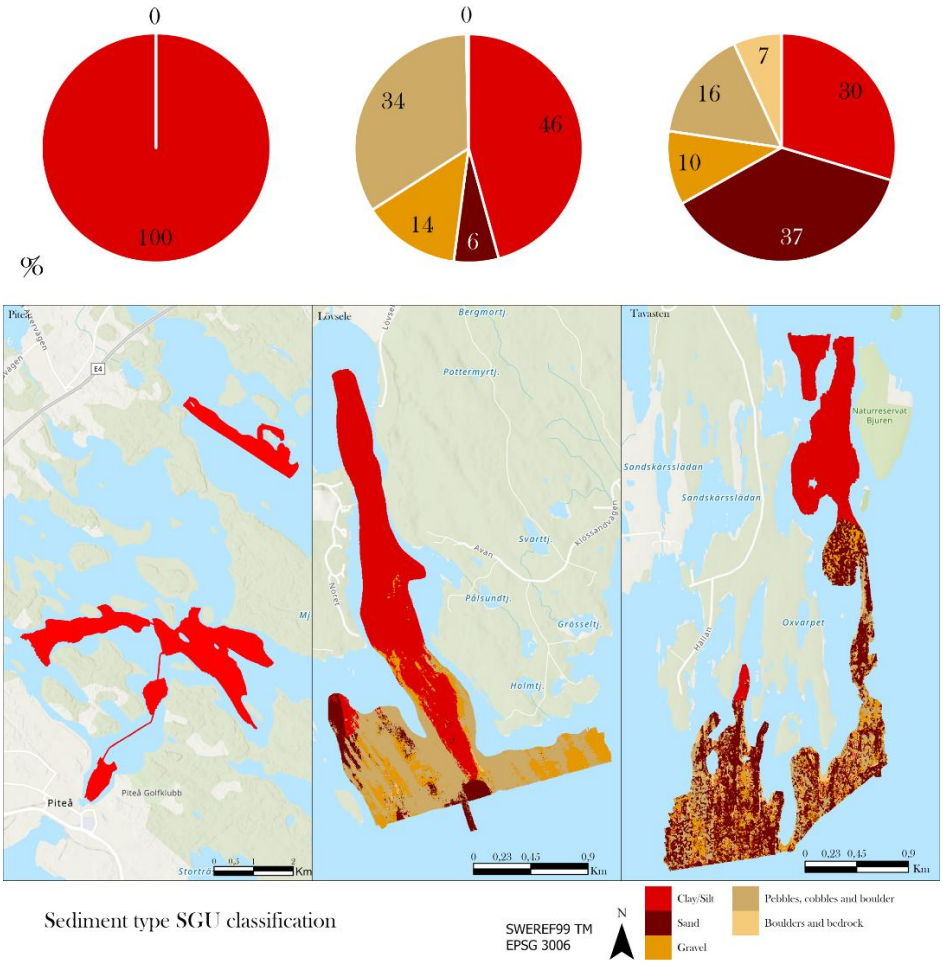

Figure 20. *Pie-charts with accompanying maps for each area that describe the coverage of sediment type according to SGU's classification scheme.*

Table 14. *Table shows the coverage in km² and percentage for each class in the SGU classification.*

Class Name	Piteå		Lövsele		Tavasten	
	Coverage (km²)	Coverage (%)	Coverage (km²)	Coverage (%)	Coverage (km²)	Coverage (%)
Clay/Silt	2,1	100	3,16	45,7	0,74	29,6
Sand	0	0	0,44	6,4	0,93	37,2
Gravel	0	0	0,96	13,9	0,26	10,5
Pebbles, cobbles and boulder	N/A	N/A	2,32	33,7	0,40	15,8
Boulders and bedrock	N/A	N/A	0,02	0,4	0,17	6,9

3.4.2.3. EMODnet Classification – seabed substrates in Sweden

Thematic maps in accordance with EMODNet have been produced according to the folk-5 classification scheme and are presented in the following section.

3.4.2.3.1. FOLK 5

The three investigated areas show noticeable differences in substrate coverage according to the EMODNet Folk-5 classifications (Fig. 21). *Mud to muddy sand* dominates in Piteå with a total coverage of 98%, where it covers 37% and 26% in Lövsele and Tavasten respectively. *Sand* is absent from Piteå but covers 3% in Lövsele and 4% Tavasten. *Coarse substrate* is most abundant in Tavasten with a coverage of 65% and cover 48% in Lövsele. No *coarse substrate* is found in Piteå. *Mixed sediment* covers 12% in Lövsele, 5% in Tavasten and 2% in Piteå. *Rock and boulders* as a class that covers the least amount of the areas and is absent from Piteå and only covers 0,2% in Tavasten and 0,03% in Lövsele. Area size and pixel count for each class can be seen in Table 15.

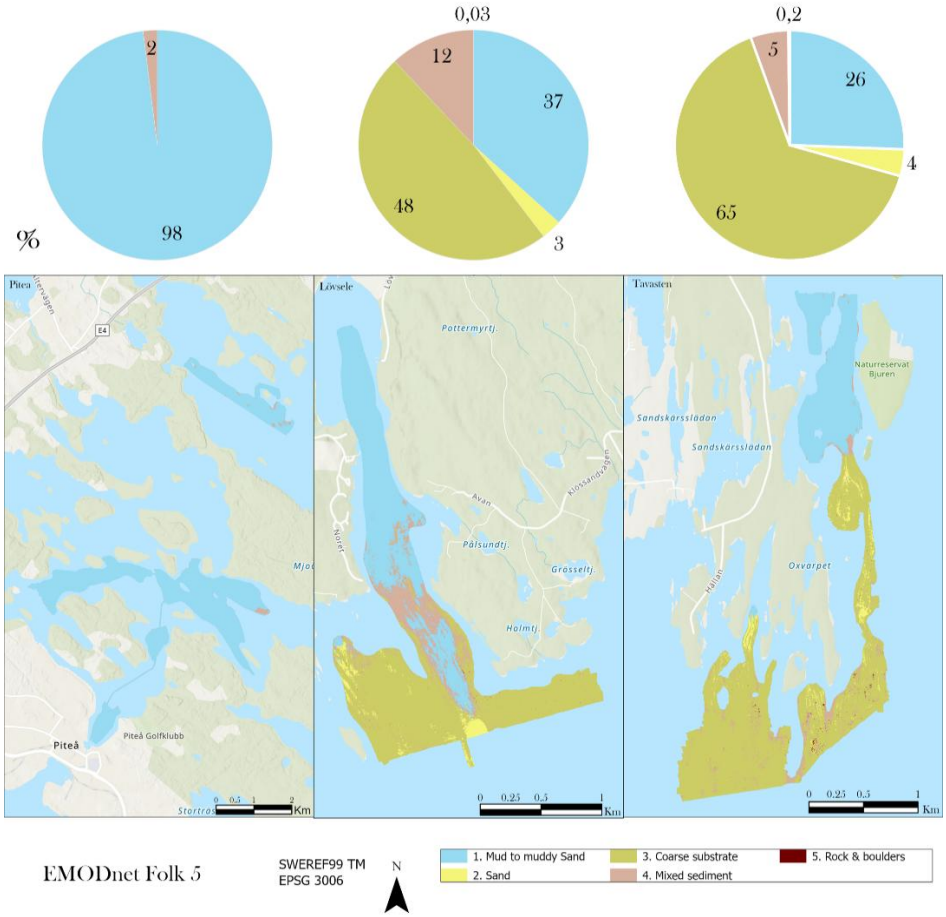

Figure 21. *Pie-charts with accompanying maps for each area that describe the coverage of sediment type according to the EMODNet Folk-5 classification scheme.*

Table 15. *Table showing the coverage in km² and percentage for each class in EMODNet Folk-5.*

Class Name	Piteå		Lövsele		Tavasten	
	Coverage (km²)	Coverage (%)	Coverage (km²)	Coverage (%)	Coverage (km²)	Coverage (%)
Mud to muddy sand	6,81	98,0	0,74	36,7	0,61	25,6
Sand	N/A	N/A	0,06	2,9	0,09	3,7
Coarse sediment	N/A	N/A	0,98	48,4	1,54	65,1
Mixed sediment	0,14	2,0	0,24	12,0	0,13	5,3
Rock & boulders	N/A	N/A	0,00	0,0	0,01	0,2

3.4.2.4. HELCOM HUB

Like the thematic EMODNet folk 5 maps, HELCOM HUB maps have also been produced according to levels 3, 4 and 5 classification schemes and are presented in the following section.

3.4.2.4.1. Level 3

Similar to the coverage variability in the EMODNet Folk-5 classification scheme, the HELCOM HUB Level 3 classifications show that the three areas have a stark difference in terms of substrate type and coverage (Fig. 22). *Baltic photic rock and boulders* has the lowest coverage in all three areas and is absent in Piteå and covers 0,007% in Tavasten and 0,004% in Lövsele. *Baltic photic muddy sediment* is most abundant in Piteå with a coverage of 98%, whereas it covers 38% and 25% in Lövsele and Tavasten respectively. Lövsele inhibits the most amount of *baltic photic coarse sediment* which covers 18% of the surface, 8,7% of the surface in Tavasten and cannot be found in Piteå according to the model and this classification. *Baltic photic sand* is absent from Piteå and covers 6,5% in Tavasten and 2,2% in Lövsele. The most abundant substrate class in Tavasten is *Baltic photic mixed substrate* which covers 60% of the area. This is also the substrate class that dominates in Lövsele with a coverage of 42%, whereas the coverage in Piteå is only 2,3%. Area size and pixel count for each class can be seen in Table 16.

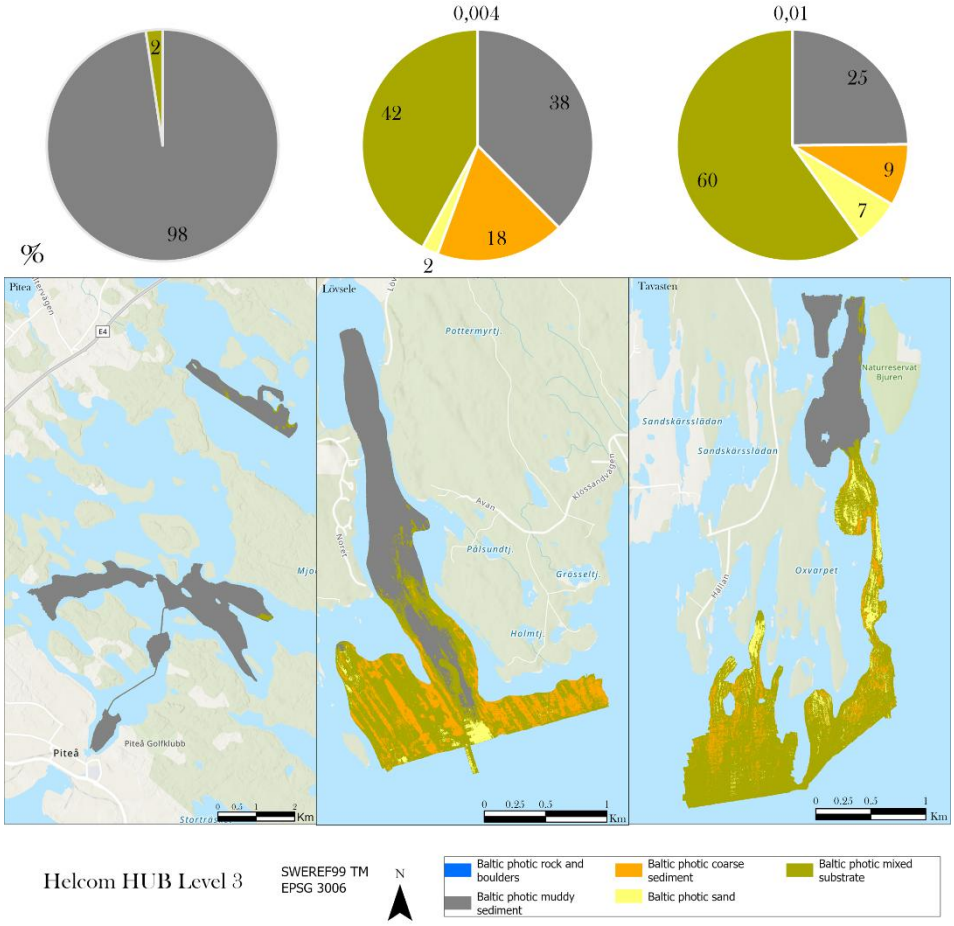

Figure 22. *Pie-charts accompanying maps for each area that describe the coverage of sediment type according to the HELCOM HUB Level 3 classification scheme. The table shows the pixel-count, coverage in km2 and coverage in percentage.*

Table 16. *Table showing the classification code, coverage in km2 and percentage for each class in HELCOM HUB level 3.*

Class Name	Class Code	Piteå		Lövsele		Tavasten	
		Coverage (km^2)	Coverage (%)	Coverage (km^2)	Coverage (%)	Coverage (km^2)	Coverage (%)
Baltic photic rock & boulders	AA.A	N/A	N/A	0,00	0,0	0,00	0,0
Baltic photic muddy sediment	AA.H	6,79	97,7	0,76	37,6	0,59	24,8
Baltic photic coarse sediment	AA.I	N/A	N/A	0,37	18,1	0,21	8,7
Baltic photic sand	AA.J	N/A	N/A	0,05	2,2	0,15	6,5
Baltic photic mixed substrate	AA.M	0,16	2,3	0,85	42,1	1,42	59,9

3.4.2.4.2. Level 4

Due to the long classification name, the coverage will be referred to the classification code that can be seen in Figure 23. The most predominant

substrate class in Piteå is AA.H4 that covers 83% of the surface, which is followed by AA.H4 at 14%. The remaining area is covered by AA.M1; 0,6% and AA.M2; 1,7%. Tavasten and Lövsele contain the same classes but in varied coverage. AA.M1 is the dominant class in Tavasten and covers 41% where it covers 12% in Lövsele. AA.H4 covers the largest area in Lövsele with 34% coverage and 7,1% of the surface in Tavasten. The second highest substrate class coverage in Lövsele is AA.M2 with 30% coverage, and 18% in Tavasten. AA.H1 also covers roughly 18% of the surface in Tavasten, but only 3,8% in Lövsele. AA.I1 is the fourth largest class in Lövsele with a coverage of 11%, where it's only 6,6% in Tavasten. The remaining substate classes that cover both Lövsele and Tavasten can be seen in Table 17.

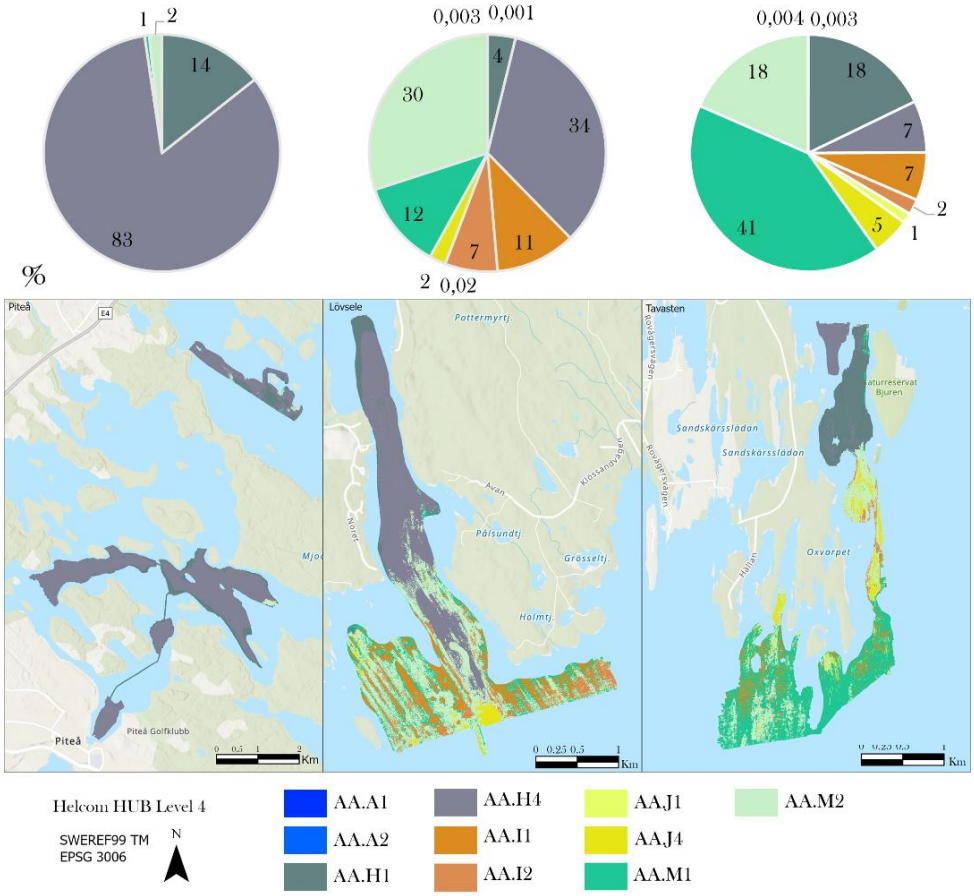

Figure 23. *Pie-charts accompanying maps for each area that describe the coverage of sediment type according to the HELCOM HUB Level 4 code classification scheme.*

Table 17. *Table shows the classification code, coverage in km² and percentage for each class in HELCOM HUB level 4.*

Class Name	Class Code	Piteå		Lövsele		Tavasten	
		Coverage (km²)	Coverage (%)	Coverage (km²)	Coverage (%)	Coverage (km²)	Coverage (%)
Baltic photic rock & boulders characterised by epibenthic biotic structures	AA.A1	N/A	N/A	0,00	0,0	0,00	0,0
Baltic photic rock & boulders characterised by sparse macroscopic epibenthic biotic structures	AA.A2	N/A	N/A	0,00	0,0	0,00	0,0
Baltic photic muddy sediment characterized by macroscopic epibenthic biotic structures	AA.H1	1,00	14,3	0,08	3,8	0,42	17,8
Baltic photic muddy sediment characterized by no macroscopic biotic structures	AA.H4	5,79	83,3	0,68	33,9	0,17	7,1
Baltic photic coarse sediment characterized by macroscopic epibenthic biotic structures	AA.I1	N/A	N/A	0,22	11,0	0,15	6,6
Baltic photic coarse sediment characterized by sparse macroscopic epibenthic biotic structures	AA.I2	N/A	N/A	0,14	7,2	0,05	2,1
Baltic photic sand characterized by macroscopic epibenthic biotic structures	AA.J1	N/A	N/A	0,00	0,0	0,03	1,4
Baltic photic sand characterized by no macroscopic biotic structures	AA.J4	N/A	N/A	0,05	2,2	0,12	5,2
Baltic photic mixed substrate characterized by macroscopic epibenthic biotic structures	AA.M1	0,04	0,6	0,24	11,9	0,98	41,4
Baltic photic mixed substrate characterized by sparse macroscopic epibenthic biotic structures	AA.M2	0,12	1,7	0,61	30,0	0,44	18,5

3.4.2.4.3. Level 5

As with HELCOM HUB Level 4, the coverage will be referred to the classification code that can be seen in Table 10. The most predominant substrate class in Piteå is AA.H4U that covers 83% of the surface which is followed by AA.H1S at 14%. The remaining area is covered by AA.M2T: 1,7%, AA.M1V; 0,5%, AA.H1B; 0,1%, AA.M1R; 0,06% and AA.M1B; 0,04%. The dominant class in Lövsele is AA.H4U with a coverage of 34% and is found in the northern part of the area (Fig. 24). This is followed by AA.M2T at 30% and AA.M1B at 12% coverage. The lesser abundant classes in Lövsele are distributed as follows: AA.I1V; 9,8%, AA.I2T; 7,2%, AA.H1B; 3,7%, AA.J4U; 2,3%, AA.I1B; 1,2%, AA.H1V; 0,1%, AA.J1V; 0,02%, AA.A1C; 0,002%, AA.J1B; 0,002%, AA.A2T; 0,001% and AA.A1V; 0,0006%. AA.M1B is the most abundant substrate class in Tavasten with 41% coverage. This class is followed by AA.M2T with 18% coverage, that is in turn closely followed by AA.H1B at 17%. The remaining classes and their respective coverage can be seen in Table 18.

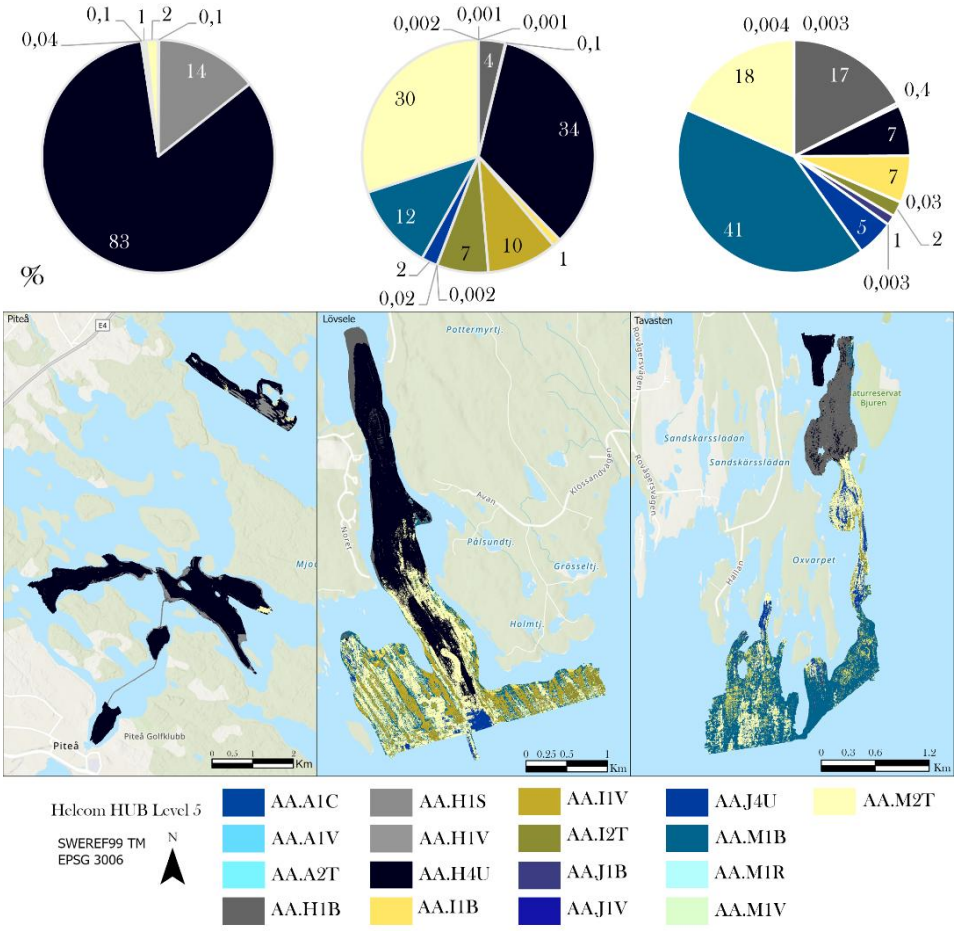

Figure 24. *Pie-charts with accompanying map for each area that describes the coverage of sediment type according to the HELCOM HUB Level 5 code classification scheme.*

Table 18. *Table showing the classification code, coverage in km² and percentage for each class in HELCOM HUB level 5.*

Class Name	Class Code	Piteå		Lövsele		Tavasten	
		Coverage (km²)	Coverage (%)	Coverage (km²)	Coverage (%)	Coverage (km²)	Coverage (%)
Baltic photic rock and boulders characterized by perennial algae	AA.A1C	N/A	N/A	0,00	0,0	N/A	N/A
Baltic photic rock and boulders characterized by mixed epibenthic macrocommunity	AA.A1V	N/A	N/A	0,00	0,0	0,00	0,0
Baltic photic rock and boulders characterized by sparse epibenthic macrocommunity	AA.A2T	N/A	N/A	0,00	0,0	0,00	0,0
Baltic photic muddy sediment characterized by submerged rooted plants	AA.H1B	0,01	0,1	0,07	3,7	0,41	17,4
Baltic photic muddy sediment characterized by annual algae	AA.H1S	0,99	14,3	N/A	N/A	N/A	N/A
Baltic photic muddy sediment characterized by mixed epibenthic macrocommunity	AA.H1V	N/A	N/A	0,00	0,1	0,01	0,4
Baltic photic muddy sediment characterized by no macrocommunity	AA.H4U	5,79	83,3	0,68	33,9	0,17	7,1
Baltic photic coarse sediment characterized by submerged rooted plants	AA.I1B	N/A	N/A	0,02	1,2	0,15	6,5
Baltic photic coarse sediment characterized by mixed epibenthic macrocommunity	AA.I1V	N/A	N/A	0,20	9,8	0,00	0,0
Baltic photic coarse sediment characterized by sparse epibenthic macrocommunity	AA.I2T	N/A	N/A	0,14	7,2	0,05	2,1
Baltic photic sand characterized by submerged rooted plants	AA.J1B	N/A	N/A	0,00	0,0	0,03	1,4
Baltic photic sand characterized by mixed epibenthic macrocommunity	AA.J1V	N/A	N/A	0,00	0,0	0,00	0,0

Baltic photic sand characterized by no macrocommunity	AA.J4U	N/A	N/A	0,05	2,2	0,12	5,2
Baltic photic mixed substrate characterized by submerged rooted plants	AA.M1B	0,00	0,0	0,24	11,9	0,98	41,4
Baltic photic mixed substrate characterized by soft crustose algae	AA.M1R	0,00	0,1	N/A	N/A	N/A	N/A
Baltic photic mixed substrate characterized by mixed epibenthic macrocommunity	AA.M1V	0,04	0,5	N/A	N/A	N/A	N/A
Baltic photic mixed substrate characterized by sparse epibenthic macrocommunity	AA.M2T	0,12	1,7	0,61	30,0	0,44	18,5

3.4.2.5. Biological distribution, grouped species

3.4.2.5.1. Vascular plants

Across the three different geographic locations, vascular plants were found in varying abundance. The coverage percentage was 0-30% in Piteå; 0-85% in Lövsele but up to 90% in Tavasten (Table 19). In terms of dominant of plant groups, submerged aquatic vascular plants were more prevalent in the northern tip of Lövsele but in the southern part of Tavasten from the model images. Higher occurrence of vascular plants was found for Tavasten (Fig. 25). The model shows that all three areas had between 0-20% of vascular plant coverage as most dominant percentage-class, but Tavasten showed a higher percentage in the 20-40% and 40-60% classes. The accuracy of the modelled data at the ground-truthing location was 99%, 99%, and 98% respectively in Piteå, Lövsele and Tavasten. This means that the modeled data for vascular plants, in Lövsele for example, 99% correspond to the interpreted coverage of vascular plants from the samples at the sampling location.

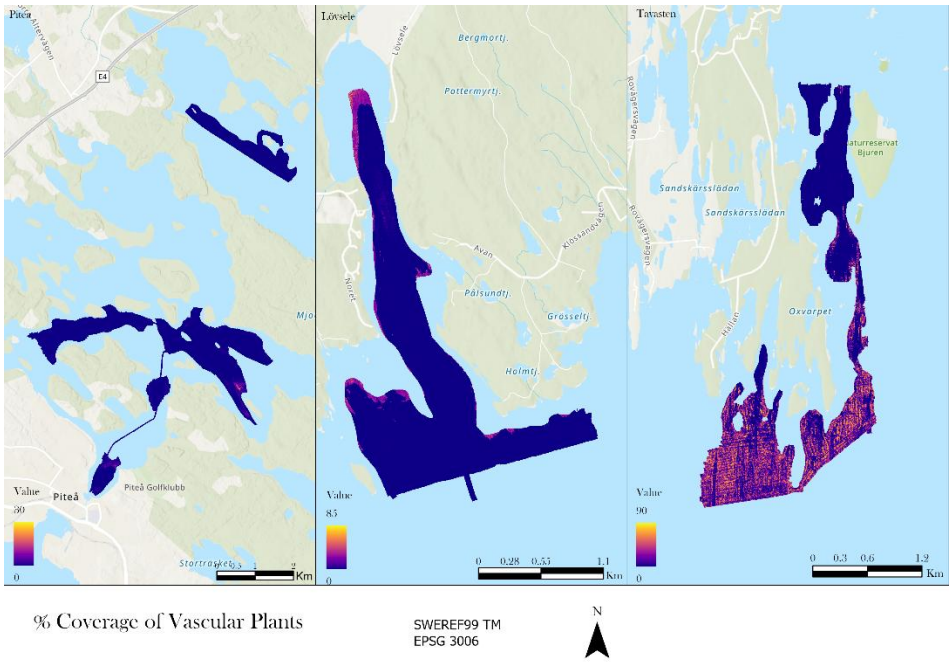

Figure 25. *Continuous coverage map showing the coverage of vascular plants in % as indicated by the color-bar for each area.*

Table 19. *Table showing the classification percentage, coverage in km2, coverage in percentage for each class and accuracy percentage in modelled vascular plants.*

Classes	Piteå		Lövsele		Tavasten	
	Coverage (km^2)	Coverage (%)	Coverage (km^2)	Coverage (%)	Coverage (km^2)	Coverage (%)
0–20%	6,95	100,0	1,93	95,4	1,66	70,7
20–40%	0,00	0,0	0,09	4,2	0,30	12,9
40–60%	N/A	N/A	0,01	0,4	0,25	10,8
60–80%	N/A	N/A	0,00	0,0	0,12	5,3
80-100%	N/A	N/A	0,00	0,0	0,01	0,3
Accuracy of model compared to sample (%)	99		99		98	

3.4.2.5.2. Green algae

In the case of green algae, the overall coverage percentage was in the range between 0-100% for Piteå and Lövsele but 0-90% for Tavasten (Fig. 26). A higher percentage of green algae has been observed in Tavasten per pixel compared to the other two areas, returning an overall higher coverage. Among the total pixels in Piteå areas, about 96% of pixels were in range of 0-20% coverage for green algae, which was 93% in Lövsele and 86% in Tavasten (Table 20). The accuracy of the modelled data at the ground-truthing location was 100%, 93% and 86% in Piteå, Lövsele and Tavasten respectively. This

means that the modeled data for *green algae*, in Tavasten for example, 86% correspond to the interpreted coverage of *green algae* from the samples at the sampling location.

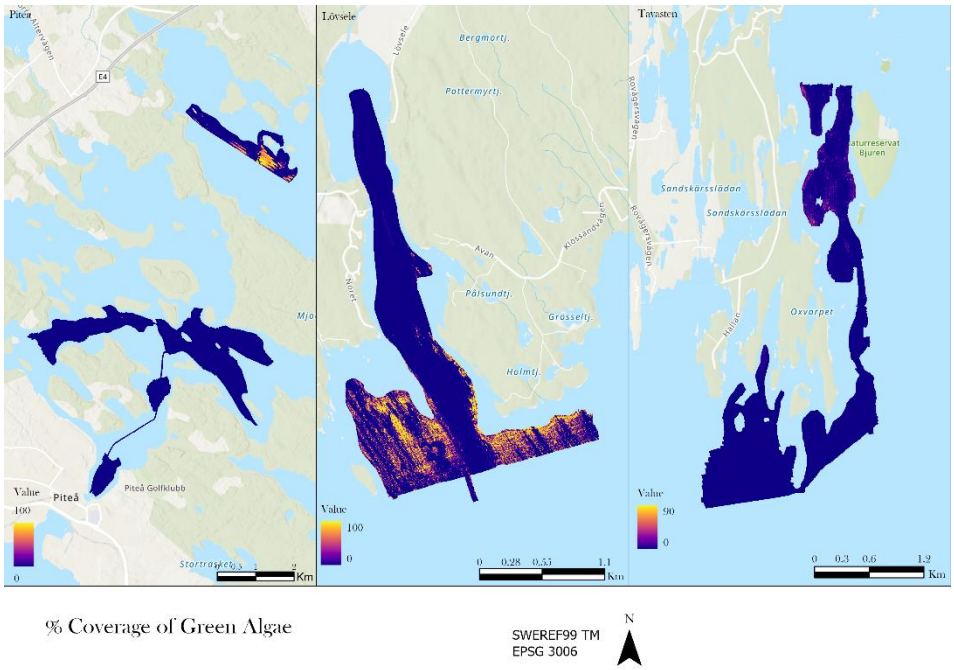

Figure 26. *Continuous coverage map showing the coverage of green algae in % as indicated by the color-bar for each area.*

Table 20. *Table showing the classification percentage, coverage in km², coverage in percentage for each class and accuracy percentage in modelled green algae.*

Classes	Piteå		Lövsele		Tavasten	
	Coverage (km²)	Coverage (%)	Coverage (km²)	Coverage (%)	Coverage (km²)	Coverage (%)
0-20%	6,71	96,5	1,63	80,5	1,66	70,7
20–40%	0,02	0,3	0,09	4,5	0,30	12,9
40–60%	0,05	0,6	0,08	3,8	0,25	10,8
60–80%	0,06	0,9	0,08	4,1	0,12	5,3
80-100%	0,11	1,6	0,15	7,2	0,01	0,3
Accuracy of model compared to sample (%)	100		93		86	

3.4.2.5.3. Dominant plant species

The dominant plant species was different in the three different survey areas (Figure 27 and Table 21). In Piteå, the perennial filamentous green algae *Aegagropila* was more frequent than other plant species (*Myriophyllum spp, Potamogeton spp, Ceratophyllum spp, Moss spp, Vaucheria, and Diatoms*) covering between 0 to 100%. The dominant plant species in Lövsele was

Cladophora, another filamentous green algae which outnumbered other submerged vascular plant species like *potamogeton perfolitus*, *Nazas marina or Stuckenia pectinata* covering again between 0 to 100% of the pixels in the area. Considering the most dominant species in Tavasten, it was not green algae but, submerged the vascular plant *Stuckenia pectinata* with a pixel value ranging between 0 to 83%. The other plant species in this region were either submerged vascular plants like-*Najas marina*; *Myriophyllumsibricum*; *Potamogeton perfolitus*; green algae eg. *Cladophora spp* or Charophytes eg. *Chara spp*. Considering the direction of distribution for the dominant species it was found that all three species were more commonly distributed in non-clay type sediments. The accuracy of the modelled data at the ground-truthing location was 100%, 93% and 66% in Piteå, Lövsele and Tavasten respectively. This means that the modeled data for *Cladophora spp*, in Lövsele for example, 93% correspond to the interpreted coverage of *Cladophora spp* from the samples at the sampling location.

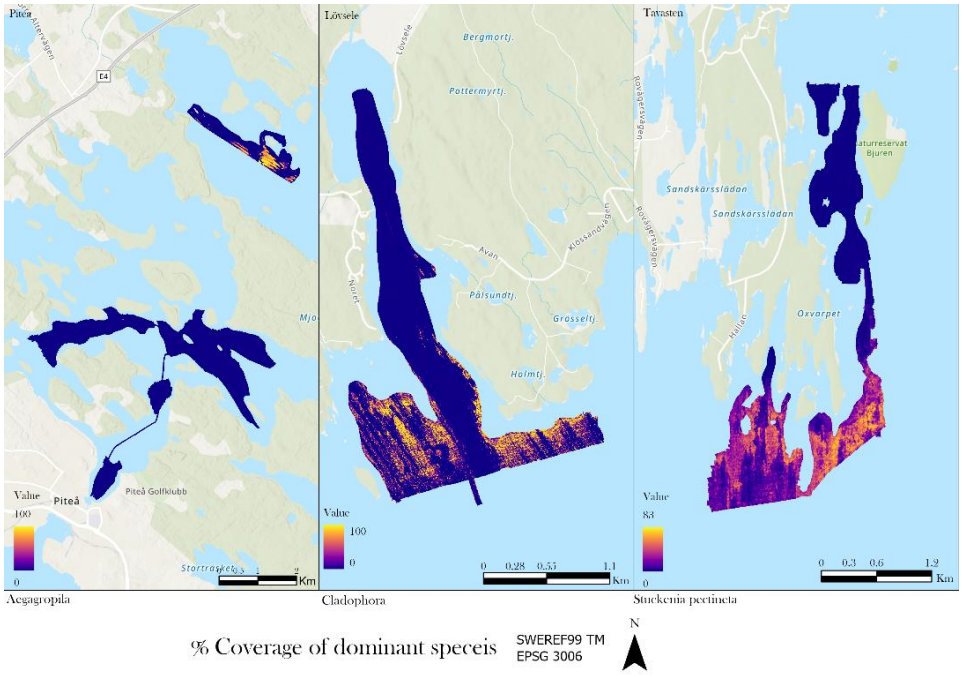

Figure 27. *Continuous coverage map showing the coverage of the dominant species for each area in % as indicated by the color-bar for each area.*

Table 21. *Table showing the classification percentage, coverage in km², coverage in percentage for each class and accuracy percentage in modelled dominant species in three study areas.*

Classes	Piteå (*Aegagropila spp*)		Lövsele (*Cladophora spp*)		Tavasten (*Stuckenia pectinata*)	
	Coverage (km²)	Coverage (%)	Coverage (km²)	Coverage (%)	Coverage (km²)	Coverage (%)
0–20%	6,70	96,4	1,64	81,0	1,53	65,1
20–40%	0,03	0,5	0,09	4,4	0,47	20,0
40–60%	0,04	0,6	0,07	3,7	0,28	12,0
60–80%	0,06	0,8	0,08	3,9	0,07	2,8
80–100%	0,12	1,7	0,14	7,0	0,00	0,0
Accuracy of model compared to sample (%)	100		93		66	

3.5. Shipborne bathymetry and seabed characteristics (GTK)

3.5.1. Iijoki

The Iijoki, located in the northernmost study area, is marked by high river discharge. This results in seabed sediments that are significantly coarser, consisting mainly of sand. At the confluence of the river and the sea, extensive underwater sandy dune fields were identified, with dune heights ranging from 0.2 to 1 m and widths between 10 and 20 m (Fig. 28). These features indicate a highly dynamic depositional environment shaped by strong fluvial input. Toward, the open sea finer sediments accumulate within deeper and more sheltered basins. The shallowest area corresponds to the river channel itself, and after the river opens into the sea the bathymetry gradually deepens offshore. Water depths in this area range from 1.3 to 19 m.

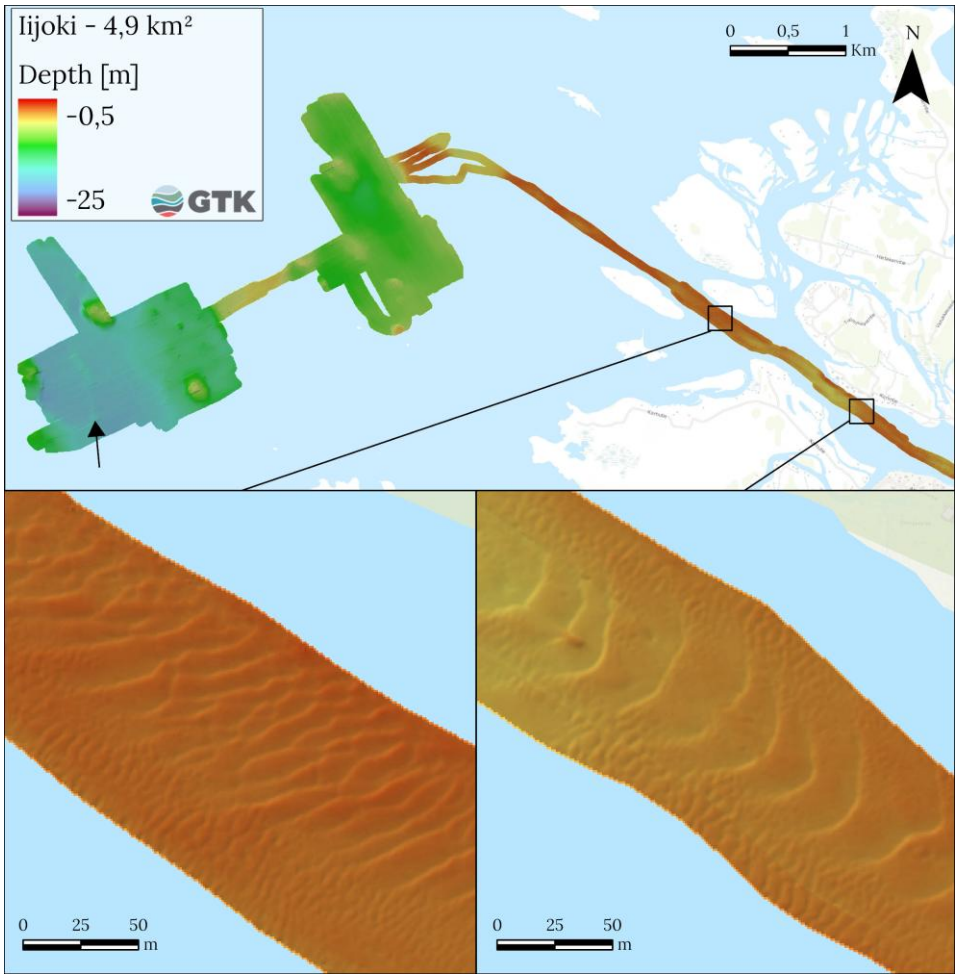

Figure 28. *Bathymetry map of the Iijoki area and detailed pictures of the sand dunes in the river. The arrow indicates a small esker feature, that can be seen in the bathymetry map. In the deeper area the bathymetry is collected with PDBS and the raster resolution is 5x5m. In the shallower river area, the data is collected with MBES and the raster resolution is 1x1m.*

Hydroacoustic surveys can also reveal clear signs of human activity. In addition to natural structures, anthropic marks such as trawl tracks and dredging deposits are often identifiable in side-scan images like in Figure 29.

The left side-scan image shows a soft seabed dominated by recent brackish water mud with numerous trawl marks. These marks form a dense pattern, indicating repeated trawling events. The right image displays a series of unusual seabed piles, which were also detected in sub-bottom profiles. In the profiles these piles were up to about 1 m high. These features occur only in the northeastern corner of the study area and do not resemble any known geological structures. Their morphology and restricted distribution suggest that they were formed by the deposition of dumped dredging material.

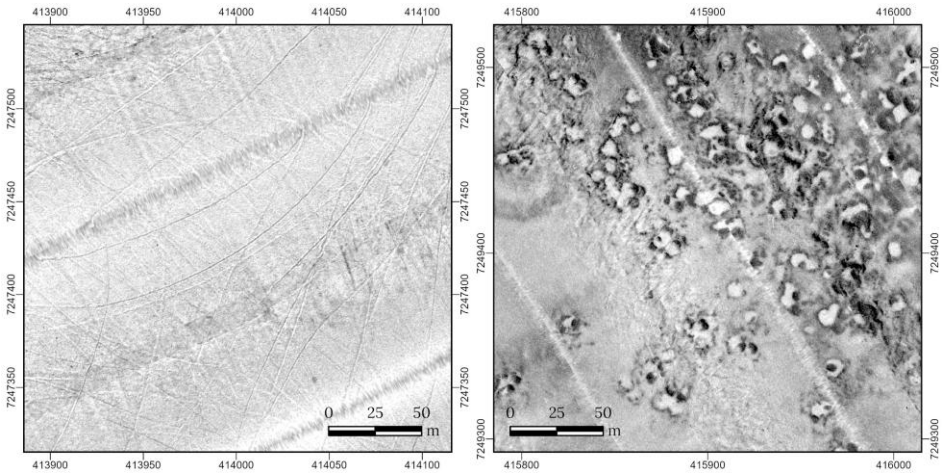

Figure 29. *Side-scan sonar images showing trawl-marked soft seabed (left) and localized seabed piles interpreted as dredging deposits (right).*

3.5.2. Kiiminkijoki

In Kiiminkijoki area the river and the nearshore environment represent the shallowest parts of the study area. Progressing toward open sea, the seafloor steepens and forms deeper gullies resembling small submarine canyons, where water depths reach up to 41 m. Overall, the seafloor topography is highly variable in this area; between these deeper gullies are very shallow rocky shoals that pose challenges for navigation. Depths vary from 1 to 41.4 m (Fig 30).

The Kiiminkijoki estuary shows transitional characteristics between sheltered depositional zones and more exposed sandy environments. Sediment composition varies spatially, with finer material accumulating in deeper basins, while coarser sands dominate shallower regions subject to wave and current activity. The variability reflects the dual influence of riverine input and open-sea dynamics.

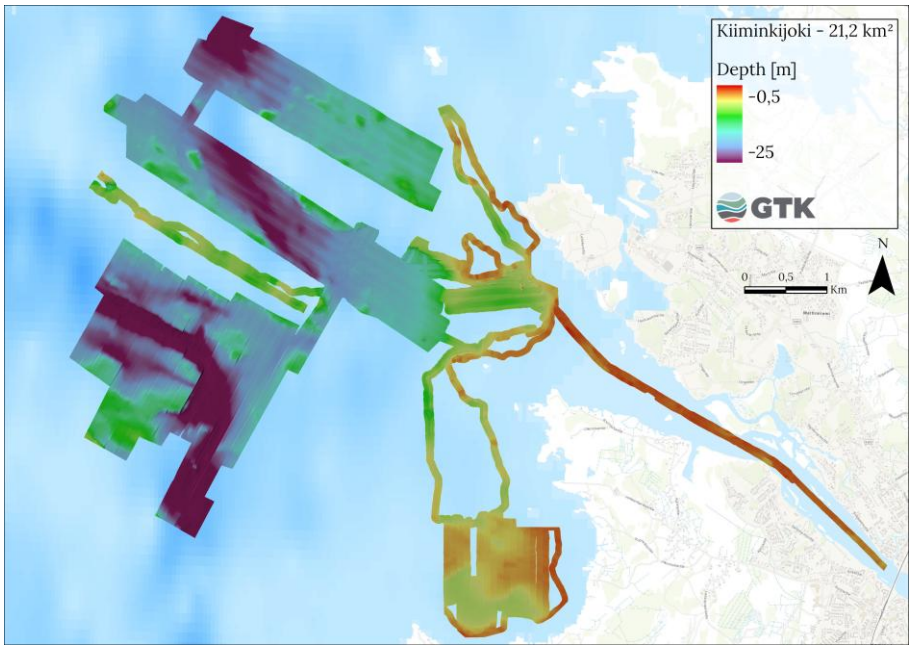

Figure 30. *Bathymetry map of the Kiiminkijoki area. In the deeper area the bathymetry is collected with PDBS, and the raster resolution is 5x5m. In the shallower river area and close to the shoreline the data is collected with MBES, and the raster resolution is 1x1m.*

3.5.3. Kalajoki

In the Kalajoki estuary, water depth ranges from 1.1 to 25 m, with the shallow coastal zone primarily shaped by dunes and sandbars. Similar to the Lohtajanjoki, the Kalajoki area contains submarine extensions of terrestrial eskers; however, these features are heavily eroded, and the seafloor deepens notably where the esker extending from land into the marine environment terminates (Fig 31). The seabed substrate consists exclusively of sand, and the area is characterized by sandy dunes. The geomorphology and the dominance of coarse material reflect strong influence of marine processes, with limited preservation of finer sediments. These conditions point to a high-energy environment where sediment transport and redistribution are continuous.

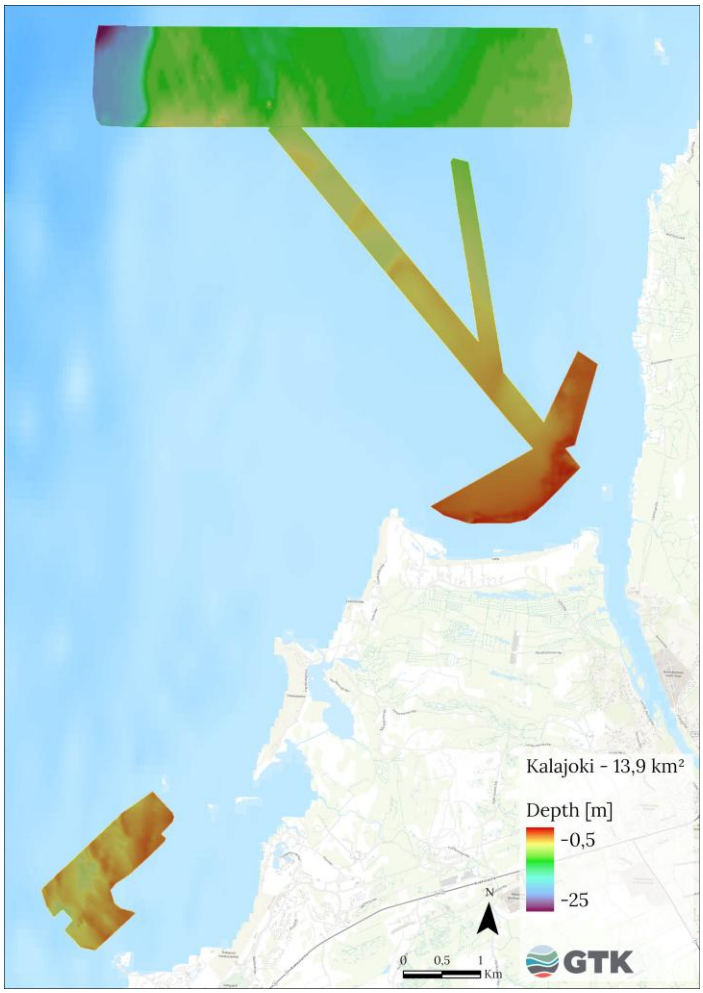

Figure 31. *Bathymetry map of the Kalajoki area. This bathymetry map is produced by interpolating depth points from sub bottom profiles. The resolution is 5x5m.*

3.5.4. Lohtajanjoki

In Lohtajanjoki area the seabed across the entire area is covered by a sand layer of variable thickness. Geomorphological features such as eskers observed on land extend onto the seabed. However, these features are strongly eroded, and the uppermost substrate predominantly consists of secondary sand derived from erosion. Drop-camera observations revealed distinct ripple marks, indicating active sediment transport. The thickest sand accumulations occur near the shoreline, while elsewhere, underlying brackish-water mud and glacial clay are overlain by at least a thin layer of sand. Water depths vary from 0,7 to 15,4 m. The shallowest areas are in the inner parts of the estuary and along the sandy shoreline. The northern part of the study area is the deepest, where depressions and pits can be seen (Fig 32).

The presence of erosional structures indicates highly dynamic environmental conditions, likely driven by wave action and seasonal sea ice movement. At the mouth of the estuary, where it opens to the sea, depression zones are present, with the seabed composed primarily of till and bordered

by sharp-edged hard clay. These features are likely formed through erosion driven by bottom currents or the mechanical action of packed sea ice. The area is particularly susceptible to thick ice masses accumulating against the shoreline. The seabed here is less suitable for fine sediment accumulation, reflecting the openness of the estuary to marine influences. In contrast, the innermost part of the estuary is shallow and sheltered, with substrates dominated by organic-rich mud. These soft sediments, coupled with shallow depths and sheltered conditions, emerge as potential habitats for dense vegetation.

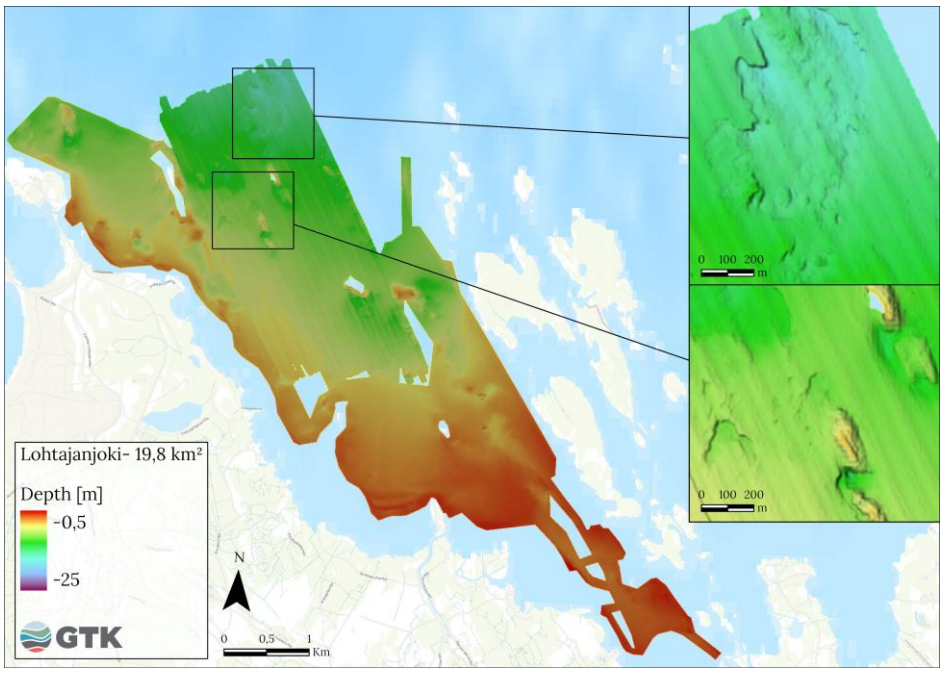

Figure 32. *Bathymetry map of the Lohtajanjoki area and detailed pictures of the depressions and scrape marks. In the deeper area the bathymetry is collected with PDBS and the raster resolution is 1x1m. The shallower area is modelled by interpolating depth points from sub bottom profiles. The resolution for the shallow area is 5x5m.*

The side-scan imagery provides more detailed information on substrate composition and the structure of the depression and the smaller scrape marks in Figure 33. The left side-scan image shows the larger depression, with its bottom appearing dark, indicating a till-dominated hard substrate. The surrounding walls are steep, and the adjacent plateau consists of softer material, mainly glacial clay. The right image displays smaller scrapes and pits, where darker areas correspond to harder material and lighter areas to softer sediments.

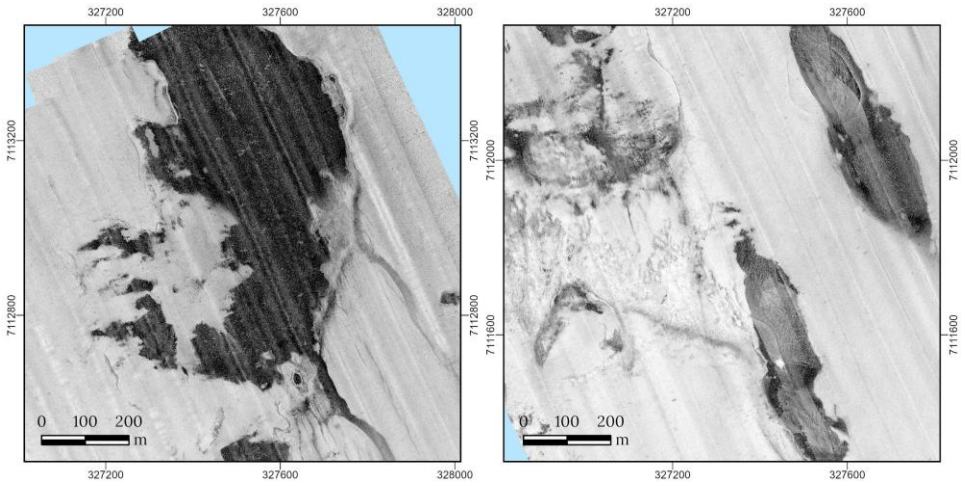

Figure 33. *Sidescan images showing the larger depression with hard substrate (left) and the smaller pits and scrape marks (right).*

3.5.5. Lapuanjoki

In the Lapuanjoki estuary the water depth varies from 0,5 to 21,7 m and the area is its shallowest within the inner parts of the estuary. The immediate vicinity of the river mouth is a clear sediment accumulation zone, dominated by loose, organic-rich mud. Further offshore, where wave action exerts greater influence, the seabed transitions into a highly dynamic depositional environment. The most interesting finding was elongated linear bedforms within a narrow strait-like channel as the estuary opens toward the sea. These linear dunes, with heights of 0.1 to 0.6 m and average widths of about 10 m, extend for almost 1 km (Fig. 34). They are composed of mixed mud and gyttja clay layers.

Longitudinal dunes are long, straight ridges that form when two forces of similar strength act from directions separated by a large angle; this causes sediment to accumulate and elongate parallel to the mean transport direction, producing stable dunes that persist over long distances and times (Reffet et al., 2010) . A small part of the Lapuanjoki study area was surveyed in 2024 and 2025 with MBES, and the results showed that these linear features are quite persistent and they did not move or deform significantly during the year. The dunes are aligned parallel to the dominant current and wind direction, yet they also experience wave energy arriving from a more perpendicular direction. In this estuarine system, strong wind driven currents from north aligned with the strait may interact with wave-driven oscillatory flows arriving from a different direction and be the main force forming these dunes. Alternatively, cohesive or stabilized sediments can also produce linear dune forms under unimodal winds (Rubin et al., 2009). In coastal estuarine settings, factors such as mud admixture, biologically mediated binding, or periodic exposure and consolidation can stabilize portions of the bed. Stabilized cells within the dune system could act as elongating lee features, encouraging deposition and crest extension parallel to the channel, even where flow is largely unidirectional.

The incoming river discharge together with the action of waves shapes the seabed, reflecting the continuous interplay between fluvial input and marine processes. To fully understand the seabed dynamics in the area further studies are needed.

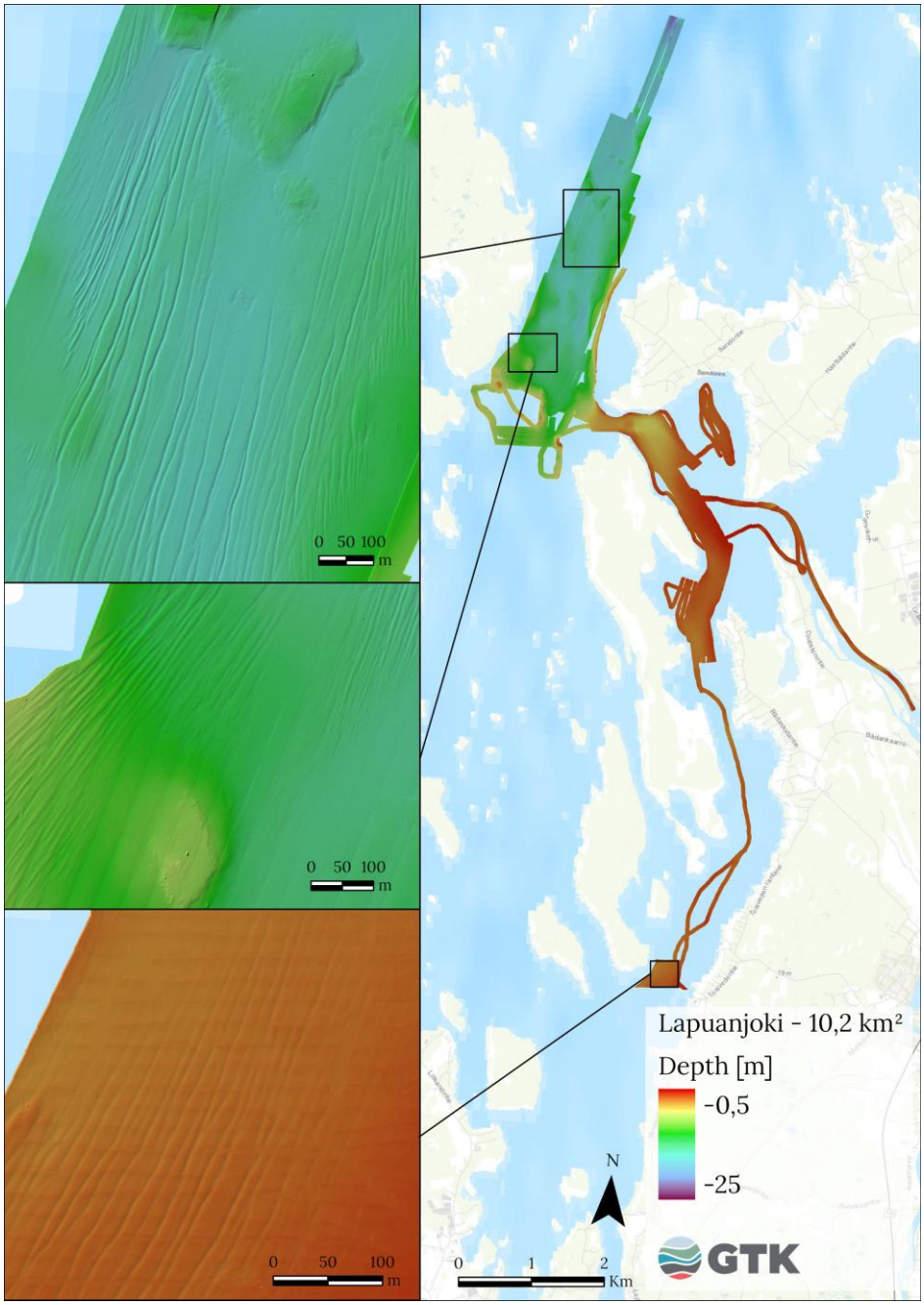

Figure 34. *Bathymetry map of the Lapuanjoki area and detailed pictures of the linear dunes. All the bathymetry data in Lapuanjoki is collected with MBES.*

3.5.6. Lapväärtinjoki

In the southernmost area, Lapväärtinjoki, water depths range from 1.6 to 13.6 m. The seafloor is relatively flat, characterized by bedrock or till-based

mound formations (Fig. 35). In the area, the seabed is dominated by soft sediments, with thick mud layers indicating ongoing sediment accumulation. The combination of sheltered conditions and shallow depths creates a favourable depositional environment, allowing fine-grained material transported by the river to settle and form a distinct sediment sink. The geomorphological setting shows minimal influence from wave action, resulting in relatively stable substrates. Notably, the seismic profiles consistently revealed a distinct layer of recently deposited sediment throughout the area.

Figure 35. *Bathymetry map of the Lapväärtinjoki area. In the deeper area the bathymetry is collected with PDBS, and the raster resolution is 1x1m. The shallower*

area is modelled by interpolating depth points from sub bottom profiles. The resolution for the shallow area is 5x5m.

3.6. Satellite derived bathymetry (GTK)

Bathymetry estimations were carried out in six locations in west coast of Finland. Each of them was in the vicinity of river estuary. As a reference data, in-situ depth measurements were done in six location using research vessel Gridi. Additional bathymetry measurements were done with research vessel Geomari, but it couldn't cover the intended shallower shores. SeaMoreEco project partners from Centre for Economic development, Transport and Environment Northern Ostrobothnia collected vegetation and depth information from depths of 0 to 3 meters in Kalajoki area. However, bathymetry modelling was done only with data from R/V Gridi.

In all the six locations best correlation between measured and modeled values was obtained with values from band 1 (coastal aerosol) and band 4 (red). Only in Lohtaja were bands B1 and B3 nearly as good as B1 and B4. Typically, however, bands 2 (blue) and 4 (red) gave nearly similar results as with bands 1 and 4. The curves in Figure 36 shows best fit trendline between calculated satellite image values and measured depth in the six locations.

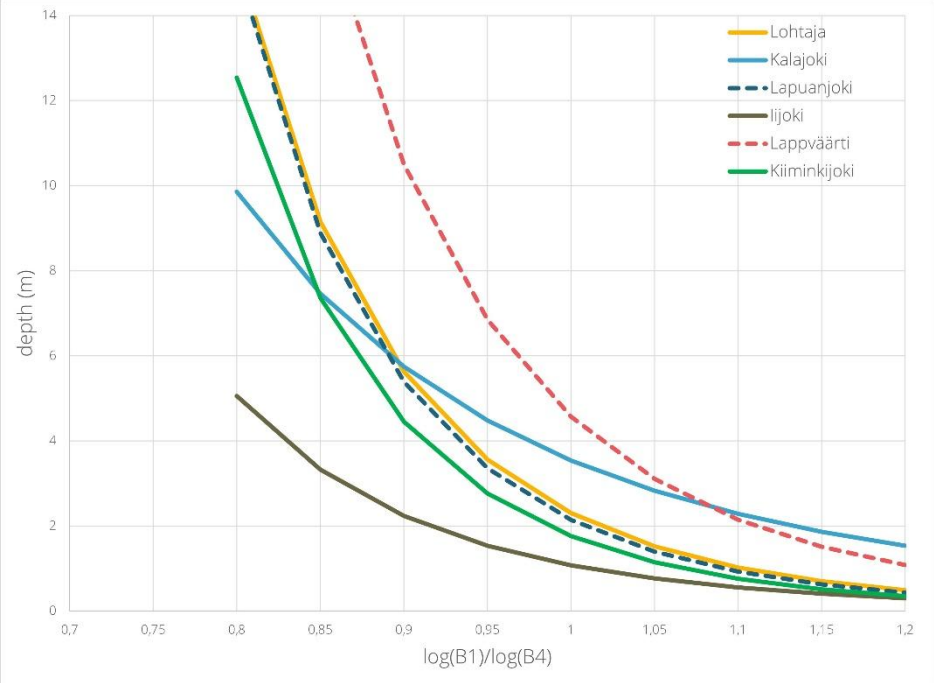

Figure 36. *Trendlines to calculate bathymetric map.*

Interestingly, Lohtaja, Pietarsaari (Lapuanjoki) and Haukipudas (Kiiminkijoki) are closely similar equations with each other. Kalajoki, Kristiinankaupunki (Lapväärtinjoki) and Iijoki each following their own optical response.

Table 22 shows the equation, which was used to calculate bathymetry values from Sentinel-2 image derivative log(Band1)/log(Band4). Four, five and two

in the names tells how many best images were averaged to get the best results.

Table 22. *Equations to calculate bathymetry from Sentinel-2 images.*

Study area	Equation
Lohtaja_CAdR_four	2,3006*X^-8,494
Kalajoki_CAdR_five	3,5403*X^-4,588
Pietarsaari_CAdR_four	2,1378*X^-8,767
Kristiinankaupunki_CAdR_four	4,5659*X^-7,899
Iijoki_CAdR_two	1,0762*X^-6,937
Haukipudas_CAdR_meanfour	1,7605*X^-8,799

Kalajoki and Lohtaja are two research sites, which are located next to each other. The two areas resemble each other, both being situated next to sandy peninsula. Both are next to open sea, allowing occasional alqae/pollen rich surface water change with clearer water. Modeled bathmetry correlates rather well with acoustic measurements, with R2 values of 0,752 and 0,796, respectively. Modelled bathymetry and resulting graph of Kalajoki area are shown in Figure 37 and Modelled bathymetry and resulting graph of Lohtaja area are shown in Figure 38.

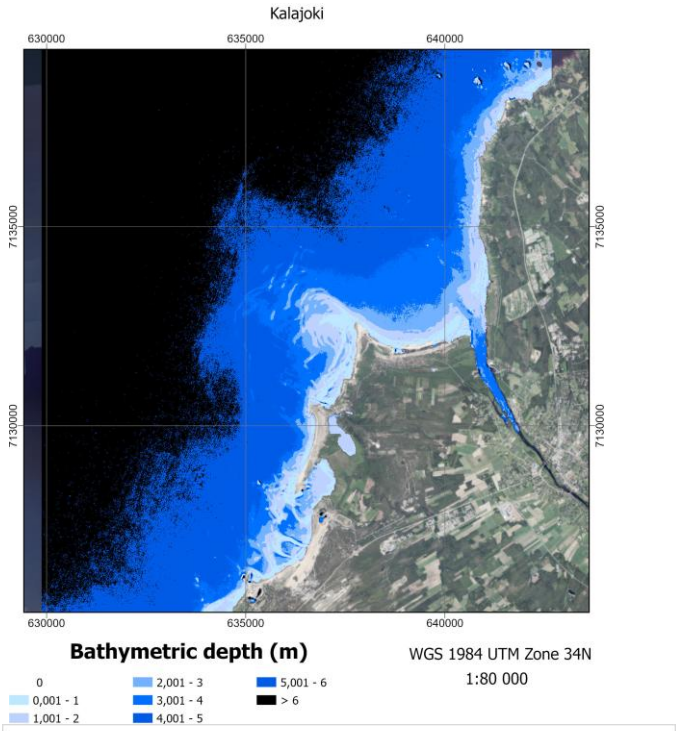

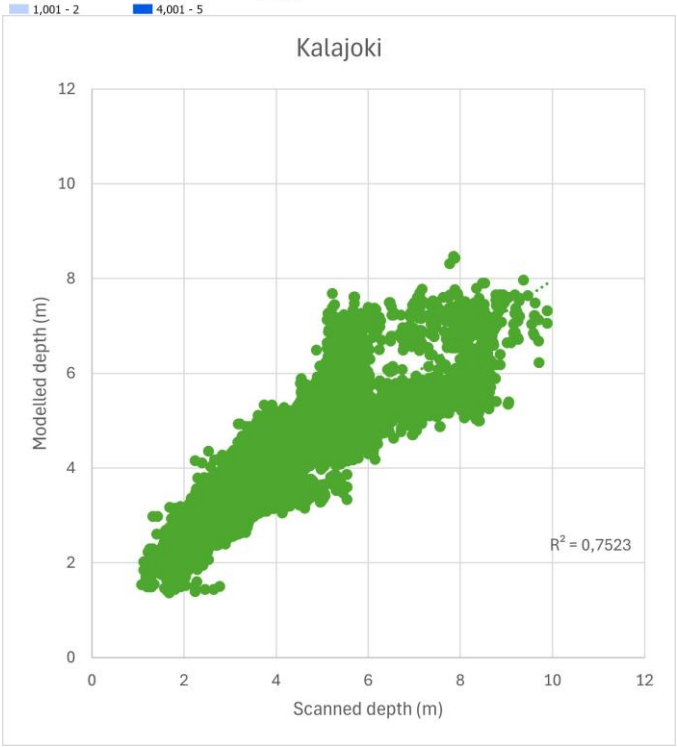

Figure 37. *Bathymetry in Kalajoki and comparison graph of modelled and measured water depth.*

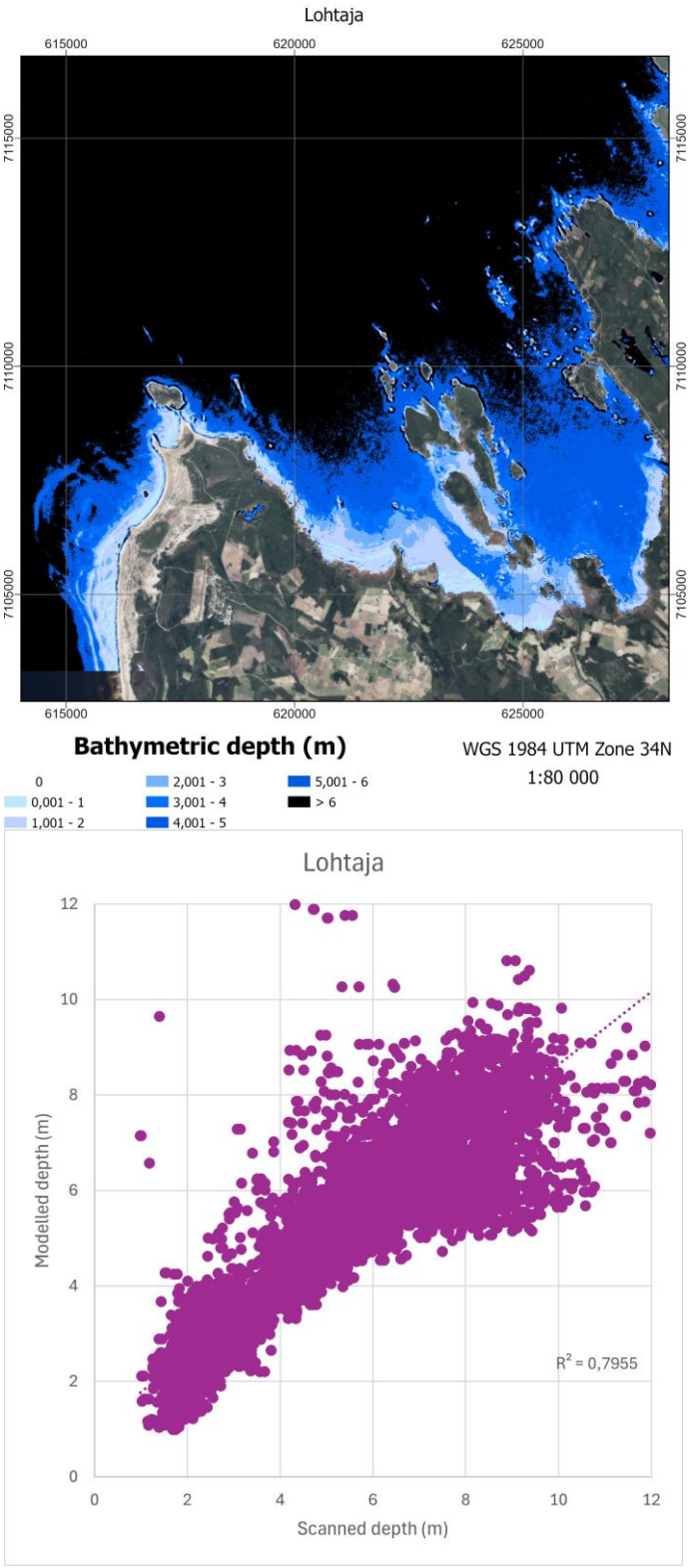

Figure 38. *Bathymetry in Lohtaja and comparison graph of modelled and measured water depth*

In Lapväärtinjoki area majority of the survey line points were from deeper water depths, and Sentinel-2 images didn't show reliable difference between water depths deeper from 6 m (Fig. 39).

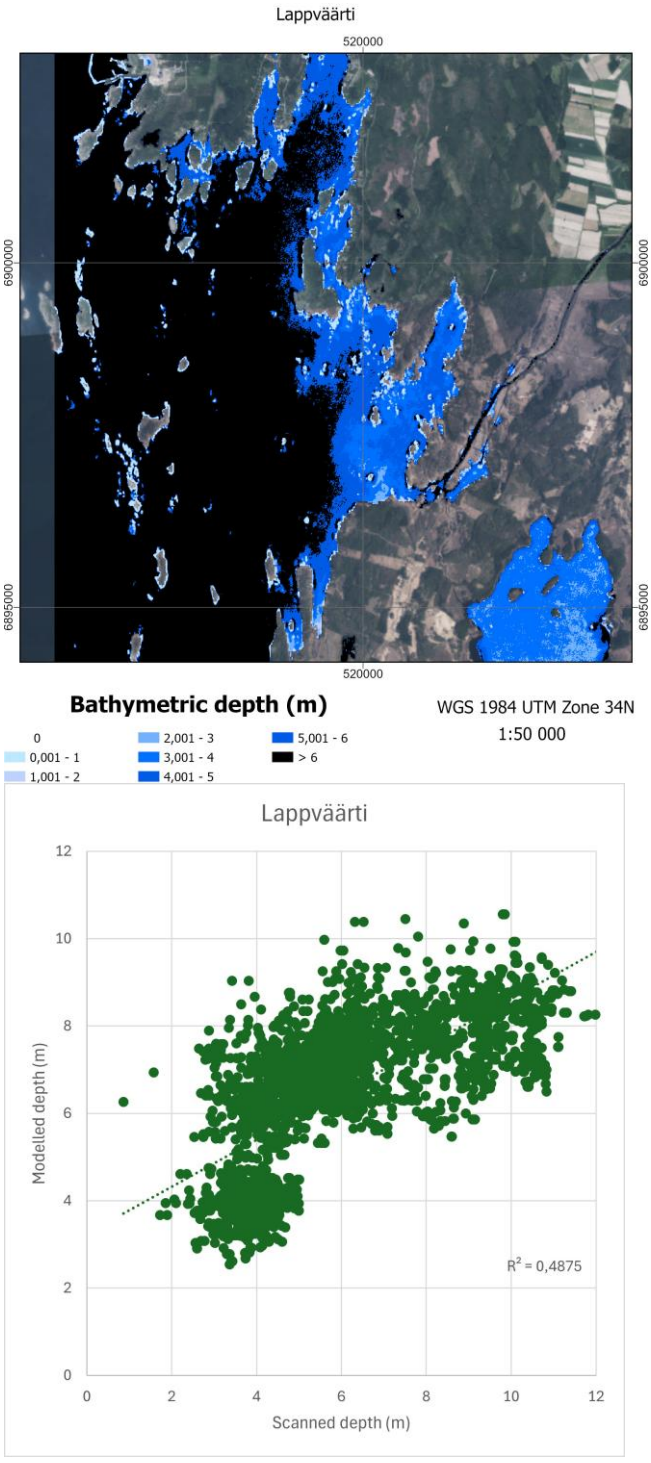

Figure 39. *Bathymetry in Lapväärtti and comparison graph of modelled and measured water depth.*

In Lapuanjoki the area surveyed with echo sounders was partly river estuary and mainly sheltered inland bay with river influx. Sediment rich water from

inland river dominates in our research area. Depth estimations showed rather low reliability. (Fig. 40).

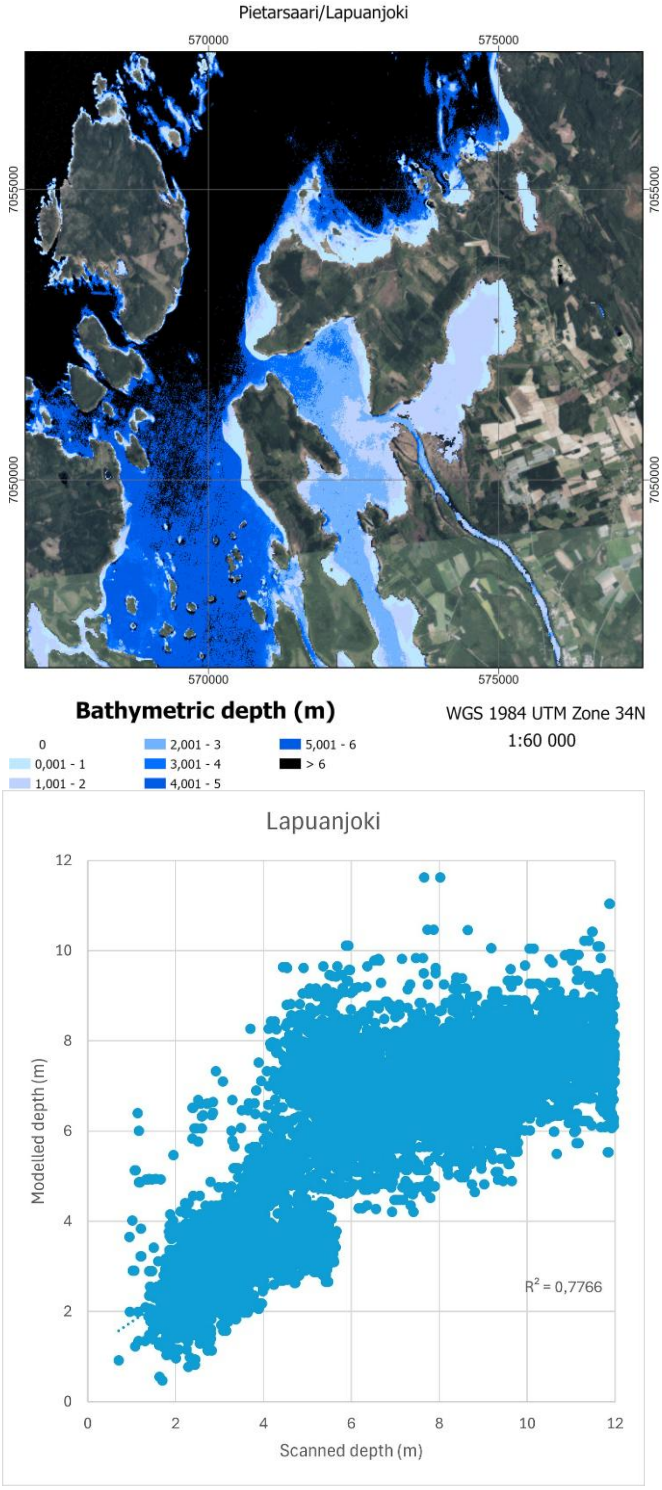

Figure 40. *Bathymetry in Lapuanjoki and comparison graph of modelled and measured water depth.*

The survey lines in Kiiminkijoki area were mainly done in too deep waters, to be of good help in bathymetry estimations (Fig. 41).

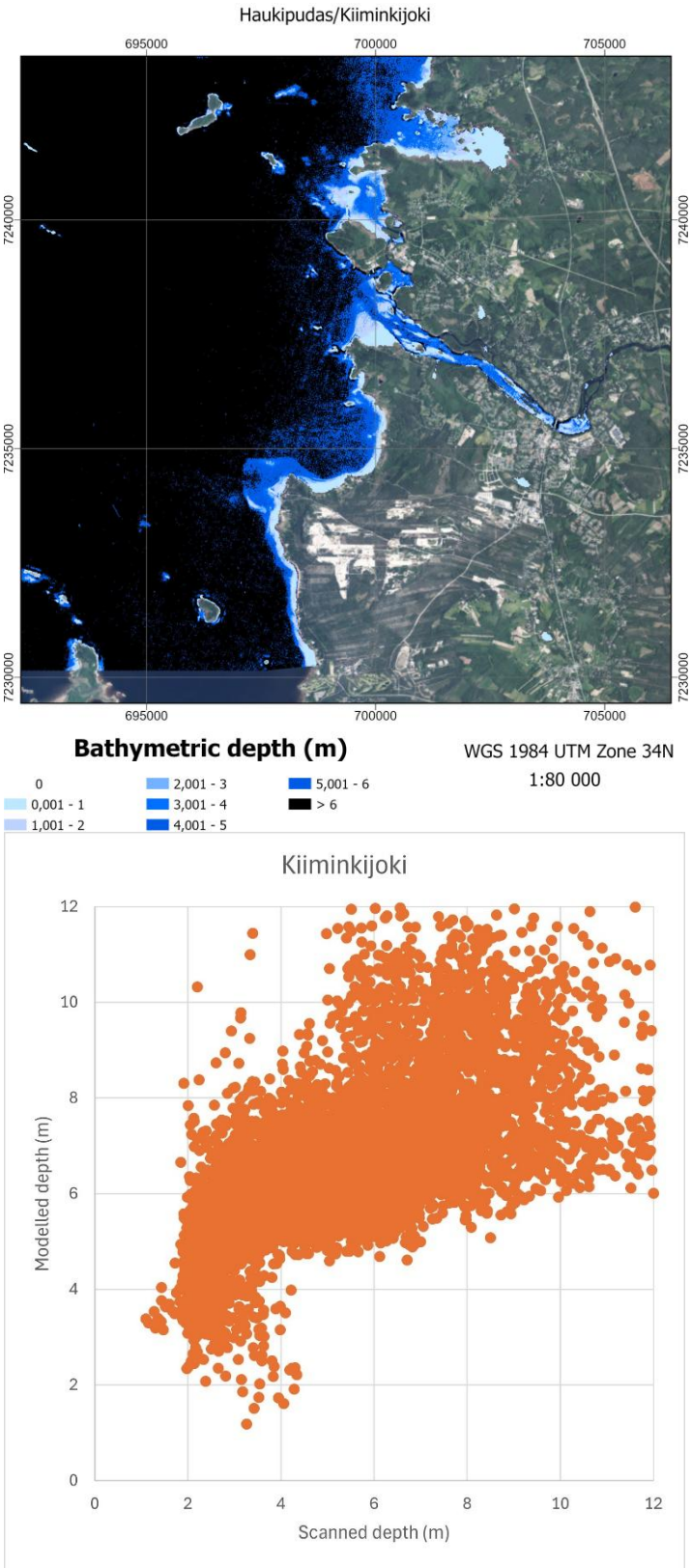

Figure 41. *Bathymetry in Kiiminkijoki and comparison graph of modelled and measured water depth.*

In Iijoki area, the only scanned survey line was along the river, and it proved to be impenetrable by visual light. All the water showed similar signals, disregarding the scanned depths of the water (Fig. 42).

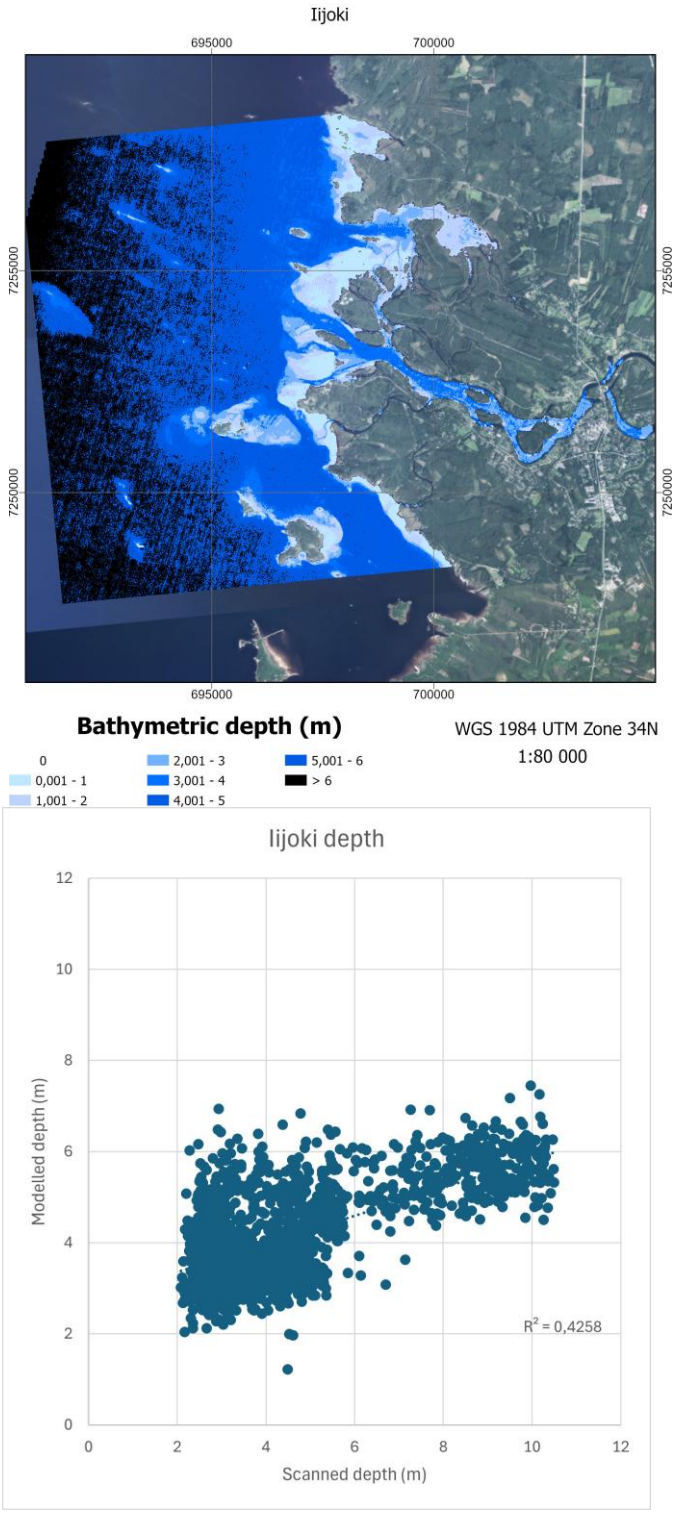

Figure 42. *Bathymetry in Iijoki and comparison graph of modelled and measured water depth.*

In generally, shallow area bathymetry estimation with Sentinel-2 seems to be reasonably reliable, at least in most of the locations. Main issue is to choose cloud free images at the time with no algae, sedimentation/sediment in suspension or other interference to water optical properties. Referencing depth measurements should cover different kind of marine sub areas. Flowing rivers, deltas and stagnant bays as well as open sea should all be covered within survey lines. Furthermore, reference soundings deeper than 10 m provide only a little to help with bathymetry estimations.

3.7. Satellite derived seabed substrates and vegetation coverage (GTK)

Satellite derived substrate mapping was done only for Kalajoki area where shallow seabed substrate consists exclusively of sand (Figure 43). According to aerial image (Land Survey of Finland) and Superficial deposits map (GTK) the coast located on the north-eastern side of the Kalajoki river estuary consists of moraine. This could not be distinguished due to the coarse resolution of satellite imagery.

The maximum mapping depth was about 6–7 m. Even shallower areas were partly optically deep or possibly covered by vegetation, which is why seabed substrate types could not be classified more detailed than unvegetated/vegetated.

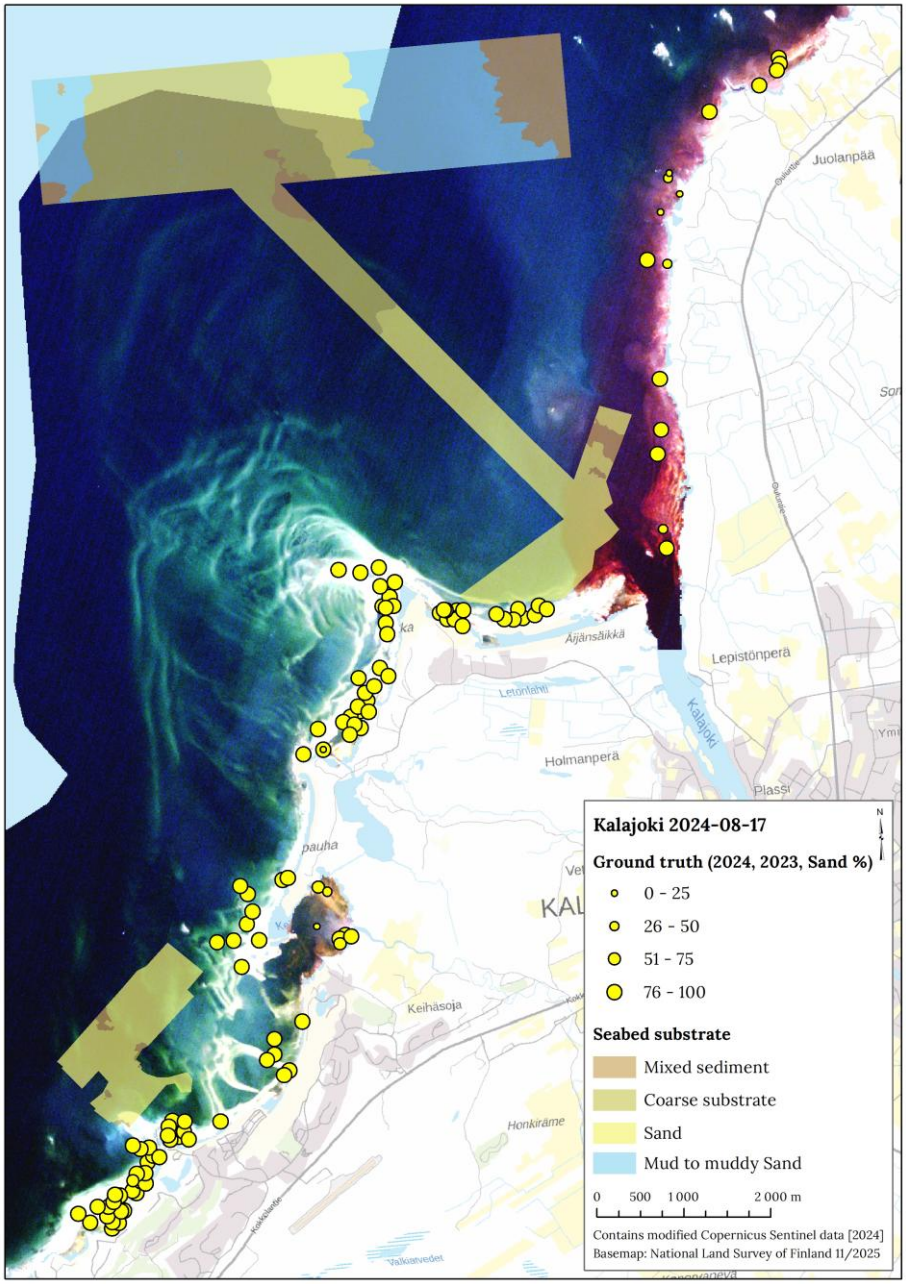

Figure 43. *Seabed substrates in Kalajoki.*

Substrate mapping was done using the satellite image acquired on 2024-08-17. Different band combinations were tested. For this site, the best results were obtained using bands 3–4 and bands 2–5 along with their depth-invariant indices (Fig. 44). As seen in Figure 44, the classification results (unvegetated and vegetated areas) are well-defined in the shallow near shore areas, whereas in deeper regions the classification appears more fragmented using bands 3–4. Areas that are likely unvegetated at greater depths seem to be often misclassified as vegetated. Using bands 2-5, the classification is more uniform in the shallow near shore areas but fails to resolve deeper

areas. In the eastern Kalajoki river estuary the unvegetated zones are often misclassified as vegetated.

Scuba divers collected vegetation and depth information from depths of 0 to 3 meters in the Kalajoki area. This ground truth data is classified according to amount of vegetation (%). No ground truth data were available from the deeper parts of the study area, which prevents validation of the classification in those zones. It should be noted that the ground truth points in the eastern part of the study area were collected in 2023 and include very few observations of vegetation. This limitation affects the reliability of classification in that region.

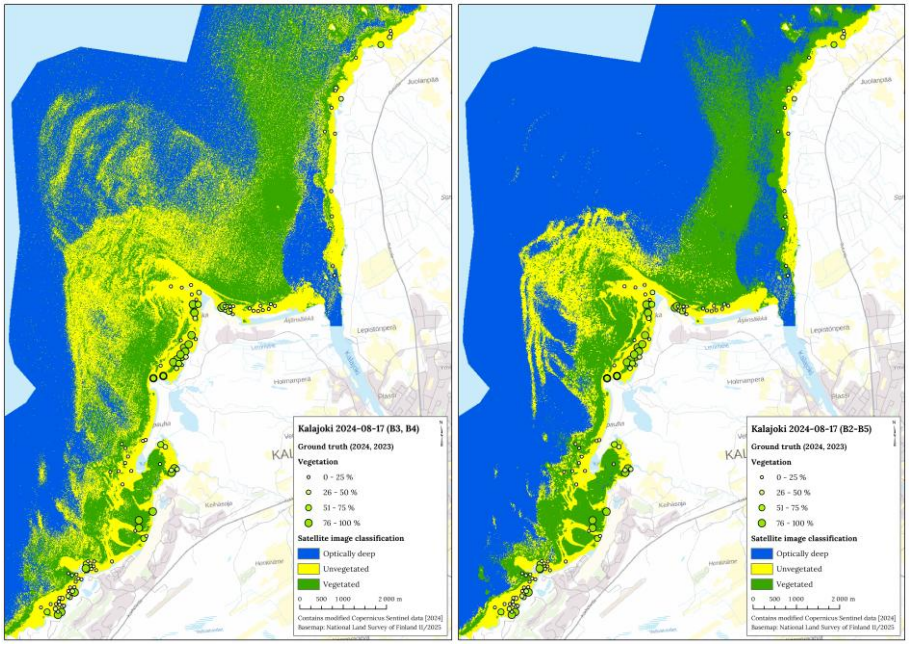

Figure 44. *Classified distribution of submerged aquatic vegetation (SAV) and unvegetated bottom in Kalajoki area from Sentinel-2 satellite image 2024-08-17 using bands 3 -4 and bands 2 -5 along with their depth-invariant indices and showing the ground - truth data (2024, 2023) as points.*

Drone based classification in Kalajoki wetlands area was used to evaluate the accuracy of the satellite image classification results (Fig. 45). Resolution of the drone-based classification is 1 m x 1 m. Resolution of the satellite-based classification is 10 m x 10 m. Broad unvegetated shallow areas are rarely classified vegetated from the satellite image in the entire study area. There are some areas in the southern part of the wetland area where regions identified as unvegetated by drone-based observations have been classified as vegetated in the satellite-derived data (Fig. 45). The classifications of broad shallow areas covered by dense vegetation are quite consistent. Small, patchy vegetated areas seem to be classified as unvegetated from satellite image. Using bands 2-5, the spatial patterns of classes are more consistent and cover broader extents.

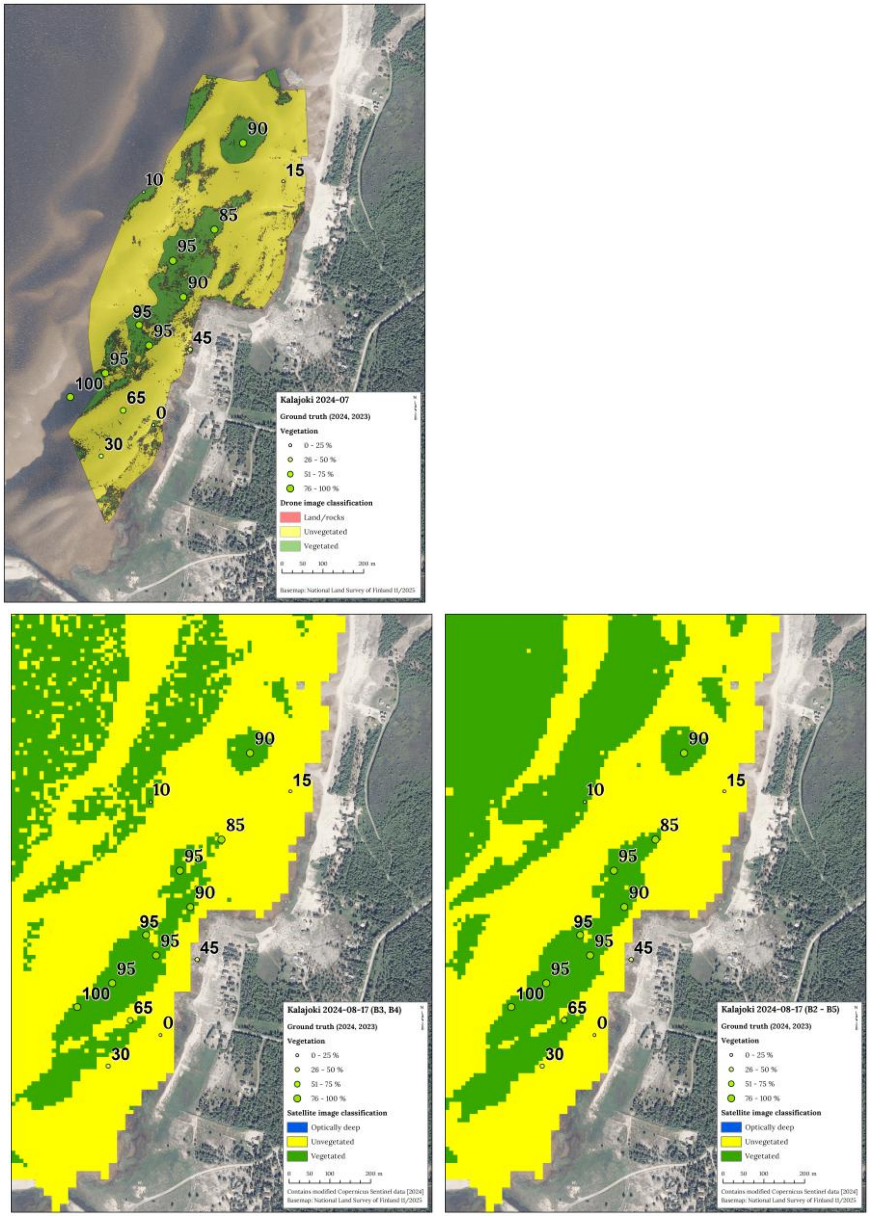

Figure 45. *Classified distribution of SAV and unvegetated bottom in Kalajoki area from drone and Sentinel-2 satellite images using bands 3–4 and bands 2–5 along with their depth-invariant indices and showing the ground-truth data as points.*

As shown in Figure 43, the river water has a distinct coloration compared to other parts of the study area. The depth-invariant index (DII) is calculated under the assumption of uniform water properties across the entire area. Therefore, it was studied if areas influenced by river or turbid water could be identified from the data. Sentinel-2 data from different bands is shown in Figure 46.

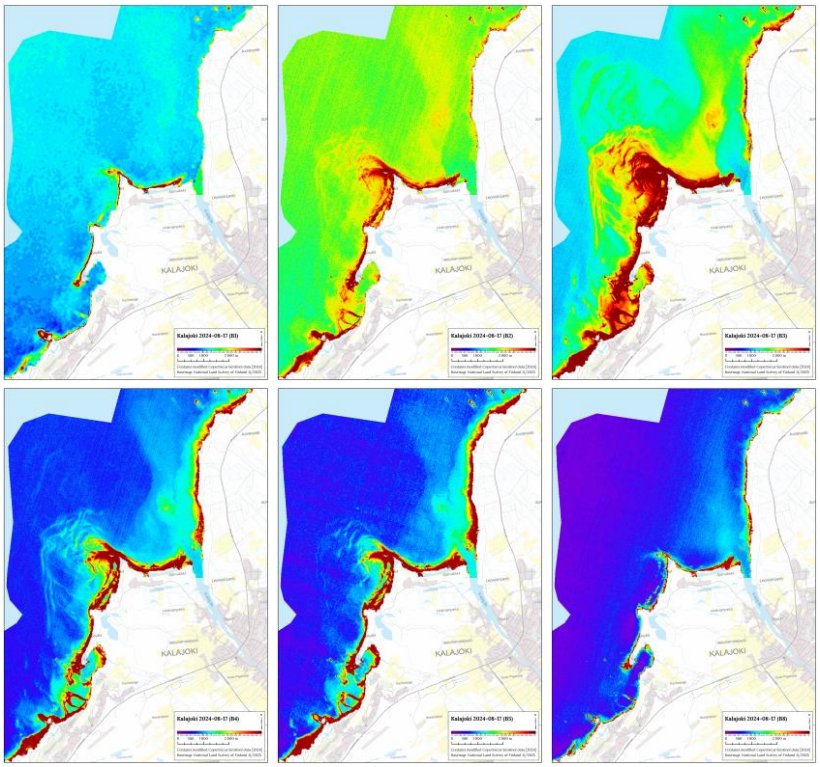

Figure 46. *Sentinel-2 data from different bands (2024-08-17).*

Some indices were tested for identification of different water types. The Normalized Difference Turbidity Index NDTI (= (red_factor * red - green_factor * green) / (red_factor * red + green_factor * green) algorithm was developed for the measurement of water turbidity in small ponds (Lacaux et al. 2007). High NDTI values represent high turbidity, while low values represent low turbidity. Turbid water can be seen in front of the Kalajoki river mouth (Fig. 47). However, there are shallow, unvegetated and sandy areas in the central part of the area, which appear relatively clear in the true color image, but have slightly high NDTI values.

The Redness Index RI (= (red_factor * red * red_factor * red) / (green_factor * green * green_factor * green * green_factor * green) algorithm was developed to identify soil color variations (Pouget et al. 1991). It may be used in identifying zones affected by river water as seen in Figure 47. High RI values appear in front of the Kalajoki river mouth. Higher RI values can be seen also further south in Keihäslahti in front of the river mouth.

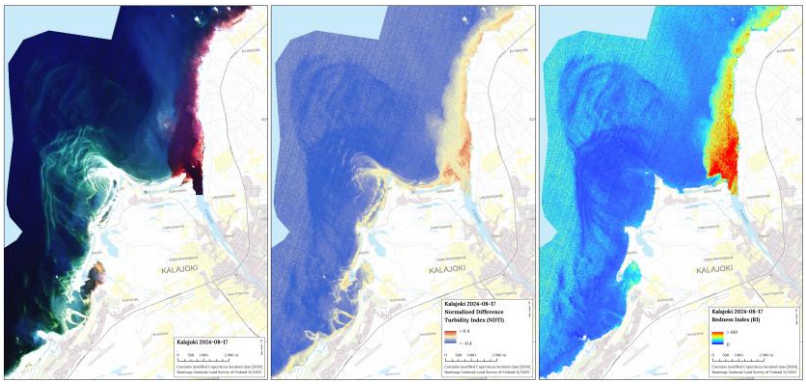

Figure 47. *True Color image, The Normalized Difference Turbidity Index and The Redness Index in Kalajoki area from Sentinel-2 satellite image (2024-08-17).*

It may be possible to identify different water types/qualities (clear, turbid, riverine influenced waters) and use them to improve substrate classification. Segmenting areas based on water characteristics prior to classification or using water type as auxiliary data may give more reliable results.

Substrate classification was tested using redness index (RI) as auxiliary data. A new class, unvegetated seabed in turbid water, was created and training vectors were placed in the high RI areas. Classification was done using different bands, their depth-invariant indices and Redness Index (RI). Classification results are in Figure 48. Although the differences compared to previous classification are minor, the area of unvegetated bottom near the shore expands somewhat in the east. This corresponds slightly more closely to ground truth points in the riverine influenced water zones. It should be noted that also the optically deep zones expand in the north-east.

Substrate classification cannot be further examined with the current dataset, as there are only a few vegetation observations from the turbid water areas, and no ground truth data are available from deeper regions.

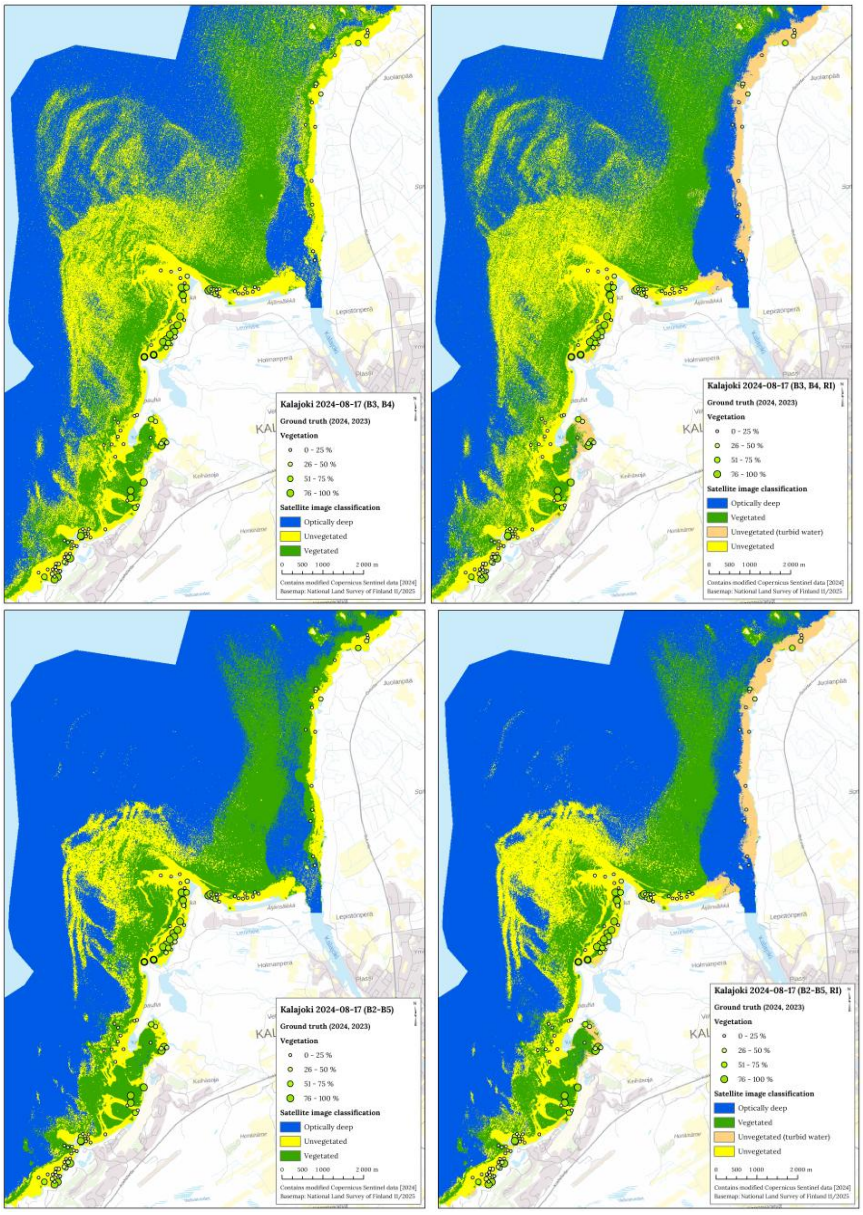

Figure 48. *Classified distribution of SAV, unvegetated bottom and unvegetated bottom in turbid water in Kalajoki area from Sentinel-2 satellite image 2024-08-17 using bands 3 -4 and their depth-invariant index and Redness Index (RI) and bands 2 -5, their depth-invariant indices and Redness Index (RI) and showing ground - truth data (2024, 2023) as points.*

In Lohtajanjoki some acoustic-seismic profiles showed dense vegetation. It was visible especially in high-frequency sub-bottom profiler data, where tall vertical vegetation stood out. This enabled the estimation of vegetation height in the region using Chirp profiles. Meridata MDPS software was used to determine the seabed depth/seabed surface and the upper boundary of the vegetation (Fig. 49). It is important to note that the estimated height is approximate due to the limited resolution of the survey equipment in depicting vegetation. The height was interpolated using the IDW

geoprocessing tool in ArcGIS Pro, resulting in a map that illustrates hot spots of dense vegetation.

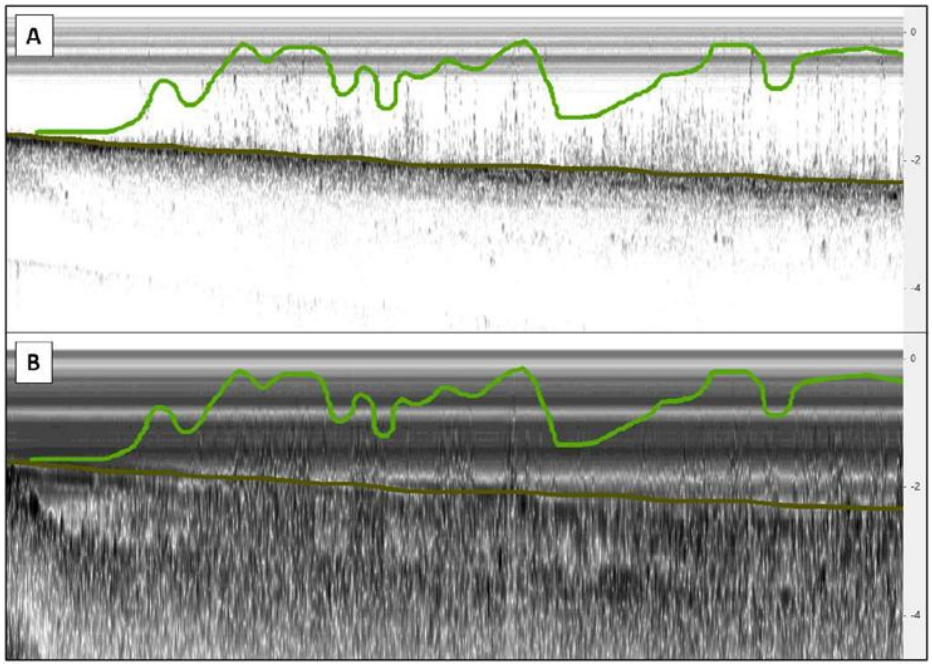

Figure 49. *High-frequency sub-bottom profiler. B: Low-frequency sub-bottom profiler. In both pictures the vegetation layer is marked with green and the seabed surface with brown.*

Map in Figure 50 illustrates the height of the dense aquatic vegetation, that was mainly recognized as Potamogeton perfoliatus in the field. The vegetation reaches heights of over 2.5 meters at its peak. The highest vegetation in Lohtajanjoki area is found in the 2.5 – 3.5-meter depth zone near river mouths. It appears in patches primarily on top of the brackish water mud. However, the densest clusters are found in regions of organic-rich recent mud. There is also erosional sand on top of the seabed and mixed into to the surface sediment. The sand makes the reflection of the seabed stronger making it easier to distinguish the seabed from the vegetation.

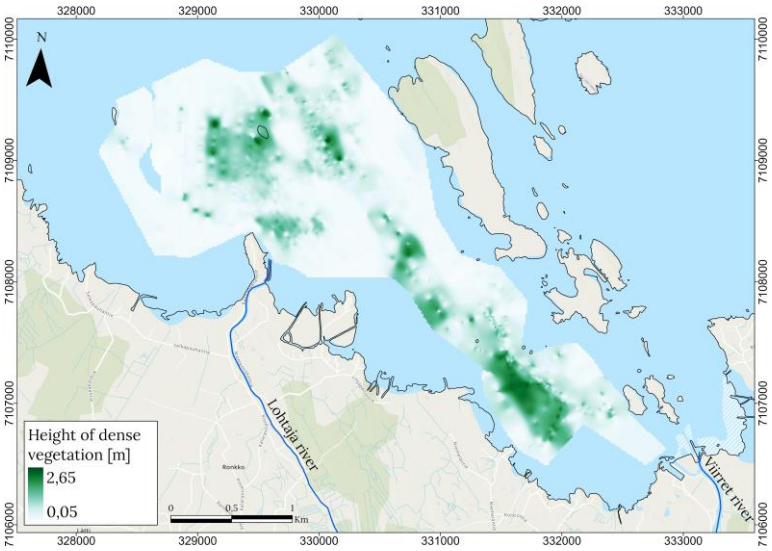

Figure 50. *Estimated height of the dense vegetation in Lohtaja area. The darker green shows the areas where the highest vegetation is growing.*

Vegetation coverage was estimated using Sentinel-2 satellite image acquired on 2023-08-26. No ground truth data was available for the area, which limits the validation of the results.

The surveyed area includes rocks, boulders and mud which could not be distinguished in the satellite imagery. Additionally, turbid water zones occur in study area, especially in the south-eastern part, which increases the complexity of classification (Fig. 51). Substrates could not be classified more detailed than unvegetated/vegetated.

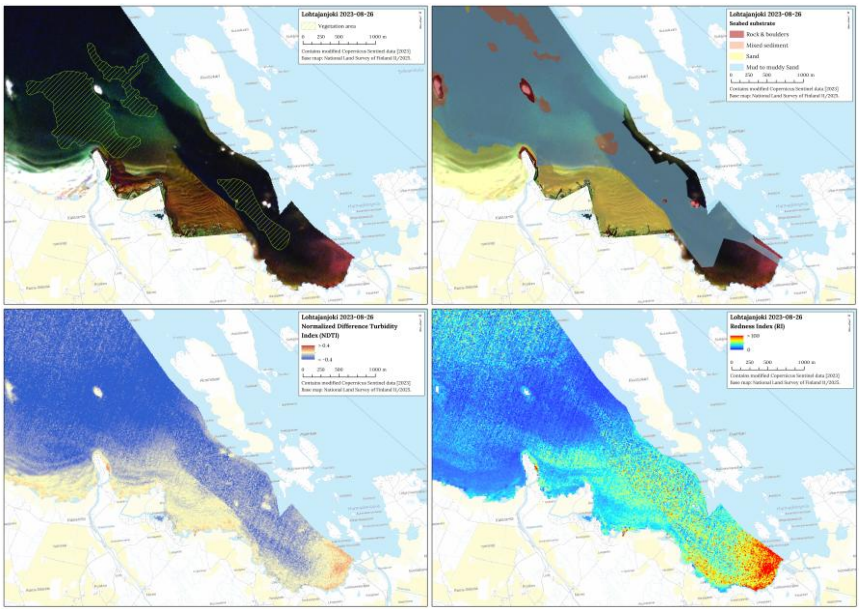

Figure 51. *True color image with vegetation area based on side-scan image, Seabed substrates from acoustic-seismic profiles, The Normalized Difference Turbidity Index and The Redness Index in Lohtaja area from Sentinel-2 satellite image 2023-08-26. True color images include drone image.*

Based on the available imagery, a rough estimate of the vegetation-covered area was made using bands 3–4 along with their depth-invariant index (Fig. 52). The reliability of the estimate cannot be confirmed due to the lack of ground truth or drone-based classification data. The vegetated area appears to partially coincide with the vegetation zones previously interpreted from side-scan images.

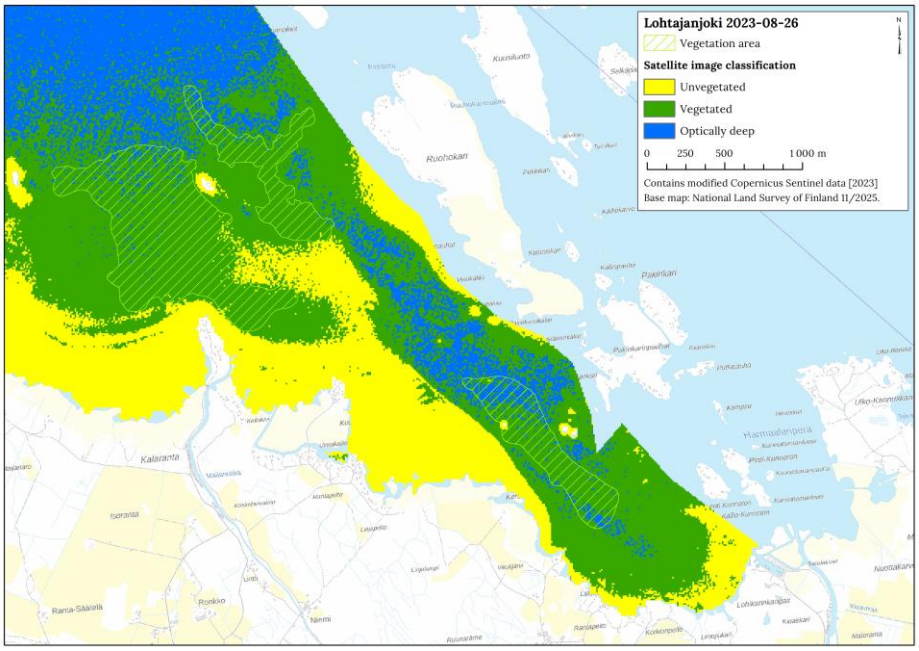

Figure 52. *Classified distribution of SAV and unvegetated bottom from satellite image 2023-08-26 using bands 3–4 along with their depth-invariant index and vegetation area based on side-scan images.*

3.8. Integrated data on seabed geology

Figure 53 presents a combined visualization of phase differencing bathymetric sonar (PDBS) data, point-derived bathymetry from sub-bottom profiles, and satellite-derived bathymetry. The PDBS dataset provides the highest spatial resolution at 1 × 1 m, while the SBP-derived bathymetry has a resolution of 5 × 5 m, interpolated from depth points extracted along the sub-bottom profiles. The satellite-derived bathymetry represents the coarsest dataset at 10 × 10 m.

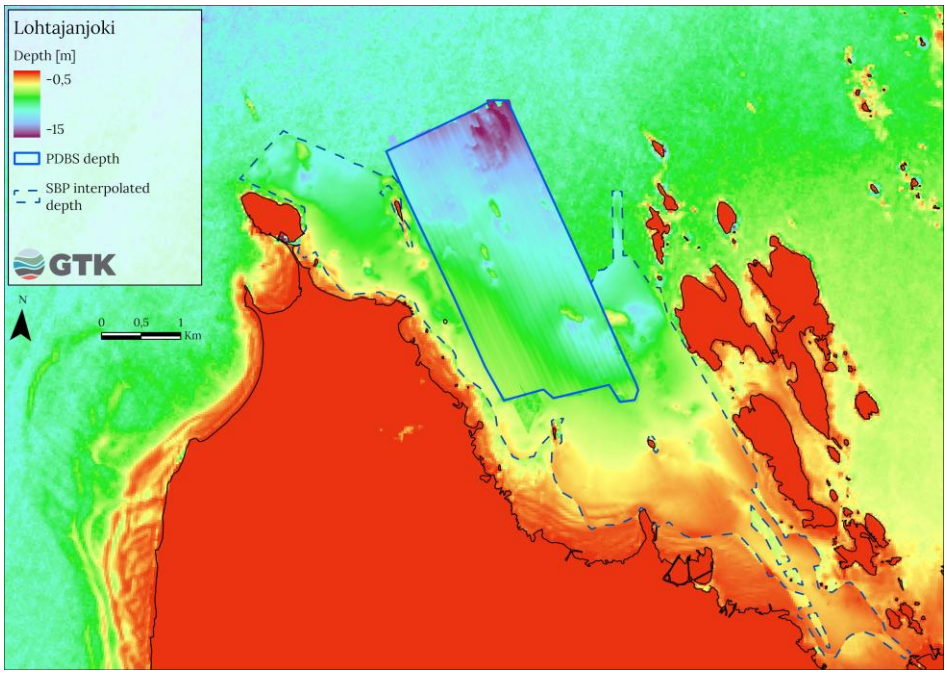

Figure 53. *Combined bathymetry data from satellites, echo sounders and sub bottom profiles in Lohtajanjoki area. The satellite derived bathymetry is on the background. Blue border indicates the bathymetry collected with PDBS (Phase Differencing Bathymetric Sonar). And the dashed line indicates the area where the bathymetry is interpolated from sub bottom profiles.*

As shown in the image, satellite data performs reasonably well in very shallow areas, where it captures the general morphology of coastal dunes and sandbars. These larger depositional features are clearly visible and align broadly with the higher-resolution acoustic datasets. However, the performance deteriorates rapidly with increasing depth. The ability of satellite data to capture true seabed morphology rapidly declines beyond approximately 3 m depth, and fine-scale features are progressively lost. In deeper areas, particularly toward the boundary between the PDBS and satellite datasets at around 15 m depth, the satellite product fails to detect the actual seafloor and is clearly outperformed by the higher-resolution acoustic data.

These results indicate that satellite-derived bathymetry can complement acoustic and seismic surveying, particularly in shallow waters where it reliably captures depths of roughly less than 3 m. However, in the deeper and typically turbid waters of the Bothnian Bay, satellite data cannot detect the seabed, and its spatial resolution is too coarse to resolve small-scale morphological features. Consequently, fine structures such as the dunes off the Lapuanjoki and Iijoki estuaries remain beyond its detection capability. Larger seabed features such as major sandbars in the Kalajoki and Lohtaja areas can nevertheless be identified, making satellite data useful for monitoring broad-scale seabed morphology, shoreline change, and land uplift. Detailed investigation or monitoring of small-scale geological features still requires vessel-based or unmanned surface vehicle-based surveys

equipped with sufficiently high-resolution bathymetry sonars. In clear-water environments, drones can provide additional insight into vegetation patterns, shallow structures, and general seabed conditions, but precise mapping always requires complementary sampling or high-resolution acoustic data.

3.9. Sediment analysis/studies

Sedimentation rates

To estimate recent sedimentation rates in the study areas, a total of 28 sites (out of 92) were examined. The sampling locations, from water depths between 1–23.2 m, were selected carefully using acoustic-seismic profiles. Sediment cores were recovered from five different areas in Finland, from the vicinity of Lapväärtinjoki estuary, Lohtajanselkä area, Kalajoki area, and from Lapuanjoki, Kiiminkijoki, and Iijoki estuary (Fig. 7).

In most of the sediment cores, 21 of the 28 cores, 137Cs activity content in the deeper part of the sediment core was zero or close to zero. In four sediment cores, 137Cs profile was unclear. Typically, 137Cs profiles show a sharp or a relatively sharp upward increase that forms the peak or maximum 137Cs value (Fig. 54A, C and D). Values then decrease gradually towards the sediment surface. Most sediment cores clearly showed these subsurface 137Cs activity content maxima. Maximum 137Cs values in the sediment cores occurred from 1.5 to 67 cm depths with an average depth of 18.5 cm for maximum 137Cs contents. This maximum here corresponds to the Chernobyl nuclear power plant accident in April 1986, and it is used for calculations of sedimentation rates.

Four sediment cores showed increasing 137Cs contents downcore without clear maxima. The lack of maxima (or maxima at the bottom of the sediment core) may arise from their young age range (Fig. 54B).

The deepest examples of a 137Cs maxima occurred in sediment cores from Lapuanjoki estuary (core MGGN-2024-20, 67 cm; and core MGKA-2024-3, 34.5 cm) and Lapväärtinjoki estuary (core MGKA-2023-7, 31.5 cm).

The depths of 137Cs maximum in cores indicate relatively high sedimentation rates. Post-Chernobyl, i.e. after AD 1986, linear sedimentation rates varied from 0.18 to 1.76 cm/year with an average value of 0.55 cm/year.

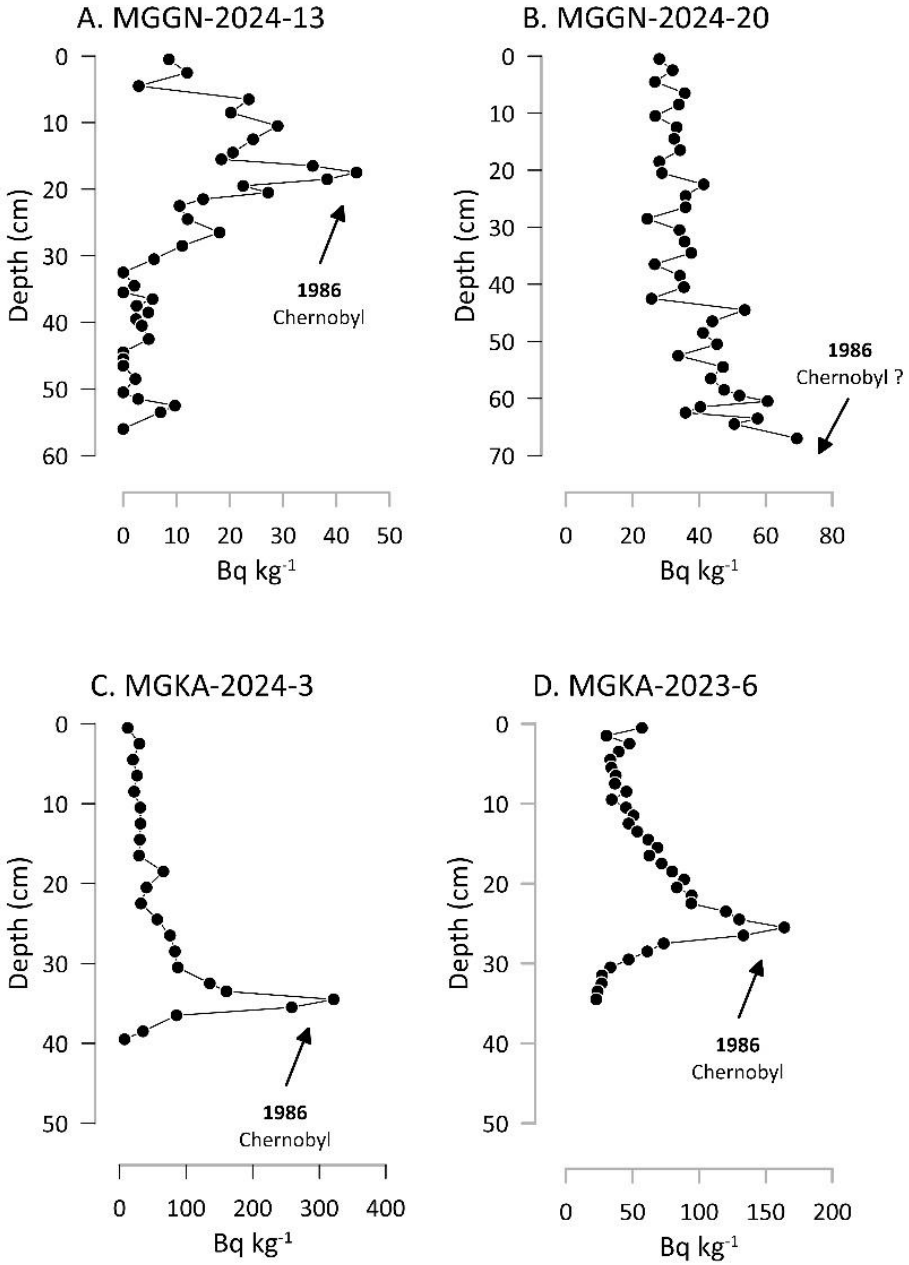

Figure 54. *137Cs activity contents (Bq kg-1) down-core vs. depth (cm) profiles from selected sediment cores (A–D) taken in the Gulf of Bothnia. Stratigraphical marker horizons are labelled, and ages are given in years AD.*

Harmful substances in the sediments

To investigate the occurrence and concentrations of environmentally harmful substances in sediments, 24 sampling sites were examined within the SeaMoreEco area of the Gulf of Bothnia. In total, 58 elements were analyzed; this report focuses on four major heavy metals: cadmium (Cd), lead (Pb), zinc (Zn), and mercury (Hg).

Cadmium concentrations in sediment cores generally increase upward from the bottom of the sediment core toward subsurface maxima, which occur at depths of ca 10-30 cm depending on sedimentation rates. Above these maxima, concentrations decline toward the surface, representing present-day conditions (Fig. 55 and 56). The highest subsurface Cd concentrations (>1.3 mg/kg) were observed in the core MGGN-2024-16 from the Iijoki area.

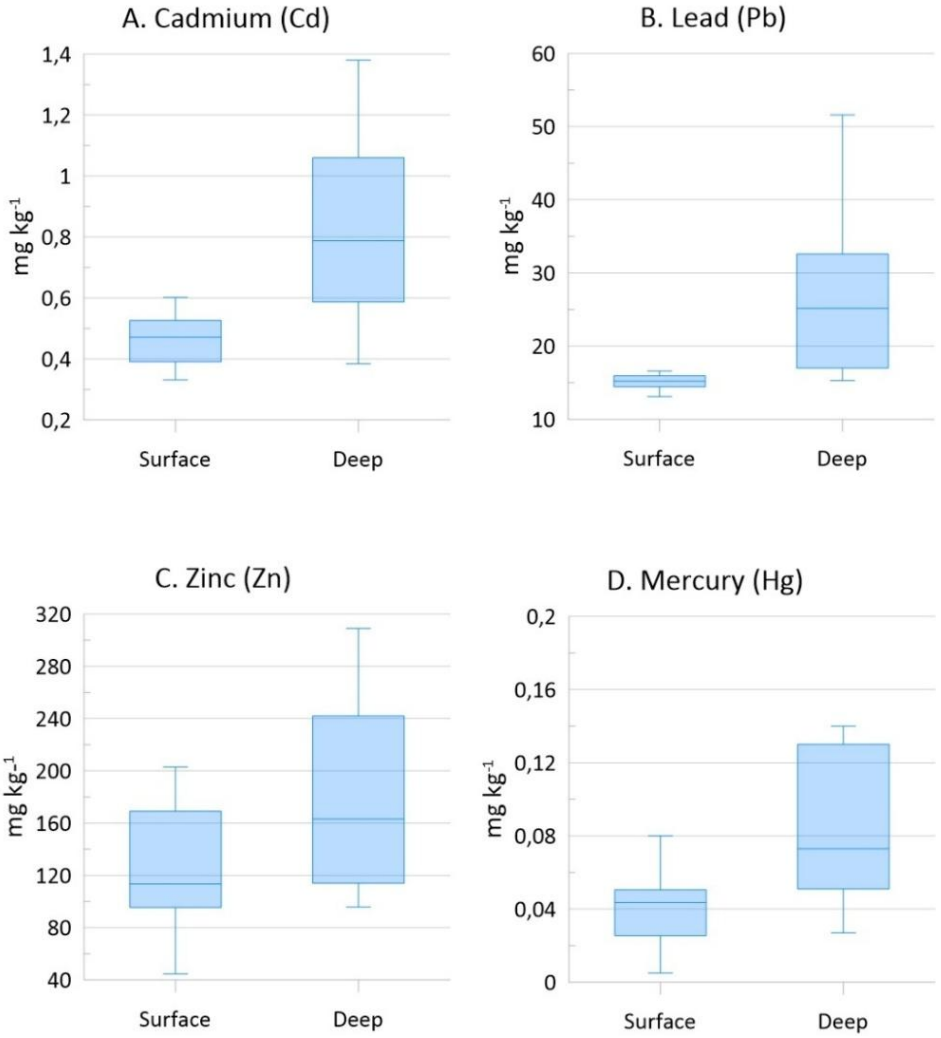

Figure 55. *Box plots of lead (A), cadmium (B), zinc (Zn) and mercury (Hg) contents (mg/kg) in the seabed surface (0-1 cm) sediment and in the deeper sediment core. For every site/core the surface sediment (Surface) value and maximum elemental value in the deeper sediment (Deep) are presented in the plot.*

The vertical distribution of lead exhibits a similar pattern, with concentrations increasing from the bottom toward subsurface maxima and subsequently decreasing toward the surface (Fig. 55 and 56). The highest Pb concentration (92.7 mg/kg) was recorded at 18–19 cm depth in core MGGN-2023-4 from the Lapväärtinjoki area.

Zinc profiles closely follow those of Pb (Fig. 56), showing an upward increase toward subsurface maxima, followed by a decline toward the surface. The

highest Zn concentrations (>150 mg/kg) were found in several cores from the Iijoki, Lapuanjoki, and Lapväärtinjoki areas. These values exceed the ERL (Effects Range-Low) toxicity threshold for heavy metals (150 mg/kg; Long et al., 1995).

Mercury distributions also display an upward increasing trend toward subsurface maxima, followed by a decrease toward the surface (Fig. 56). Surface Hg concentrations are consistently below 0.1 mg/kg across all sites. Maximum Hg concentrations (0.35–0.36 mg/kg) were detected at depths of 25–27 cm in core MGGN-2023-3 and 25–26 cm in core MGGN-2023-4, both from the Lapväärtinjoki area.

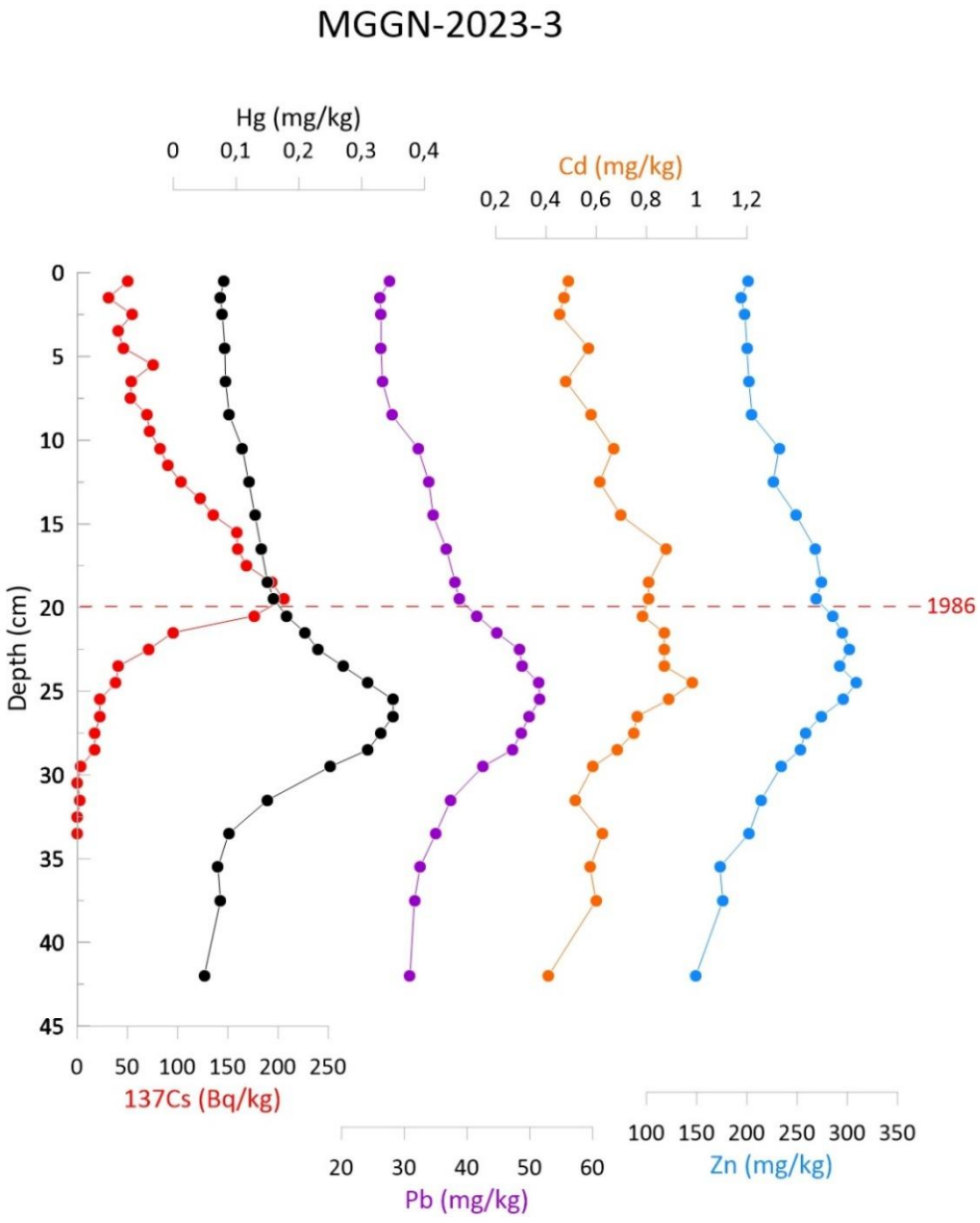

Figure 56. *137Cs activity (Bq kg-1), mercury (Hg), lead (Pb), cadmium (Cd) and zinc (Zn) contents (mg/kg) down-core vs. depth (cm) profiles from sediment core MGGN-2023-3 taken in the Lapväärtinjoki area, in the Bothnian Sea. Stratigraphical marker horizon is labelled, and age is given in years AD.*

Overall, all sites exhibit a clear decreasing trend in heavy metal concentrations toward the sediment surface. Figure 55 illustrates that present-day surface concentrations are substantially lower than subsurface values. Based on 137Cs activity concentration profiles, the highest heavy metal concentrations correspond to deposition during the late 1960s and 1970s.

4. Discussion

4.1. Seabed composition – changes in both place and time

The seabed composition within the six study areas in Finland is characterized by a predominance of unconsolidated sediments overlying solid bedrock, which is largely covered by glacial or more recent deposits. Fine-grained substrates, including brackish water mud, recent mud, and secondary sand, dominate most areas. Iijoki and Kiiminkijoki are primarily composed of these soft sediments, reflecting a depositional environment influenced by river discharge as well as brackish water conditions. Lohtajanjoki also exhibits a muddy substrate but contains notable sandy sections, consistent with its proximity to an esker system; thin sand layers occur widely on top of glacial clay or brackish water mud. Lapväärtinjoki differs by combining fine-grained mud with a substantial proportion of coarse-grained till. Lapuanjoki is almost entirely composed of mud, forming a uniform soft sediment cover. In contrast, Kalajoki is dominated by coarse-grained deposits, with extensive sand and sand/gravel layers, a feature linked to nearby esker formations extending onto the seafloor. Some bedrock outcrops occur locally in Lohtajanjoki and Lapväärtinjoki, although in all areas the bedrock is predominantly buried beneath sedimentary cover. Seabed features such as mud lineations and dunes found in some areas suggest very dynamic seafloor environment. In addition, seabed erosion marks, both anthropogenic (trawl marks) and natural (erosional features formed by pack ice) were also observed at seabed, suggesting that shallow water environment here is under constant pressure. Moreover, the land uplift continuously, slowly but gradually, raises the seabed/new material into shallower areas of active erosion by waves and ice.

We calculated the linear sedimentation rate estimates here using the subsurface depths of the 137Cs maxima for a placement of the Chernobyl nuclear power plant accident event (April 1986) 1986. Post-Chernobyl linear sedimentation rates at sites studied around the Gulf of Bothnia varied from

0.2 to 1.8 cm/year with an average value of 0.55 cm/year. Interestingly these sedimentation rate estimates in the Gulf of Bothnia study areas were in average similar than shown in the earlier studies (e.g., Kotilainen et al. 2021). It is notable that sedimentation rate estimates concern only the areas of accumulation (like here only 20,7 %). Also, the study sites exhibiting high rates of sedimentation according to acoustic soundings received priority in the sampling site selection process. Studied sites thus likely represent upper estimates of sediment deposition for the entire study area.

Regarding harmful substances in the sediments, we did study heavy metal contents in seabed sediments. Heavy metal input into the Gulf of Bothnia began to increase in the 1950s. The dating results of the seabed sediments suggest that heavy metal input peaked from the 1960s to the 1970s. Sedimentary records indicate that the concentrations of heavy metals have generally declined since that time. However, in some SeaMoreEco study areas cadmium and zinc concentrations in the subsurface sediments are still relatively high.

“Contaminated sediments” on the seabed can present major environmental risks when resuspending in water and pollute marine life. There is a relatively good overall understanding of the harmful substances present in seabed sediments, but there is a lack of knowledge about the more precise concentrations, more precise regional location and extent of the harmful substances present in the bottom sediments. This is especially true/valid in estuaries that are under heavy human pressure. The new HIDDEN project aims to reduce this knowledge gap.

4.2. Fieldwork challenges (SGU)

The basis for a thorough and accurate assessment of seafloor conditions is a carefully conducted field data collection approach. During the three summers that SGU conducted fieldwork, various problems arose which affected not only the fieldwork itself, but also the quality of the collected data. During the fieldwork of 2023 and 2024, the position of samples and video was logged by Ugglan’s fixed-mounted RTK positioning system. This, along with Ugglan’s ability for dynamic positioning, provided centimeter level accuracy. During the fieldwork of 2025, Ugglan wasn’t available which resulted in positions were logged by a hand-held GPS, with a meter-level accuracy. This compromises the comparability between the data collected during different field auctions. It could also lead to misinterpretation of substrate class and environmental conditions. Due to the nature and purpose of this project, that is, however, not of significant concern. This is because of the inherent uncertainty of not having underwater positioning of the underwater cameras and sampler, which makes the radius of uncertainty greater than the accuracy of the positioning system.

SGU has developed methods for incorporating underwater positioning in the sampling process that will likely be incorporated in the upcoming HIDDEN

(Habitat Investigation in Diverse and Dynamic Estuarine Networks) project. If this method is utilized, highly accurate RTK-positioning is essential to ensure high quality data collection. This will enhance the data quality and result in even higher model accuracy.

4.3. Model vs Reality (SGU)

The methodological framework applied in this study combines hydroacoustic surveys, seabed sampling, and machine learning based spatial modelling to produce high-resolution substrate and habitat maps for shallow coastal areas in the northern Gulf of Bothnia. Together, these approaches provided a robust foundation for understanding spatial patterns in sediment composition and benthic habitats, while also offering a reproducible workflow that can be applied in future marine mapping initiatives. Also, the use of open-source data analysis tools (e.g., R, CARET, XGBoost) also supports long-term applicability.

The modelling workflow produced continuous maps for different sediment fractions and biological types, which could then be transformed into thematic habitat classes that adhere to the requirements of many regional sediment and habitat mapping schemes. However, the use of such a novel approach, while efficient, repeatable and standardized, has also its own shortcomings. For example, due to limited time and resources, there was not a sufficient number and diversity of ground-validation sites in some areas, which can affect model training and model output. This shortcoming was partially addressed by using XGBoost algorithm, which resolved the problem by internally shuffling the training and predictor arrays to the optimal model once an optimal loss function was reached. However, in some cases this was not enough as shown in one of our study areas (i.e., Piteå) where the result showed that the model struggled to predict other substrate types and produced a thematic map that have a mostly (98%) clay sediment distribution. This can be attributed to the lack of diversified ground validation points for other sediment classes. Additionally, another limitation of the study was that it focused solely on percentage coverage, without evaluating alternative approaches such as presence-absence or probability-based for species and sediment classification.

HELCOM HUB classification proved highly useful for identifying suitable habitats based on sediments and observed species in the Bothnian Gulf. The HELCOM HUB system in the present study was limited to only level 5 classification, as the survey data did not include biomass information needed for the level 6 classification. Additionally, coverage of one species could overlap with others, making identification from video observations challenging, which further constrained the classification to level 5.

In the Piteå region, one species was identified as dominant, as noted in the results. However, this presented a challenge when using the HELCOM HUB classification. For example, the species is classified under rock and boulders

as "AA.A1C5 *Baltic photic rock and boulders dominated by perennial filamentous algae*," whereas in muddy sediments, it is classified as "AA.H1Q5 *Baltic photic muddy sediment dominated by stable aggregations of unattached lake ball (Aegagropila linnaei).*" This required careful observation, since misidentification could lead to incorrect habitat classification. Special attention was also given to unattached rigid hornwort (*Ceratophyllum spp.*), which occurs only in muddy or mixed sediments.

The EMODnet classification was a useful and standardized way for identifying and comparing the geological status of the study areas. However, applying the Folk 5 classification system aslo proved challenging, as many observations and modeled data did not align precisely with its categories. The modeled data struggled to fit these classes, as the percentage coverage for rock and boulders (25%), coarse sediment (gravel and stones-pebbles, 75%), sand (0%), and clay (0%) did not correspond neatly to any single category, necessitating classification as a mixed type. With support from the Finnish Geological Survey, the classification of the modeled locations was refined further, but this did not fully resolve the classification challenge.

Sediment sampling, sub-bottom interpretations and modeling all produced relatively similar results with distinct areas of fine sediment accumulation and clear signs of erosional or transport bottoms in others. This emphasizes the importance of collecting multiple datatypes and integrating different data processing skills in the post processing workflow. By using both marine geological expertise, as in the case of sub-bottom interpretation and substrate sampling, and advanced machine learning and AI techniques, as in the case of the modeled maps, reliable products and a more thorough assessment of critical areas can be highlighted.

4.4. Filling the knowledge gap in the white ribbon zone – some observations

Near shore areas can be too shallow for efficient seabed survey methods, but too deep for land-based survey methods and thus often appear as unmapped patches or "white ribbon" zones. To fill this knowledge gap integrated methods are needed. In the SeaMoreEco project we have tested to integrate satellite and airborne derived data with shipborne data.

Satellite-derived bathymetry is a useful complement to acoustic and seismic surveys in shallow, clear waters, where it can reliably map depths down to about 3 meters water depths. However, in deeper and turbid areas such as in the estuaries, its limitations become evident: the seabed cannot be detected, and spatial resolution is insufficient for small-scale features like submarine dunes. While major seabed structures such as large sandbars can be identified, enabling broad-scale monitoring of morphology, shoreline change, and land uplift, detailed mapping of fine geological features still requires vessel-based or unmanned surveys with high-resolution sonar. In

clear-water environments, drones can provide additional insights into vegetation and shallow structures, but precise mapping always depends on complementary sampling or acoustic data.

Airborne drones and ground truth data have the best resolution, but they cover only small areas. Satellite data covers large areas, but the resolution is coarse, and data fails in deep and/or turbid water.

Satellite-based substrate classification requires supporting background data to improve accuracy. Based on the findings of this study, it is recommended that ground truth data should be collected not only from shallow coastal areas, but also from deeper zones. Data should be collected also from vegetated areas and areas representing different water types. Drone imagery should be done for areas representing different water types as well. The optimal time for drone surveys is during calm weather conditions, ideally synchronized with satellite image acquisition, to ensure comparability and minimize water surface disturbance.

Using water characteristics (clear, turbid) as auxiliary data may improve substrate classification. More data and validation are required to study this further.

Different band combinations should be tested to determine the best results in different areas. The SAV mapping is difficult for vegetation growing in deep water and areas with fragmented vegetation and poor water quality, as pointed out by Huber et al. (2022). They also recommended to use “dense” and “sparse” SAV classes to differentiate between vegetation growth densities.

4.5. The project significance to present and future projects and collaborations

The methodological framework applied in this study combines hydroacoustic surveys, seabed sampling, and machine learning based spatial modelling to produce high-resolution substrate and habitat maps for shallow coastal areas in the northern Gulf of Bothnia. In addition, satellite and airborne drone derived data were used to fill the knowledge gap in “the white ribbon zone”, a shallow water area from shore down to the water depths around 3 meters. Together, these approaches provide a robust foundation for understanding spatial patterns in sediment composition and benthic habitats, while also offering a reproducible workflow that can be applied in future marine mapping initiatives.

The use of MBES and SBP are effective methods for recording seafloor- and sub-seafloor features. The dynamic line planning strategy minimized the risk of missing shallow features and ensured full coverage mapping with high positional accuracy. However, the reliance on vessel availability introduced methodological variability, particularly in 2025 when the high-precision RTK

positioning system was replaced with a handheld GPS. Although this did not compromise the general usability of the dataset, it does introduce slight uncertainty in sample positioning that should be acknowledged in data interpretation.

Ground truthing through sediment samples and underwater video observations is important for validating and correcting hydroacoustic interpretation as well as satellite data. The Van Veen grab sampler functioned well in fine grained sediments, but was not suitable for coarse substrates, which limited direct sampling in some areas. Underwater cameras therefore played a critical role in confirming substrate types and providing biological observations, reinforcing the importance of using multiple verification methods in habitat mapping projects.

An important strength of this study is the integration of geophysical, geospatial, and environmental predictors within a machine learning process. The use of XGBoost allowed flexible modelling of both continuous and categorical substrate variables, and the iterative predictor selection process ensured that only ecologically and geologically meaningful variables were retained. This approach improves model interpretability and reduces noise from irrelevant predictors. By combining modelling outputs with established classification systems such as EMODnet Folk and HELCOM HUB, the results are directly comparable with regional and international mapping products.

The modelling workflow produced continuous maps of substrate fractions and biological cover, which could then be transformed into thematic habitat classes. These two processes provide both quantitative information and standardized categorical outputs. However, the accuracy of biological predictions remains partly dependent on the density and representativeness of the field observations. Increasing the number of biological validation points in future surveys would further strengthen the reliability of future models.

Despite these limitations, the workflow demonstrated high reproducibility. The standardized data processing workflow, unified raster architecture, and documented modelling procedures ensure that the methodology can be replicated both within and beyond the study area. The use of open-source statistical tools (R, CARET, XGBoost) also supports long-term applicability.

4.5.1. A foundation for future marine management

The products generated in this project provide a valuable foundation for multiple future applications in marine management and research. The results reveal where sensitive habitats occur, how substrates are distributed, and which areas may require protection or careful use. The unified raster structure and standardized classification systems (EMODnet Folk, HELCOM HUB) ensure that the output can be directly integrated into national and regional mapping efforts, long-term monitoring programs, and future

modelling initiatives. These datasets can support environmental impact assessments, marine spatial planning, and conservation measures by offering detailed information on bottom types and habitat distributions in shallow coastal areas. The continuous prediction layers also enable future reclassification without the need to repeat field surveys, making it possible to update habitat maps as new frameworks or management needs emerge. Furthermore, the products can serve as training datasets for future machine-learning models, facilitate comparison between years, and provide a baseline for detecting environmental change.

The project partners have a history of collaboration that dates to the implementation of SEAmBOTH-project in 2018 (Bergdahl, et al., 2020). This partnership has evolved and resulted in exchange of experience and information that has benefited the current project significantly. The project organized workshops and meetings that consisted of presentations and discussions about how to integrate and harmonize data from the different organizations. The produced products in this study provide an avenue for comparability between Sweden and Finland and make it easier to plan joint environmental actions, identify shared ecological values and evaluate the effectiveness of cross-border initiatives. Overall, the generated products form a long-term asset that can be reused, refined, and expanded to support evidence-based decision-making and ecosystem-based management that aligns with EU environmental directives and supports regional coherence.

4.5.2. Recommendations for advancing shallow coastal mapping

Studying shallow coastal waters requires continuous development of both field methods and analytical approaches. Based on the results and experiences from this project, several key steps are recommended for future work to increase biological and geological ground-truthing. While the current models provide substrate predictions, biological classifications in shallow areas would benefit from additional validation data. Future surveys should include more underwater video transects, more targeted sampling in diverse sediment and biological areas, even seasonal observations to capture temporal variability, as this will improve species-level predictions and strengthen HELCOM HUB classification mapping. The upcoming shallow-water fieldwork for the HIDDEN project is challenging due to shallow water obstacles and equipment limitations. The use of smaller, more agile floating drones can aid data collection by being able to reach shallower waters without concerns for human safety. In addition, data generated by satellites and airborne drones is also very useful in these demanding very shallow water environments.

4.5.3. Integrating the methodology and results into future projects

The results and methods of the SeaMoreEco project can be further elaborated in HIDDEN to enhance transparency, accessibility, and usability for future studies and marine management initiatives. By documenting detailed field methodologies including hydroacoustic surveys, seabed sampling procedures, satellite and airborne drone imaging, and data processing workflows alongside metadata for each dataset, users can better understand how the data was collected and validated. Interactive visualization of bathymetry, backscatter, underwater videos, and thematic sediment and habitat maps would allow stakeholders to explore spatial patterns and ground-truth observations more effectively. Linking datasets to model parameters, predictor variables, and accuracy metrics ensures reproducibility and clarity, while comparative analyses across years and survey areas provide insights into temporal and spatial changes. Additionally, incorporating downloadable products, shapefiles, and guidance for interpreting maps supports practical applications in ecosystem-based management and regional planning, including Interreg initiatives. Overall, integrating the SeaMoreEco results and methods into HIDDEN creates a comprehensive resource that not only documents past research but also facilitates ongoing monitoring, adaptive management, and further scientific exploration of shallow coastal ecosystems.

4.5.4. The importance of cross-border multidisciplinary collaboration

Networking between project partners is crucial for projects like SeaMoreEco because it fosters the exchange of knowledge, expertise, and resources across institutions and countries. Collaborative networks allow partners to share field methods, modeling approaches, and data processing techniques, which improve consistency and quality of results. They also enable faster problem-solving by combining different experiences and perspectives when challenges arise, such as logistical issues during field surveys or data interpretation difficulties. Importantly, networking strengthens the scientific and managerial impact of the project by linking local observations to regional and European-scale initiatives, ensuring that outputs are aligned with broader environmental monitoring and management frameworks, in this case, HELCOM and EMODnet. Additionally, strong partnerships facilitate capacity building, knowledge transfer, and training opportunities for less experienced team members, enhancing the overall competence and sustainability of future research efforts. Finally, effective networking increases visibility and credibility of the project, which can attract further funding and foster long-term collaborations beyond the current project's scope.

Potential collaborations with other projects could significantly enhance the impact and applicability of the SeaMoreEco results. For instance, linking with

regional monitoring programs or marine conservation initiatives in the Gulf of Bothnia could help integrate the high-resolution seabed and habitat maps into broader environmental management frameworks. Collaboration with projects focusing on climate change impacts on coastal ecosystems could allow the SeaMoreEco products to support predictive modeling of habitat shifts under different scenarios. Cross-border initiatives, such as other Interreg or HELCOM-funded projects, could benefit from sharing methodologies, datasets, and modeling approaches, fostering harmonization of habitat mapping standards and conservation strategies across the northern Baltic region. Additionally, partnerships with academic research programs or citizen science initiatives could expand biological monitoring, validate modeling outputs, and support long-term ecological studies, creating synergies that enhance both scientific knowledge and practical management outcomes.

4.6. Where to find maps and data

The reports and accompanying appendices will be available for download in the Doria portal (https://www.doria.fi/).

Results from thematic and continuous modeling that SGU produced within the project will be uploaded to the SeaGIS map portal (https://seagis.org/) and will be available for download.

Data-products produced by GTK will be published in the Hakku portal (https://hakku.gtk.fi/en) and available for download. Sedimentation rates data will be available in the EMODnet Portal (https://emodnet.ec.europa.eu/en)

REFERENCES

Ahlberg, P. (1986). Den svenska kontinentalsockelns berggrund. The Geological Survey of Sweden. Uppsala: The Geological Survey of Sweden.

Avellan, L., Haldin, J., Kontula, T., Leinikki, J., Näslund, J., & Laamanen, M. (2013). Technical Report on the HELCOM Underwater Biotope and habitat classification. Helsinki, Finland: Baltic Marine Environment Protection Commission - HELCOM.

Bergdahl, L., Gipson, A., Haapamäki, J., Heikkinen, M., Holmes, A., Kaskela, A., Keskinen, E., Kotilainen, A., Koponen, S., Kovanen, T., Kågesten, G., Kratzer, S., Nurmi, M., Philipson, P., Puro-Tahvanainen, A., Saarnio, S., Slagbrand, P., & Virtanen, E. (2020). Seamless Maps and Management of the Bothnian Bay SEAmBOTH - Final report. Metsähallitus, Parks & Wildlife Finland, Vantaa, 2020. ISBN 978-952-295-268-4 (pdf). p 149.

Berggrund 1:50 000 250 000. (2025, 10 29). Retrieved from SGU Kartvisaren: https://apps.sgu.se/kartvisare/kartvisare-berg-50-250-tusen.html

Boden, A. (2005). Bodenkundliche Kartieranleitung (KA5). Bundesanstalt für Geowissenschaften und Rohstoffe und Geologische Landesämter der Bundesrepublik Deutschland (Hrsg.). Stuttgart, Germany: Schweitzerbart'sche Verlagsbuchhandlung.

Chen, T., & Guestrin, C. (2016). XGBoost: A Scalable Tree Boosting System. Washington: University of Washington. HAV. (2017). DRAFT: Visuella undervattensmetoder för uppföljning av marina naturtyper och typiska arter. Gothenburg: Swedish Agency for Marine and Water Management.

Grinsted, A. (2015). Projected Change – Sea level. In: The BACC II Author Team, Second Assessment of Climate Change for the Baltic Sea Basin. Regional Climate Studies, 253–263.

HAV. (2017). DRAFT: Visuella undervattensmetoder för uppföljning av marina naturtyper och typiska arter. Gothenburg: Swedish Agency for Marine and Water Management.

Hjulström, F. (1935). Studies of the morphological activity of rivers as illustrated by the River Fyris. Uppsala: The Geological institution of the University of Upsala.

Huber, S., Hansen, L. B, Nielsen, L. T., Rasmussen, M. L., Sølvsteen, J., Berglund, J., Paz von Friesen, C., Danbolt, M., Envall, M., Infantes, E., & Moksnes, P. (2022). Novel approach to large-scale monitoring of submerged aquatic vegetation: A nationwide example from Sweden, Integrated Environmental Assessment and Management, Volume 18, Issue 4, 1 June 2022, Pages 909–920, https://doi.org/10.1002/ieam.4493

Ilus, E. (2007). The Chernobyl accident and the Baltic Sea. Boreal Environ. Res. 12, 1–10.

Janowski, L., Wroblewski, R., Dworniczak, J., Kolakowski, M., Rogowska, K., Wojcik, M., & Gajewski, J. (2021). Offshore benthic habitat mapping based on object-based image analysis and geomorphometric approach. A case study from the Slupsk Bank, Southern Baltic Sea. Gdansk: ScienceDirect.

Kakkuri, J. (2012). Fennoscandian land uplift: Past, present and future. In: Haapala, I. (ed.) From the Earth's core to outer space. Dordrecht: Springer, 127–136.

Kankaanp¨ää, H., Vallius, H., Sandman, O., & Niemist¨o, L. (1997). Determination of recent sedimentation in the Gulf of Finland using 137Cs. Oceanol. Acta 20, 1–14.

Kaskela, A.M., Kotilainen, A.T., Alanen, U., Cooper, R., Green, S., Guinan, J., van Heteren, S., Kihlman, S., Van Lancker, V., Stevenson, A., & the EMODnet Geology Partners (2019). Picking Up the Pieces—Harmonising and Collating Seabed Substrate Data for European Maritime Areas. Geosciences 2019, 9, 84.

Kotilainen, A.T., Kotilainen, M.M., Vartti, V.-P., Hutri, K.-L., & Virtasalo, J.J. (2021). Chernobyl still with us: 137Caesium activity contents in seabed sediments from the Gulf of Bothnia, northern Baltic Sea. Marine Pollution Bulletin. 172.

Kuhn, M. (2008). Building Predictive Models in R Using the caret Package. Journal of Statistical Software.

Kulha, N., Ruha, L., Väkevä, S., Koponen, S., Viitasalo, M., & Virtanen, E.A. (2024). Satellite bathymetry estimation in the optically complex northern Baltic Sea. Estuarine, Coastal and Shelf Science, Volume 298, 2024, 108634.

Kågesten, G., Baumgartner, F., & Freire, F. (2020). High-resolution benthic habitat mapping . Uppsala: The Geological Survey of Sweden.

Lacaux, J.P. Tourre, Y.M., Vignolles, C., Ndione, J.A., & Lafaye, M. (2007). Classification of ponds from high-spatial resolution remote sensing: Application to Rift Valley Fever epidemics in Senegal, Remote Sensing of Environment, Volume 106, Issue 1, 2007, Pages 66-74.

Long, E.R., Macdonald, D.D., Smith, S.L., & Calder, F.D. (1995). Incidence of adverse biological effects within ranges of chemical concentrations in marine and estuarine sediments. Environ. Manage. 19, 81–97.

Meili, M., Jonsson, P., & Carman, R. (1998). Cs dating of laminated sediments in swedish archipelago areas of the Baltic Sea. In: S¨ateilyturvakeskus, Raportti STUK-A, 145, pp. 127–130.

Mattila, J., Kankaanp¨ää, H., & Ilus, E. (2006). Estimation of recent sediment accumulation rates in the Baltic Sea using artificial radionuclides 137Cs and 239,240Pu as time markers. Boreal Environ. Res. 11, 95–107.

Moros, M., Andersen, T.J., Schulz-Bull, D., H¨ausler, K., Bunke, D., Snowball, I., Kotilainen, A., Zillén, L., Jensen, J.B., Kabel, K., Hand, I., Leipe, T., Lougheed, B.C., Wagner, B., & Arz, H.W. (2017). Towards an event stratigraphy for Baltic Sea sediments deposited since AD 1900: approaches and challenges. Boreas 46, 129–142.

Over, J.R., Ritchie, A.C., Kranenburg, C.J., Brown, J.A., Buscombe, D., Noble, T., Sherwood, C.R., Warrick, J.A., & Wernette, P.A. (2021). Processing coastal imagery with Agisoft Metashape Professional Edition, version 1.6—Structure from motion workflow documentation: U.S. Geological Survey Open-File Report 2021–1039, 46 p., https://doi.org/10.3133/ofr20211039.

Pouget, M., Madeira, J., Le Floc'h, E., & Kamal, S. (1991). Caractéristiques spectrales des surfaces sableuses de la région cotière nord-ouest de l'Egypte: application aux données satellitaires SPOT. In Proc. 2éme Journées Télédétection. Caractérisation et Suivi des Milieux Terrestres en Régions Arides et Tropicales, ORSTOM, Bondy, France, pp. 27–38.

Poutanen, M., & Steffen, H. (2014). Land Uplift at Kvarken Archipelago / High Coast UNESCO World Heritage area. Geophysica, 50(2), 49–64.

R Core Team. (2024). R: A Language and Environment for Statistical Computing. Vienna, Austria: R Foundation for Statistical Computing. Retrieved from https://www.R-project.org/

Reffet, E., Courrech du Pont, S., Hersen, P., & Douady, S. (2010). Formation and stability of transverse and longitudinal sand dunes. Geology, 38(6), 491-494.

Rubin, D.M., & Hesp, P.A. (2009). Multiple origins of linear dunes on Earth and Titan. Nature Geoscience 2.9 (2009): 653-658.

Schiewer, U. (2008). The Baltic Coastal Zones. Berlin: Springer. SGF. (2016). Jordarternas indelning och benämning. Luleå: Swedish Geotechnical Society

Virtasalo, J.J., Hämäläinen, J., & Kotilainen, A.T. (2014). Toward a standard stratigraphical classification practice for the Baltic Sea sediments: the CUAL approach. Boreas. Volume 43, Issue 4, 924–938.

Zaborska, A., Winogradow, A., & Pempkowiak, J. (2014). Caesium-137 distribution, inventories and accumulation history in the Baltic Sea sediments. J. Environ. Radioact. 127, 11–25

Zhao, D., Yang, F., Wu, Z., Zhu, C., & Liu, H. (2020). Chapter 2 Multi-beam Bathymetric Technology.

Acknowledgements

GTK and SGU would like to thank and acknowledge the following individuals, organizations and stakeholders who have helped the project to reach its goals. The following list is not in any particular order.

- Anders Wallin from the County Administrative Board of Norrbotten for expert biological advice and assistance during the early parts of the fieldwork.
- Carlos Paz von Friesen from the County Administrative Board of Västerbotten for the generosity of lending SGU their boat Skorven during the 2025 fieldwork. And Anniina Saarinen and Vanessa Fontana for their biological interpretations of the underwater video that SGU collected during the project, that was the biological basis for the species modeling that SGU conducted.
- Lars Ringnér from Gattulven AB, along with his staff Alexandra Bäck and Bo Lindnér for boat driving expertise with S/V Ugglan and Skorven.
- Field working members from SGU: Cecilia Edbom Blomstrand, Max Holmström & Erik Westberg
- Anna Eklöv Petterson from the Swedish University of Agricultural Sciences for PARIO grain size analysis of the collected samples.
- The crews of R/V Geomari, and R/V Gridi as well as other GTK persons assisting with field work: Mika Aartola, Janne Arvilommi, Eija Eräkare, Sami Jokinen, Iina Karomäki, Mikko Kinnunen, Matti Laatikainen, Pekka Marttila, Lasse Miettinen, Olli Sallasmaa, Nikolas Sanila, Valtteri Savilaakso and Antti Sainio.
- Eveliina Lampinen and Anton Pajukoski from Centre for Economic development, Transport and Environment Northern Ostrobothnia for the shallow water field work and providing validation data on water depth, seabed substrates and underwater vegetation.
- Anu Kaskela and Susanna Kihlman from the EMODNet team at GTK for excellent discussions and their help with clearing up issues with the folk-5 classification scheme.
- Satu Vuoriainen for performing the 137Cs analyses at GTK. And Nana Sulander taking care of administration at GTK.
- The study utilized research infrastructure facilities provided by FINMARI (Finnish Marine Research Infrastructure network).
- The whole SeaMoreEco project team: For excellent discussions, workshops, meetings and a fantastic final seminar.